

Journal of Materials Chemistry B

Materials for biology and medicine

Accepted Manuscript

This article can be cited before page numbers have been issued, to do this please use: N. G. Sahoo, N. Karki, H. Tiwari, C. Tewari, A. Rana, N. Pandey and S. Basak, *J. Mater. Chem. B*, 2020, DOI: 10.1039/D0TB01149E.



This is an Accepted Manuscript, which has been through the Royal Society of Chemistry peer review process and has been accepted for publication.

Accepted Manuscripts are published online shortly after acceptance, before technical editing, formatting and proof reading. Using this free service, authors can make their results available to the community, in citable form, before we publish the edited article. We will replace this Accepted Manuscript with the edited and formatted Advance Article as soon as it is available.

You can find more information about Accepted Manuscripts in the [Information for Authors](#).

Please note that technical editing may introduce minor changes to the text and/or graphics, which may alter content. The journal's standard [Terms & Conditions](#) and the [Ethical guidelines](#) still apply. In no event shall the Royal Society of Chemistry be held responsible for any errors or omissions in this Accepted Manuscript or any consequences arising from the use of any information it contains.

1 **Functionalized Graphene Oxide as a Vehicle for Targeted Drug Delivery and** 2 **Bioimaging Applications**

3
4 Neha Karki¹, Himani Tiwari¹, Chetna Tewari¹, Anita Rana¹, Neema Pandey¹, Souvik Basak²,
5 Nanda Gopal Sahoo^{1*}

6 ¹Prof. Rajendra Singh Nanoscience and Nanotechnology Centre, Department of Chemistry, Kumaun
7 University, D.S.B. Campus, Nainital, 263002, India

8 ²Dr.B.C. Roy College of Pharmacy & Allied Health Sciences, Durgapur, West Bengal, 713206, India
9

10 **Abstract**

11 Graphene Oxide (GO) has attracted tremendous attention as a most promising nanomaterial
12 among the carbon family since it emerged as a polynomial functional tool bearing rational
13 application in diverse fields such as biomedical engineering, electrocatalysis, biosensing, energy
14 conversion, storage devices and others. Despite having certain limitations due to their irreversible
15 aggregation performance owing largely to the strong vander Waals interactions; efforts have been
16 made to smartly engineer its surface chemistry for multimodal realistic applications. The use of
17 such GO based engineered devices has galloped rapidly in last few years principally due to its
18 excellent properties such as huge surface area, honeycomb like structure allowing vacant
19 interstitial space to accommodate compounds, sp² hybridized carbon, improved biocompatibility
20 and cell surface penetration due to electronic interactions. Amongst multifaceted GO dynamics, in
21 this review, attempts have been made to discuss the advanced applications of GO or graphene
22 based materials (GBNs) in biomedical field involving drug or therapeutic gene delivery, dual drug
23 or drug-gene concoction targeting, special delivery of drug cocktail to brain, stimuli responsive
24 release of molecular payloads, Janus structured smart applications for polar-nonpolar combination
25 drug loading followed by targeting together with smart bioimaging approaches. In addition, the
26 advantages of dual drug delivery systems have been discussed in details. We have also discussed
27 various electronic mechanisms, detailed surface engineering to meet microcosmic criteria for its
28 utilizations, various novel implementations of engineered GO as mentioned above together with
29 discussions of its inevitable toxicity or disadvantages. We hope that target audience, belonging to
30 biomedical engineering, pharmaceutical or material science field, may acquire relevant
31 information from this review which may further help them design future studies in this field.

32

33 **Keywords:** Bioimaging; controlled release; dual drugs; drug delivery; Janus structure.

34

35 ***Corresponding author: Email address:** ngsahoo@yahoo.co.in (N. G. Sahoo)

36

37 Contents

38 1. Introduction

39 2. Functionalization of GO

40 2.1. Non-covalent Functionalization

41 2.2. Covalent Functionalization

42 3. Advantages and disadvantages of GO

43 3.1. Advantages of GO

44 3.1.1. pH responsive GO for Controlled Release

45 3.1.2. Temperature Sensitive GO

46 3.1.3. Near Infrared (NIR) or Laser sensitive photodynamic therapy (PDT)

47 3.1.4. Janus Structured GOs for Multivariant (differentially polar dual drug) Release

48 3.2. Disadvantages of GO

49 3.2.1. Aggregation in Biological Media

50 3.2.2. Irregular size

51 3.2.3. Toxicity study of GO

52 4. Drug Targeting Strategies of GO

53 4.1. Active Targeting

54 4.2. Passive targeting

55 5. Drug Delivery Profiles and Systems

56 5.1. Delivery of single drug

57 5.2. Delivery of binomial drugs

58 6. Dual Drug Delivery Systems over Single Drug Delivery System

59 7. Role of GO in Bioimaging

60 7.1. Optical Imaging

61 7.1.1. Fluorescence Imaging

62 7.1.2. Two Photon Fluorescence Imaging

63	7.1.3. Raman Imaging
64	7.2. Radionuclide Imaging
65	7.3. Magnetic Resonance Imaging
66	7.4. Photoacoustic Imaging
67	7.5. Computed Tomography
68	7.6. Multimodal Imaging
69	8. Challenges and Outlooks
70	8.1. Prevention of drug from biological degradation
71	8.2. Effective Targeting
72	8.3. Cost effectiveness
73	9. Conclusions and Future Prospective
74	10. References
75	

76 **Abbreviations:**

77 AuNPs, Gold Nanoparticles; APS, 3-aminopropyl triethoxysilane;bcPLu, block copolymer
78 pluronic; BSA, Bovine Serum Albumin; β -CD, Betacyclodextrin; CT,Computed Tomography;
79 CPT, Camptothecin; CAs, Contrast Agents;CEF, Cephalexin; CXCR4, C-X-C chemokine receptor
80 type 4;CuS, Coper Sulphide; CEA, CarcinoembryonicantigenCNTs, Carbon Nanotubes; CS,
81 chitosan; Ce6, chlorine6; Cis-Pt, Cis-Platin; DDSs, Drug Delivery Systems; DFT, Density
82 Functional Theory; DDMAT, 2-(Dodecylthiocarbonothioylthio)-2-methylpropionic acid; DOX,
83 Doxorubicin; 2D, FA, Folic Acid; 5-FU, 5-fluorouracil; Two Dimensional; DNA, Deoxyribo
84 Nucleic Acid; E. Coli, Escherichia coli, EPR, Enhanced Permeation and Retention;FRET,
85 Fluorescence Resonance Energy Transfer;FI, Fluorescence Imaging;GEM, Gemcitabine
86 hydrochloride; GMA, glycidyl methacrylate; GBNs, graphene based nanomaterials; GO,
87 Graphene Oxide; Glu, glucosamine; GEF, Gefitinib GQDs, GSH, glutathione; GNRs, Graphene
88 Nanoribbons;Graphene Quantum Dots; HA, hypocrellin A;IONP, Iron Oxide Nano particle; ICG,
89 Indocyanine Green; KGM/SA,Konjac glucomannan/sodium alginate; Lf, Lactoferrin;Me-LOGr,
90 Microwave-enabled Low-Oxygen Graphene;MNs, Magnetic Nanoparticles; MBs, Molecular
91 Beacons; MRI, Magnetic Resonance Imaging;MTX, Methotrexate;MI, Multimodal Imaging; MeB,
92 Methylene Blue; NIAcAcAl, N-isopropyl acrylamide-coacrylamide co-allylamine; NmPDT,
93 Nanomaterial-mediated Photodynamic Therapy;NmPTT, Nanomaterial-mediated Photothermal
94 Therapy; NGS, Nanographene Sheets;NIR, Near Infrared Regions;PEI, poly-ethyleneimide; PAI,
95 Photoacoustic Imaging; PVP, polyvinylpyrrolidone; PNIPAAm,poly(N-
96 isopropylacrylamide);PEG,poly-ethyleneglycol; PVA, poly(vinyl alcohol); PAMAM,
97 polyamidoamine; PCT, Paclitaxel; PET, Positron Emission Tomography; PNPs, polymers
98 nanoparticles; PS, Photosensitizers; PLL, poly (L-lactide); PDT, Photodynamic Therapy; PTT,P-
99 gp,P-glycoprotein; Photothermal Therapy; PCL, poly-caproyllactone;PAA, Polyallylamine; PSA,
100 polysebacic anhydride; PMMA, Poly(methyl methacrylate); QSR,Quercetin; RB, Rose Bengal;
101 RAI, Radionuclide Imaging; RI, Raman Imaging, rGO, reduced Graphene Oxide; RAFT,
102 Reversible terminated Addition Fragmentation chain Transfer; SPECT, Single-Photon Emission
103 Computed Tomography;SERS, Surface-Enhanced Raman spectroscopy; TPFI, Two-Photon
104 Fluorescence Imaging; Tf, Transferrin; UV, Ultra-Violet.

105

106 1. Introduction

107 At present, various malignant diseases have substantially affected and compromised the human
108 life and become the cause of threat all over the world [1]. Therefore, exponentially emergent call
109 for advances of the efficient treatment and diagnosis of various malignant diseases has encouraged
110 for an extensive array of interdisciplinary field to modernize an effective and nontoxic drug delivery
111 systems (DDSs). With the advancement of science and technology, various routes have been
112 emerged so far for dealing against such threat [2,3]. To enhance the persistence rate of patients
113 suffering from such diseases, the convenience of novel technologies for early diagnosis and
114 monitoring play a vital role. With current developments in nanotechnology field, the potential
115 application of nanosized materials for special types of cell target therapy such as efficient delivery
116 of biological entities to the targeted site and competent detection of diseases are being paid
117 enormous attention so far [4–6]. Since now, numerous nanostructured materials have been
118 envisioned and discovered for such highly focused biomedical applications.

119 Among these nanostructured materials, graphene based nanomaterials (GBNs) e.g. graphene
120 oxides (GO), reduced graphene oxide (rGO), graphene quantum dots (GQDs) etc., are extensively
121 explored for various drug targeting strategies, gene therapy, bioimaging application with the
122 possibility of highly engineered and efficient multi-function diagnostics and therapeutics agents
123 as they acquire exceptionally excellent physicochemical properties along with a number of
124 incomparable characteristics such as extreme small sizes, high specific surface areas and exclusive
125 arrangement of carbon atoms. At 2004, Geim and Novoselov isolated graphene by single layer
126 exfoliation technique in University of Manchester and characterized to establish it as a novel 2D
127 carbon nanomaterial with single atom layer, however, endowed with flat sp^2 hybridized structure,
128 long π - π stacking aromatic chain and polar functional group on both the surfaces [7]. In 2008, 2D
129 graphene oxide (GO), which had been synthesized by classical Hummers' method [8], was first
130 exploited in biomedical field as novel, improved drug carrier to load water insoluble anticancer
131 drugs such as Doxorubicin and SN-38 [9-10]. Interestingly, in one case pristine GO was used as
132 nanocarrier of drug [9] where in the other case [10], PEGylated GO acted as superior cargo-boat
133 to deliver SN-38 with better efficacy than Irinotecan, one FDA approved anticancer prodrug for
134 colon cancer. The superior activity of GO or functionalized GO has been attributed to their 2D
135 structures as they are reported to acquire exceptionally excellent physicochemical properties along
136 with a number of incomparable characteristics such as extreme small sizes, high specific surface

137 areas and exclusive arrangement of carbon atoms [11]. GO, an oxygenated derivative of the
138 graphene, based on its specific honeycomb lattice structures and biocompatibility, provides such
139 sites to integrate and fabricate with various types of biomolecules, such as drugs, antibodies, DNA,
140 peptide, protein, enzyme etc. In addition, graphene and its derivatives exhibit excellent optical
141 properties, thus they consider to be promising and attractive candidate for bioimaging, generally
142 for cells and tissues; GO and its derivatives are extensively applied in fluorescence bioimaging,
143 surface enhanced Raman scattering (SERS) imaging and magnetic resonance imaging (MRI) [12-
144 14] and offered the extended applications of GO based DDSs in materials science [15-17]. Such
145 biomolecules and hydrophobic drugs possess limited clinical utility as they show poor solubility
146 in the physiological environment.

147 It is well known that carbon nanomaterials aggregate in buffers solutions due to screening
148 effect of charge. Therefore, surface modification is the key to render the solubility and the
149 biocompatibility of carbon nanomaterials for biological systems. It is the physicochemical
150 characteristics of GO which make it physically and chemically versatile candidate and differentiate
151 it with other carbon nanomaterials. Hence, the principal advantage of GO over other carbon-based
152 nanomaterials is its aqueous and colloidal stability and controlled release for sustainable drug
153 release [18,19]. Owing a high surface-to-volume ratio GO enables to load more than one drug
154 simultaneously in a single nanocarrier [20]. Recently a report of a dual DDSs with cocktailing
155 two anticancer drugs Doxorubicin (DOX) and Cisplatin (Cis-Pt) has been described and found that
156 cancer cell apoptosis and necrosis rate increased by two times after the combining the drugs,
157 suggesting this dual DDS has great potential for clinical applications [21- 23].

158 Furthermore, due to its unique size and structure, Liu *et al.* investigated that in passive
159 targeting graphene appears more efficient than that of the carbon nanotubes by providing a
160 favorable environment for superior permeability and retention effect [24].

161 Interestingly, GO exhibits superior quenching abilities to the other carbon nanomaterials
162 in quenching efficiency and its kinetics. Fan *et al.* introduced a comparative study between GO
163 and CNTs based fluorescent sensor for the detection of DNA (Deoxyribo Nucleic Acid) where the
164 former resulted in detection and quantitation of lower amount of DNA than that of the latter [25].
165 Moreover, the 2D graphene sheets may be easily complexed to various other functional nano-
166 particles for potential multimodality imaging and therapy applications, while the nanoparticle
167 modification on individual nanotubes has been relatively more complicated.

168 To overcome from these complications and to explore the prospective of GO based DDSs,
169 these bio-molecules are functionalized on the surface of GBNs by means of various surface coating
170 strategies. These surface functionalization strategies are applied through non-covalent and
171 covalent bonding resulting in improved biocompatibility and regulation of their properties inside
172 the biological systems [26- 28]. To regulate the terminologies used in GO and validate the
173 toxicological consequence for the comparable results, the toxicological index of GO-based
174 formulations approach plays promising role.

175 Further to explore the optimum dosage that maintains a balance between the therapeutic
176 effects and nanotoxicity of GO-based formulations, the proper knowledge of the biocompatibility
177 of GO-based formulations with relevant pre-clinical *in vitro* and *in vivo* models are crucial, so that
178 the results obtained can be easily interpreted for the further clinical applications. Therefore, GO-
179 based nanostructured systems can encourage the development of ideological approach for the
180 expansion of novel technologies which can help to overcome against the detection limits for early
181 diagnosis and provide improved targeting approaches [29].

182 On the other hand, recently GO-based nanomaterials emerged as new alternative to address
183 the issues related with the impaired tissue penetration depths of the light sources, owing to intrinsic
184 optical (absorption in the Near Infrared Regions/NIR or Ultra-Violet/UV regions) and thermal
185 properties of these surface engineered GO which further can be utilized for selective therapies
186 through hyperthermia, recognized as one of the other promising ways to treat some malignant
187 diseases through thermal ablation [30, 31].

188 This critical review aims to update all the possible avenues related to GO or GO based
189 materials pertaining to our scope, that have been or being undertaken by various scientists across
190 the globe. In addition, we have undertaken a special note on GO based dual drug delivery with or
191 without targeting because such multimodal drug delivery based on a single carrier may take the
192 height of drug delivery application to a different level by augmenting their release pattern or
193 improving their bioactivity by synergistic mechanism. In pursuit, molecular modelling and
194 simulation approaches have been perturbed in this review to elicit role of chemistry of both carrier
195 and guests together with their loading mechanisms for achieving such polynomial drug cocktail.
196 Furthermore, application of novel Janus structured materials based on GO is being coined
197 nowadays to facilitate dual or targeted drug delivery, which has been another prime target area of
198 this critical review. Smart bioimaging, which may ease down the therapeutic decision by medical

199 practitioners through apt diagnosis, is in galore with GO based material which have been
200 summarized in this review for future benefits of the scientists and professional who are working
201 in this field. Moreover, not only we presented some perspectives on the challenges or constraints
202 counting the advanced techniques and facile methods to improve the drug loading and dispersing
203 as carriers; but innovative ideas and opportunities in this promising research field are also proposed
204 and their solutions suggested. Finally, the review also highlights the future domains and avenues
205 of implementing GO based materials in relevant biomedical applications. Thus, this review
206 provides an overview of the state of the understanding and challenges in this field and would be
207 highly beneficial not only to experienced scientist but also to graduate and undergraduate students
208 in the areas of biomedical and nanomaterials science and engineering.

209 210 **2. Functionalization of GO**

211 The functionalization of graphene sheet is an effective way which helps them to better disperse
212 and stabilize within a polymer matrix. There are two chief approaches for the functionalization of
213 graphene. (Table 1.)

214 **2.1. Noncovalent Functionalization**

215 Noncovalent modifications require moieties which show extremely high hydrophobicity
216 and usually involve Van der Waals forces, π - π interactions [32], hydrogen bonding [33],
217 electrostatic interactions [34], and coordination bonds [35] with GO. As graphene sheets also exist
218 of Van der Waals forces and π - π stacking which make their surface modification significant with
219 such moieties. In general, such noncovalent functionalization on GO surface can be attained either
220 wrapping of polymers and biomacromolecule, or via absorption of such molecules on the surface
221 of GO [36]. In this regard, Liu and coworkers [37] synthesized a composite material with graphene
222 and PNIPAAm (poly N-isopropylacrylamide) by reversible terminated addition fragmentation
223 chain transfer (RAFT) of PNIPAAm with graphene. They found pyrene functionalized polymers
224 have the property to attached both sides of the graphene sheet to form a sandwich-like structure via
225 π - π stacking which further helpful to stack higher amount of drug than the non functionalized
226 graphene. Zhi *et al.* [38] enhanced aqueous solubility of GO via reducing its excessive oxidative
227 moieties due to electrostatic noncovalent interfaces of GO with L-tryptophan (an amino acid). Their
228 study clearly explained that the increase of π - π interactions between the GO and L-tryptophan

229 molecules increased the dispersibility of GO in aqueous media. Hu *et al.* prepared a graphene
230 derivative by non-covalently functionalizing GO sheets with pluronic F127, an
231 amphiphilic triblock copolymer with excellent biocompatibility [39]. In this study, in order to
232 increase the π -conjugation before coated by F127, GO was reduced to rGO, then poly (propylene
233 oxide) (PPO) segments of F127 were used to bound to the surface of reduced GO through
234 hydrophobic interactions and the poly(ethyleneoxide) (PEO) segments of F127/rGO nanohybrid
235 results excellent solubility and stability in both of aqueous solutions and physiological
236 environment. However, the adsorption of polymers onto GO surface via a noncovalent route is not
237 as strong as the covalent linkage and susceptible to the inconsistent external environment, which
238 makes the DDSs not that much stable with biological systems *in vitro* or *in vivo*. Along with this,
239 non-covalently functionalized GO may load less quantity of aromatic drugs as compared to
240 covalently functionalized GO, because most of the conjugated sites of the GO sheets are partially
241 engaged by coated polymers.

242

243 2.2. Covalent Functionalization

244 Covalent functionalization follows the chemical bonding with surface moieties present on
245 the surface of GO with the help of strong acid-based treatment. The harsh acidic conditions might
246 also be introduced structural defects, resulting advancement in physicochemical properties of GO
247 [40]. DDSs based on covalently functionalized GO with suitable surface functional groups are
248 emerged as potential tools and widely explored for systemic targeting platforms. Xu *et al.* [41]
249 used a covalent conjunction strategy for PCT loaded on GO derivatives, whereby PCT was
250 connected with biocompatible six-armed PEG by covalent functionalization onto the GO surface.
251 The modified GO-PEG-PCT system had a high loading ratio of along with superior stability under
252 physiological conditions. The covalent functionalization for GO sheets can also be realized by
253 introducing small molecules onto the GO sheets. For example, Zhang *et al.* functionalized GO
254 sheets with sulfonic acid groups (SO_3H), followed by a covalent grafting of folic acid (FA)
255 biomolecules to the GO sheets [42]. The FA-conjugated GO i.e. FA-GO were able to well
256 dispersed and maintained stability in a physiological solution for a long time. The combination of
257 GO and FA provides a novel molecular recognition strategy to specifically carry anticancer drugs
258 into folate-receptor-positive malignant cells, which covered the way for the development of smart
259 DDSs [43]. Recently, GO was covalently functionalized with D-mannose using mannosylated

260 ethylenediamine. The mannosylation of GO drastically reduced its toxicity and improved its
261 biocompatibility in red blood cells [44]. Thus, covalent functionalization of GO contributes to
262 future biomedical applications with active biomolecules. With the help of stimuli specific polymer
263 functionalization the effective drug release rate on the tumor site can be released rapidly when the
264 modified DDSs reach at the target cells and resulted to a more effective therapy. For example,
265 Wen *et al.* [45] conjugated PEG with GO via cleavable disulfide bond (GO-SS-PEG), which
266 exhibited great biocompatibility, considerable degradability and the targeting ability of delivering
267 drugs to specific tumor cells with high intracellular glutathione (GSH) concentrations via redox
268 reaction. Similarly, Kim and collaborators developed a photothermally triggered DDSs by
269 functionalizing GO covalently with branched polyethylenimine (bPEI) and PEG successively [46].
270 The GO-bPEI-PEG nanocomposite exhibited high water stability along with high DOX loading
271 efficiency as compared with the GO alone. Chen *et al.*, developed PEGylated GO to build a highly
272 efficient drug loading and photothermally triggered DDSs [47]. The GO-PEG system shows better
273 water stability and high NIR absorbance. Conjugation of CS on GO is another example of covalent
274 functionalization which results in better biocompatibility as well as drug and gene delivery. CS is
275 used as a linker to combine FA with functional GO and also provide encapsulation, better stability,
276 biocompatibility, and controlled release of active molecules [40]. Various reports on the
277 encapsulation of DOX onto GO via charged folate conjugated CS explain the superiority of the
278 system over GO, resulting in pH responsive drug release [41]. Further, Yan *et al.* used
279 polyethylenimine (PEI) to functionalize GO covalently for an efficient nanocarrier which shows
280 high stability in both water and physiological solutions, and further combined with biomolecules
281 and markers to enhance their drug loading and delivery capacity [48]. Besides single
282 functionalization, the dual covalent functionalization of GO exhibits the attachment of distinct
283 molecules through different mechanisms. Recently, Shi and his group [49] established a scheme
284 for chemoselective dual functionalization of GO using benzoquinone. The two functional groups
285 were covalently functionalized onto GO through an epoxide ring opening reaction and the second
286 moiety with amine group was covalently attached through a Michael addition. Thus, the
287 morphology of the GO sheets was preserved and the functionalization did not cause any further
288 reduction of GO. Hence temperature and pH responsive functional groups efficiently
289 functionalized on surface of GO followed by chemical reactions and extend the application of GO
290 via preserving its structure and properties. This strategy is particularly suitable for the conjugation

291 of biomolecules and widely subjugated for modifying GO with proteins, drugs, aptamers, or
292 peptides to obtain multifunctional GO for applications in therapy, biosensing, and bioimaging [50,
293 51].

294

295 **3. Advantages and disadvantages of GO**

296 **3.1. Advantages of GO**

297 GO play a significant role in sorting out the drawbacks occurs in biomedical field. Drug release
298 can also be tuned or stimulated by the intracellular environment. In fact, drug release in a cell is
299 due to the change of the environmental condition (i.e. pH, temperature etc.) between the
300 extracellular matrix and cytoplasm. In this section, we will discuss how the characteristic
301 properties of GO provide a room for significant and effective DDSs.

302

303 **3.1.1. pH Responsive GO for Controlled Release**

304 As compared to the healthy cells, infected cells are usually sensitive and possess unique
305 physicochemical properties, microstructural features and unique micro environments which can
306 be targeted accordingly by GO. Since GO has both sp^2 and sp^3 domains within it, not only it
307 provides the π - π interaction for therapeutic molecules at surface, but also it helps to develop
308 targeted DDSs exploiting strategic ligands attached onto it [52–54]. Moreover, GO surface
309 chemistry is unique due to presence of both –OH and –COOH groups onto it. The surface is highly
310 anionic due to negative charges present on the surface arising from ionized $-O^-$ and $-COO^-$
311 functional groups. This undergoes intensive protonation in low pH where degree of protonation
312 depends on lowering of pH. The protonation of surface moieties leaves it to be non-ionic thus
313 hydrophobic. Thus, at low pH, inside aqueous solution, GO form aggregates with GO-water-GO
314 sandwich structure. On the contrary, at higher pH, the anionic surface groups remain charged,
315 thus rendering it to be hydrophilic where degree of hydrophilicity depends on elevation of medium
316 pH. This ultimately leads in dissolution of GO, altering its surface dynamics within itself as well
317 as with water. This phase transition of GO with variation of medium pH results in different
318 wettability, water penetration into GO sheets, hydrolytic cleavage of GO-guest chemical bonds
319 subsequently releasing the guest (e.g. therapeutic molecules) from GO sheets. In addition, the GO
320 response has been also dependent on layer by layer (LBL) structure of GO nanosheets which

321 regulate the entry of ions (dependent on pH) inside the same, its swelling, interfacial dynamics as
322 well as release of molecules from inside the GO nanosheet [52-54].

323 It has been reported earlier that GO has high drug loading efficiency and the release
324 behavior of the loaded drug is adjusted by varying the pH of the DDSs [55].

325 As an environmental pollutant, antibiotics increasingly affect the health issues in past few
326 years. Antibiotics overdose results in antibiotic resistant genes, which significantly cause health
327 hazards. In this context, Bytesnikova *et al.* in 2018 applied GO as a remediation of the environment
328 as it has characteristic properties to binding nucleic acids and catalyzing their decomposition.
329 They discussed the factors influencing the binding of nucleic acids and the response of antibiotic
330 resistant genes to GO, together with the presence of salts in the water pH. Finally they conclude
331 that by modifying the water conditions with the adjustment of pH and temperature one can increase
332 the efficiency of GO [56].

333 Considering the excellent dispersion of GO in water, GO was initially presumed to be
334 hydrophilic due to the presence of the hydroxyl and epoxy groups present in the GO sheet basal
335 plane [57]. Later on experiments involving pH changes and salt addition suggest that it was the
336 peripheral carboxyl groups which are actually accountable in determining the solution behavior of
337 GO [58]. Shih and his group explained the pH-dependent behavior of GO in aqueous solutions.
338 They investigated the mechanisms behind the aggregation and the surface activity of GO at
339 different pH values and found that at acidic pH, the carboxyl groups are easily protonated resulting
340 the GO sheets less hydrophilic and tends to aggregates. However, at basic medium i.e. high pH,
341 the carboxyl groups are deprotonated and thus GO shows hydrophilic character and dissolved like
342 a salt in aqueous medium [59].

343 In fact the colloidal stability of GO solutions is due to the electrostatic repulsions between
344 ionized carboxyl groups. Kim *et al.* further suggested that GO behaves like a surfactant, as it has
345 ability to adsorb at a water air interface, by lowering the surface tension of water [60]. In addition,
346 GO has been used to stabilize Pickering emulsions of organic solvents in water [61]. The basal
347 plane of GO is much more hydrophobic than the carboxyl-decorated edges, and the large
348 differences in both the hydrophilicity and structural dimensions make GO behave like an
349 amphiphile. Thus GO can perform as hydrophobic as well as hydrophilic agent according to the
350 requirement of our goal.

351 In order to that, Bai and co-workers demonstrated the pH induced sol gel transition property
352 of GO– PVA hydrogel to conclude that the hydrogel thus formed is used to selectively deliver the
353 drug to the intestine (pH 6.8-7.4) without releasing it in acidic gastric juice (pH 1-2) which
354 generally cause the stomach discomfort, therefore GO can be utilized for loading and release of
355 drug in physiological medium selectively[62]. Through proper tuning of this unique property, GO
356 can be formulated into a smart DDSs having controlled release property in various specific
357 microenvironments depending on their characteristic pH that differentiate cancer cell from the
358 normal cell e.g., Yang *et al.* reported the release behavior of water soluble anticancer drug
359 Doxorubicin and found that at acidic medium (pH-2) the release of the drug was more than 70%
360 after the time period of 30 hours which was 4 times more than the medium of pH 7 and 10, hence
361 this drug with GO give a higher drug release at acidic pH compared other pH [63].

362 The zeta potentials of GO suspensions can also render with pH as it is highly sensitive to it.
363 Chen *et al.* prepared a multilayer film of GO and branched PEI on a terephthalate substrate and
364 found a stable suspension of GO at all pH mediums [64].

365 Thus the reported pH-dependent behavior of GO originates from the degree of
366 deprotonation of the carboxyl groups present at the edges of GO sheets. The electrostatic
367 repulsions between the ionized carboxyl groups of GO are the major driving force for pH
368 dependence.

369 Also, it is found that a novel magnetic GO, grafted with brush polymer *via* surface-initiated
370 (SI) RAFT polymerization, can be applied as a nanocarrier for magnetically induced and pH-
371 triggered delivery of doxorubicin anticancer drug. In this SI-RAFT technique, first a RAFT reagent
372 called 2-(Dodecylthiocarbonothioylthio)-2-methylpropionic acid (DDMAT) was incorporated
373 onto magnetically functionalized GO nanosheet and later polymerized with glycidyl methacrylate
374 (GMA) using DDMAT. Subsequently the epoxy ring of the latter was opened with hydrazine
375 (N_2H_4) which helped to load anticancer drug DOX by SI-RAFT technique. The imine interaction
376 and π - π stacking was the major driving force for DOX coupling onto the polymer. The imine bond
377 ($-N=C_1-$) is cleavable under weakly acidic condition (\sim pH 6.0) inside body such as cancer tumor
378 microenvironment and can release DOX which is linked with Polymerized GMA via the imine
379 chain. This technique has been applied successfully to render pH responsive release of DOX from
380 such GO nanocomposite. The resulting drug-nano composite has been reported with better
381 bioavailability, lower toxicity and improved therapeutic activity when administered *in vivo* [65].

382 Recently, scientists have focused to engineered multifunctional nanomaterials with controlled
383 release of drug by sustaining a constant drug dosage in a regulated rate for a specific period of time.
384 The most intriguing properties of GO and its derivatives are their remarkable solubility and
385 stability in physiological media and biocompatibility which make them promising biomaterial
386 substrate for controlled drug delivery.

387 In this context, an efficient approach was developed by Zhao *et al.* by integrating the GO
388 with biocompatible polymer PEG and folic acid (FA) to form a nanovehicle GO-PEG-FA as an
389 efficient and targeted DDS. The release kinetics of DOX from the carrier in different medium of
390 pH was also investigated. Cumulative release of DOX at pH 7.4, 6.5 and 5 was 6.43%, 8.01% and
391 15.74%, respectively, which reveal that the drug has the favorable release in the acidic medium
392 due to the higher solubility of DOX in acidic medium, hence it can be concluded that the DOX
393 release should be regulated simultaneously by the solubility of the given drug and the designed
394 GO based carrier supports in pH dependent controlled release characteristics [85].

395 Further in order to describe novel composite materials for the controlled release Wang and
396 coworkers examined the release behavior of 5-fluorouracil (5-FU) with pH sensitive Konjac
397 glucomannan/sodium alginate (KGM/SA) and KGM/SA/GO hydrogels were prepared, where GO
398 is drug-binding agent for anticancer drug loading and release. The release amount of 5-fluorouracil
399 (5-FU) incorporated into KGM/SA/GO hydrogels was about 38.02% at pH 1.2 and 84.19% at pH
400 6.8 after 6 h and 12 h, respectively. Therefore, the release rate of 5-FU from the KGM/SA/GO
401 hydrogels could be efficiently controlled with GO. The results showed that GO has a great potential
402 for drug-binding as well as controlling the release rate of drugs from an efficient nanocarrier for
403 the site-specific drug delivery [66].

404

405 3.1.2. Temperature Sensitive GO

406 Temperature is a typical example of triggers at the diseased site that could be exploited
407 with the nanocarriers [66]. In modern drug delivery approach, the status of thermosensitive
408 nanocarriers are not only applied as traditional DDSs but also for the enhanced stability, solubility
409 and reduces immunogenicity, toxicity of the targeted drugs. GO as thermosensitive nanocarriers
410 attract enormous attention for controlled and targeted drug delivery. On the basis of this advantage,
411 Bardajee and his team synthesized a temperature sensitive nanohydrogel of NIPAAm with GO and

412 the resulting nanocomposite showed potential drug loading capacity and relative drug release
413 behaviour with increase in temperature [67].

414 Another GO based hydrogel(GO-PVA/PNIPAAm hydrogel) in which GO is the
415 crosslinker between the two biocompatible polymers i.e. PVA and PNIPAAm-GO was prepared and
416 temperature responsive behaviour of hydrogel was examined. The results demonstrated that the
417 mechanical strength of the hydrogel has been improved with increasing composition of
418 temperature sensitive GO. Furthermore, the PVA/PNIPAAm hydrogel exhibited a phase volume
419 transition temperature at around 34.9 °C, which was reduced by 1 °C when conjugated with GO.
420 This specific advantage represented that GO based hydrogel could be a potential choice in drug
421 delivery field [68].

422 Wang and coworkers demonstrated the comparative study about pure polymers
423 nanoparticles (PNPs) and their thermoresponsive hybrid with GO nanosheets for drug delivery
424 application. The loading efficiency of drug molecules (Adriamycin) with GO-PNP (~87%) has
425 been close to that with GO (~91%), but significantly higher than that with PNPs (~46%). The
426 release efficiency of GO-PNP hybrids with the highest surface coverage of PNPs (~85 PNPs /
427 mm²) has been about 22%, which was very comparable to that of PNPs (~25%) and significantly
428 higher than that of GO (~11%). The thermo-sensitive GO-PNP hybrid consisted of considerable
429 better drug loading and release performance than both PNPs and GO and thus it can be applied as
430 a novel nanocarrier for temperature-controllable drug release. The unique superiority of this drug
431 carrier system also lies in the fact that the drug loading and release are controllable by adjusting
432 temperature and PNP covering on GO surface [69].

433

434 3.1.3. Near Infrared (NIR) or Laser sensitive photodynamic therapy (PDT)

435 Compared with other light irradiation techniques, near infrared NIR (700-1000 nm) light
436 is considered as the most advantageous region in biological applications owing to its high ability
437 to penetrate tissues [70-71].

438 Sahu *et al.* non-covalently functionalized nano GO sheet (NGO) with block copolymer
439 pluronic and further conjugated the system with positively charged photosensitizer organic
440 hydrophilic dye i.e. methylene blue (MeB), through electrostatic attraction for mutual
441 photodynamic-photothermal therapy (PDT-PTT). Polymer functionalized NGO
442 exhibited relatively higher stability than non functionalized NGO in physiological medium. Also

443 the complex NGO displayed dual character of being a photothermal material as well as an
444 efficient photosensitizer vehicle. The release behavior of the photosensitizer from NGO surface has
445 been pH-responsive and acidic environment enhanced the release behavior of organic dye
446 considerably. This nanohybrid complex system explains the enhanced uptake of the targeted
447 molecules by cancer cells than non infected cells and in the absence of light, it displayed no major
448 toxicity towards the cells. On the other hand, when irradiated with selective NIR laser lights, it
449 induced significant cell death. Intravenous injection of the complex into tumor bearing mice
450 showed high tumor accumulation, and when the tumors were exposed to NIR lights, it caused total
451 ablation of tumor tissue through the combined action of photodynamic and photothermal effects.
452 This work shows the potential of NGO for synergistic complexion of both phototherapy of
453 malignant area [72].

454 In 2016, Kulluru *et al.* first investigated that NGO exhibits single-photon excitation
455 wavelength dependent photoluminescence in the visible and short NIR region, suitable for *in vivo*
456 multi-color fluorescence imaging. They demonstrated both *in vitro* and *in vivo* experiments to
457 explain that NGO is highly sensitive towards the singlet oxygen formation and hence it can be
458 applied for combined nanomaterial-mediated photodynamic therapeutic (NmPDT) and
459 photothermal therapy (NmPTT). Both NmPDT and NmPTT effectively result the destruction of
460 B16F0 melanoma tumors in mice using ultra-low intense NIR light. The average half-life time of
461 the mice examined by the GO-PEG-folate-mediated NmPDT has been beyond 30 days, which is
462 approximately 2 times longer than that of the mice treated with doxorubicin (17 days). Overall,
463 the experiment highlighted effective application of NIR using GO-PEG-folate nanocomposite as a
464 theranostic nanomedicine to exert simultaneously *in vivo* fluorescent imaging as well as combined
465 NmPDT and NmPTT effects for clinical cancer treatments [73].

466 PDT is considered as a promising therapy for cancer, because it is a non-invasive therapy
467 which has many significant advantages such as remote controllability, spatiotemporal selectivity,
468 and repeatability without cumulative toxicity [74]. Together PDT and GO represent selective
469 therapy via hyperthermic process toward cancer cells [75]. In recent years, GO-based
470 nanomaterials as photothermal sensitizers have attracted attention of researchers due to their wide
471 absorption spectrum of wavelengths from UV to NIR and the ability of converting absorbed light
472 into localized heat by surface plasmon resonance [76]. Furthermore, GO with better
473 biocompatibility and lower cost is beneficial to this application [77].

474 PDT mainly involves three components: PS, light source and oxygen. When exposed to
475 the light of specific wavelength, PS is transformed from a ground state (singlet state) into an
476 excited singlet state, then crosses to an excited triplet state. However, most of these PSs cannot
477 satisfy all the characteristics of the ideal PSs due to their low solubility, poor tumor selectivity,
478 restricted absorption wavelength, long treatment period and fast photo bleaching [78-79]. In order
479 to overcome these issues, GO has been developed as an ideal carrier of PSs mostly benefiting from
480 its large specific surface area and various surface functional groups. These characteristics enable
481 it to be functionalized with hydrophilic macromolecules and targeting ligands or active agents to
482 improve aqueous solubility and control drugs delivery toward specific types of cancer cells [80].

483 It is a promising approach to enhance PDT efficacy through sensitizing strategies. Ding *et*
484 *al.* loaded photosensitizer hypocrellin A (HA) and sensitizer TiO₂ onto GO to increase the ability
485 of producing ROS through mutual sensitization mechanism. *In vitro* cell experiments showed that
486 HA-TiO₂-GO exhibited significantly lower cell survival percent (about 30%) than HA-TiO₂ (about
487 50%) and TiO₂-GO (about 55%), suggesting the potential of HA-TiO₂-GO for improving the
488 efficacy of PDT [81]. In addition, in order to enhance the target selectivity of PSs to provide
489 accurate PDT, PSs loaded GO can also be used for activate PDT. For example, Cho *et al.*
490 conjugated photosensitizer chlorine6 (Ce6) on nano-sized GO via a redox-responsive cleavable
491 disulfide bond (GO-SS-Ce6) which was used as an active therapeutic agent for PDT. According
492 to the analysis of the UV/Vis and fluorescence spectroscopy, the fluorescence of Ce6 conjugated
493 onto GO was strongly quenched without reducing agent such as GSH though exposed to the light,
494 which avoided off-target effect caused by non-specific activation and poor target selectivity of PS.
495 They observed that cells treated with GO-SS-Ce6 exhibited strong fluorescence while very slight
496 fluorescence appeared in cells treated with free Ce6, which showed that Ce6 conjugated GO had
497 a better uptake ability than free Ce6 in cancer cells [82]. Particularly, in cancer treatment, GO-
498 based multifunctional nanomaterials have been discovered to integrate imaging and therapeutic in
499 one single platform to realize good therapeutic efficiency with minimized side effects [50, 51].

500

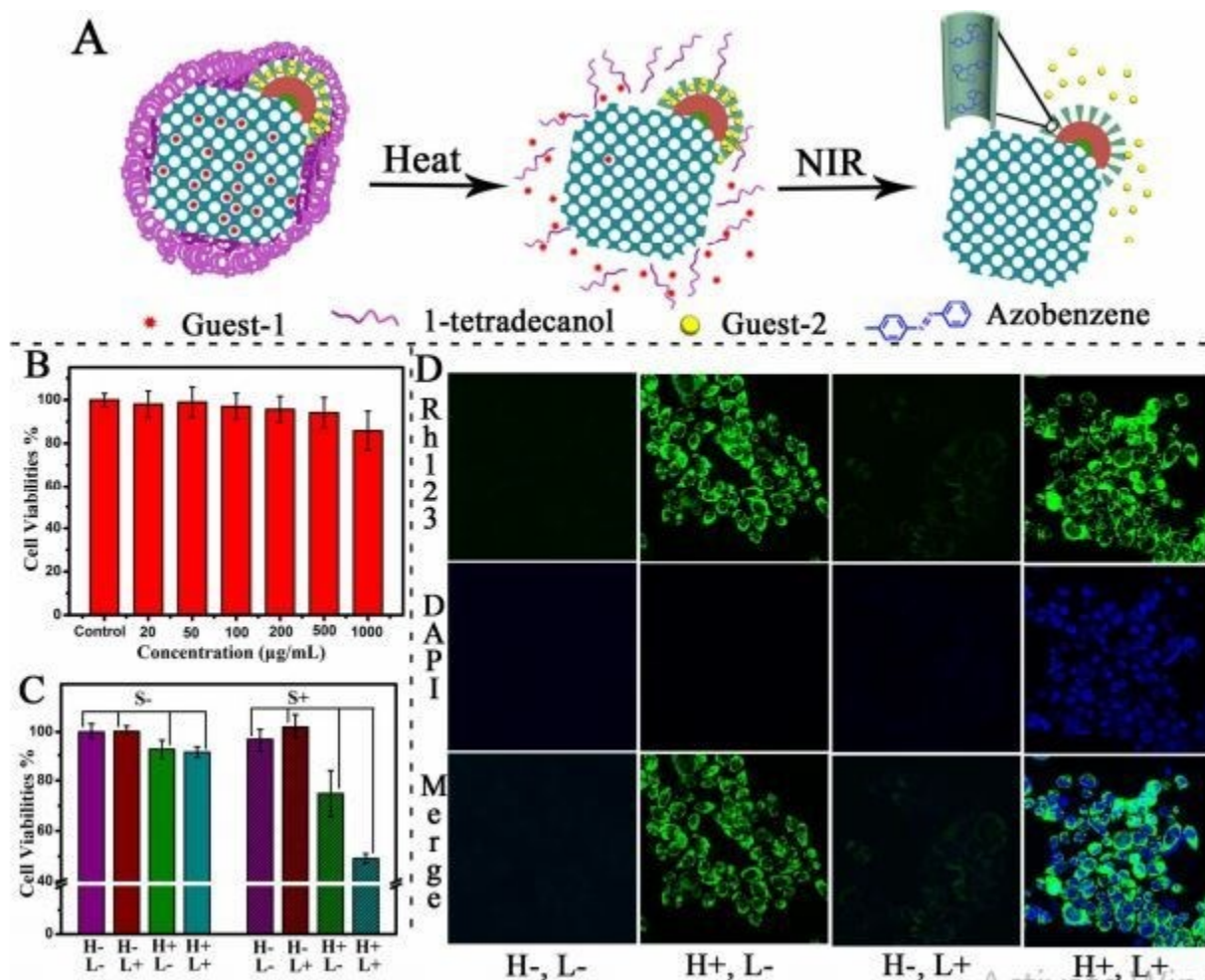
501 **3.1.4. Janus structured GOs for multivariant (differentially polar dual drugs) Release**

502 Janus structured nano-material is asymmetrically functionalized nano-material where two
503 surfaces of the material are functionalized with two polymers of differential polarity. It is named
504 on Greek God Janus with two faces. One surface of the polymer is grafted with hydrophobic

505 polymeric chain whereas the second surface is polymerized with hydrophilic one. In modern drug
506 delivery approaches, this is advantageous when cocktailed drug, loaded onto the GOs with
507 differential polarity alterations. This is particularly exploitable in case of GO because due to its
508 unique structure, GO provides the scope to convert it into anisotropic Janus structure. Due to the
509 polar functional groups such as –OH and –COOH groups, polar polymeric tails can be impregnated
510 on one surface of it. *Vis a vis*, GO has hydrophobic sp^2 and sp^3 carbon atoms too in its structures.
511 Exploiting this, on the other surface of GO, hydrophobic polymer can be attached. This
512 engineering explores the opportunity for attachment of differentially polar drug on opposite
513 surfaces of GO. For example, Khoee *et al.* in 2018 reported that GO has been converted into Janus
514 nanostructure by cross linking one surface with poly caproyl lactone (PCL) as hydrophilic polymer
515 whereas other surface being cross linked with N-isopropyl acrylamide-coacrylamide co-allylamine
516 terpolymer as hydrophobic one [83]. The author could subsequently load quercetin (QCR,
517 hydrophobic) and 5-Fluorouracil (5-FU, hydrophilic) drug duo onto this Janus structured GO and
518 successfully delivered this against cancer. The second advantage of this nanostructure was that the
519 polymers being temperature sensitive, could efficiently deliver drugs based on the temperature of
520 tumor microenvironment.

521 The Janus based GO nanomaterials are reported to produce stimuli responsive properties
522 such as pH, Near Infrared Radiation, light or combination of them. For example, Li *et al.* designed
523 Janus chorded mesoporous silica nanoparticles (UCNP-SiO₂-mSiO₂-PMO) containing hydrophilic
524 domain of UCNP-SiO₂-mSiO₂ in contrast of hydrophobic domain of PMO (Figure 1). UCNP is
525 upconversion nanoparticle (UCNP, upconversion nanoparticle = NaGdF₄:Yb,Tm@NaGdF₄,
526 mSiO₂ = mesoporous silica shell, PMO = periodic mesoporous organosilica). UCNP has been
527 reported for its towering ability to convert near IR to high energy emission such as heat energy
528 thus offering promising opportunity for the scientists to catalyze thermoresponsive release of
529 molecules bound to this. Now, SiO₂ and mSiO₂ provides the Janus structure cage dual
530 compartments to its hydrophilic surface thus aid in accommodation of multiple hydrophilic
531 molecules in a single asymmetric Janus surface. Furthermore, when this kind of Janus nucleus is
532 co-bonded with GO, it provides GO enough storage space of molecules of opposite polarity. This
533 also endows GO efficiently to catapult near IR or heat mediated release of its guest
534 molecules. Exploiting this, efficient co-loading of hydrophobic paclitaxel (PCT) and hydrophilic
535 DOX have been furnished on UCNP-SiO₂-mSiO₂-PMO and subsequently targeted against

536 malignant cells. Furthermore, the authors engineered janus nanostructured surface with
537 thermoresponsive 1-tetradecanol and photosensitive azobenzene in order to convert normal drug
538 release to smart release with the aforementioned stimuli. Interestingly, the drugs from the
539 combination revealed more tumoricidal efficiency (~50%) compared to that of their individual
540 formulation (~25%) [84].



541
542 **Figure 1.** Schematic presentation for dual-control drug release systems by using the dual-
543 dual-compartment mesoporous Janus nanocomposites. (B) MTT cell viability assay of Janus
544 UCNP@SiO₂@mSiO₂&PMO (C) Cell viabilities of paclitaxel and DOX co-loaded
545 UCNP@SiO₂@mSiO₂-Azo&PMO-PCM Janus nanocomposites under the heat (H) and NIR light
546 (L) treatment (S means sample). (D) Confocal laser scanning microscopy (CLSM) observations of
547 the HeLa cells after incubation with the Rh123 (green) and DAPI (blue) co-loaded mesoporous
548 Janus nanocomposites with or without heat (H) and NIR light (L) stimuli. Reprinted from [84],
549 Copyright 2014, with permission from American Chemical Society.

550

551

552 3.2. Disadvantages of GO

553 Although nanostructured GO-based DDSs due to various therapeutics potential have
554 achieved significant advances to improve the therapeutic efficacy and minimize the adverse side
555 effects of drugs, at the same time the clinical use of drug delivery systems often requires the
556 association of therapeutics and diagnostics to realize personalized patient treatments.

557 3.2.1. Aggregation in biological media

558 As an excellent candidate for solution processing, the colloidal stability of GO plays
559 decisiverole for controlling the excellence and performance of the proposed DDSs. Increasing the
560 ionic strength or decreasing the pH of aqueous dispersions of GO results in the coagulation of GO
561 particles and thus affect the colloidal stability [59, 87-88].

562 Colloidal stability of GO has been extensively studied in aqueous and organic media and
563 it is accomplished that both magnitude and scaling laws for the van der Waals forces are affected
564 considerably by the 2D lattice structure of GO. Also GO exfoliates and shows stable dispersions in
565 polar organic solvents. However, introducing a nonpolar solvents cause colloidal instability at a
566 critical volume fraction. Analyzing the aggregation of GO in mixtures of different nonpolar
567 solvents and N-methyl-2-pyrrolidone, Gudarzi *et al.* proposed that the solvents with dielectric
568 constants less than 24 may not be able to favor stable colloids of GO resulting in aggregation of
569 GO [89]. However, dispersions of GO in polar solvents establish surprisingly high stability at high
570 concentration of acids and salts. An exciting fact of this study was that aggregation of GO is highly
571 sensitive to pH as it shows abnormal behavior in the presence of acid and base. This evidence can
572 have advance impact on GO storage as GO, self-generates proton during interaction with water
573 [90]. Therefore, slightly basic dispersion of GO can become slightly acidic over time and becomes
574 much more sensitive to ionic impurities.

575 Meng and his group formulated a multi-step ultracentrifugation-based technique to
576 isolate the conical arrangement of GO sheets. GO sheets act as large aggregated particles than the
577 expected individual sheet which have a tendency to generate irreversible coagulation when
578 excessively high polar salts such as NaCl and MgCl₂ are introduced. On the other side, by
579 introducing amphoteric salts such as AlCl₃, the GO dispersion remains stable which attributed to
580 the inversion of surface charges of GO sheets. Although there is disadvantage of GO regarding the
581 colloidal stability in different medium due to its aggregation phenomenon, but using the different
582 inorganic salts according to the demand we can overcome by this threat [91].

583 3.2.2. Irregular size

584 GBNs are nothomogeneous, and they vary in number, lateral dimension, surface chemistry,
585 defect density or quality of the individual graphene sheets and composition or purity and the size
586 of the graphene sheet produced in bulk amount cannot be controlled [92]. To overcome these
587 obstacles, development of a facile method of synthesizing GO is required to potentially control the
588 size and quality for the targeting drug delivery approach. McAllister et al. explained that the lateral
589 size of GO obtained by complete oxidation of graphite particles was independent of the size of the
590 graphite particle, demonstrating that the controlling factor is not the size of graphite particles.
591 However, Zhao *et al.* showed that the controlled oxidation of graphite particles from Hummer's
592 method had a significant effect on the size of GO. High surface area GO sheets were obtained by
593 sonicating GO with controlled oxidation. Further, Li *et al.* recognized that the formation of epoxy
594 groups on graphene sheets could weaken the interaction between the sheets. They explained that
595 the size of the sheets might be reduced with increased oxygen content therein due to the higher
596 density of carbon-oxygen bonds, allowing cracks to form over hydroxy and epoxy coated sites on
597 the graphene sheet during oxidation. Hence previous study demonstrated that the size of the GO
598 could be controlled not only by a balance of edge-to center penetration versus crack propagation
599 rates but also by the degree of graphite oxidation.

600 3.2.3. Toxicity study of GO

601 GO is a promising candidate for targeted DDSs and its *in vivo* toxicity, cytotoxicity and
602 uniform genotoxicity attract researchers to considered GO in either biological applications. The
603 toxicity analysis of GO has not developed anynonconflict evidence in current research interest
604 [93]. However, many studies show that GO could cause cell apoptosis, lung granuloma formation,
605 pulmonary edema and platelets aggregation [94]. Furthermore, hemocompatibility is also an
606 important toxicity assessment of GO [95]. The hemolytic properties of GO are caused by the strong
607 electrostatic interaction between the GO surface and the lipid bi-layer of the erythrocyte membrane
608 [96]. Many detection methods have suggested that the material properties of GO such as reactive
609 oxygen species, high surface area and charge, unique particle size and functional groups on its
610 surface and edges can affect its toxicity in organism [97]. In addition, *in vivo* and *invitro*
611 experiments have shown that GO displayed observable dose-dependent toxicity [98]. Surface
612 modification is a suitable and effective method to reduce toxicity and improve biocompatibility of
613 GO by eliminating the fabrication of reactive oxygen species and tuning the strong hydrophobic

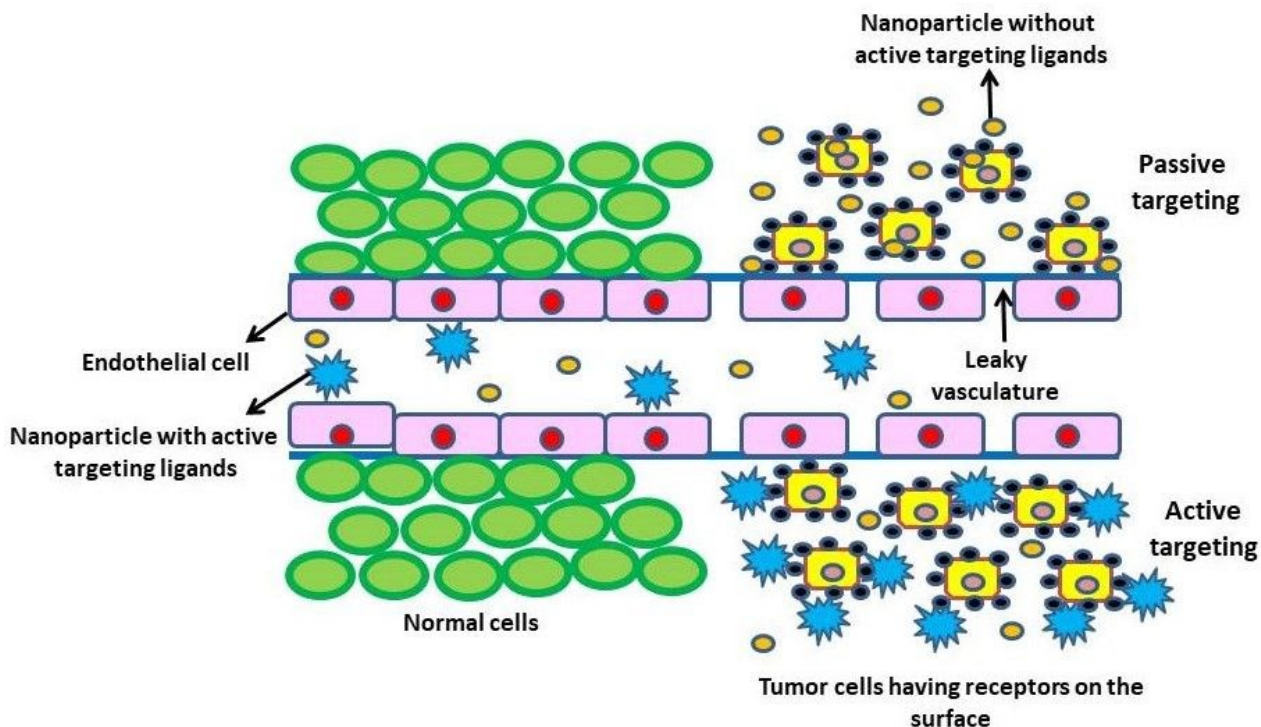
614 interaction between GO and organelles [99], which has been confirmed by integrating GO with
615 various biocompatible molecules such as polymer macromolecules, serum protein, antibodies,
616 antigens, genes and others to reduce toxicity [100]. Zhi *et al.* [101] found that tumor necrosis
617 factor α (TNF- α), interleukin-1 (IL-1) and interleukin-6 (IL-6) increased significantly in the
618 presence of GO, leading to strong immunogenicity. While after functionalization of GO with
619 polyvinyl pyrrolidone (PVP), the apoptotic process of T-lymphocytes got delayed and improved
620 the anti-phagocytosis aptitude of GO against macrophages. Thus, immunological evaluation has
621 been a key factor for GO *in vivo* compatibility assessment. Furthermore, biocompatible polymer
622 such as PVP, PEG or PVA (Poly Vinyl Alcohol) or macromolecule functionalized GO (as
623 discussed in section 2) is expected to exhibit improved immunological compatibility and reduced
624 toxicity than non-functionalized GO. A synopsis of advantages and disadvantages of GO has been
625 summarized in Table 1.

626

627

628 **4. Drug Targeting Strategies of GO**

629 This section highlights both the physicochemical characteristics of the GO based nanocarriers
630 and the physiological features and microenvironment of site of action to outline what strategies
631 should be undertaken to deliver the molecules of interest specifically to certain targeted site. This
632 segment discusses about the respective properties of carrier and targeted site, describing the
633 convenient choice between passive and active targeting mechanisms. Herein, we will discuss about
634 the principles for both processes and their correlation with the tumor microenvironment. The
635 previous literature illustrates how the nanocarriers and the enhanced permeation and retention
636 effect (EPR) influence the passive targeting. Whereas the active targeting depends on the ligand-
637 receptor binding, which improves selective accumulation to targeted sites. Here we highlight the
638 passive and active targeting processes to enable such nanoparticles to be targeted to desired
639 binding sites efficiently (Figure 2).



640

641 **Figure 2.** Passive and Active targeting of nanoparticles towards target cells.

642

643 **4.1. Passive targeting**

644 Passive targeting takes advantage of the unique pathophysiological characteristics of
 645 tumor vessels, enabling nanodrugs to accumulate in tumor tissues. Passive targeting mechanisms
 646 are attractive to target drug delivery because this diffusion does not need any extensive
 647 functionalization, and these have been exploited using graphene. Passive targeting involves the
 648 transportation of nanocarriers through permeable tumor vessel into the tumor cells by means of
 649 passive diffusion. In passive diffusion, movement of molecules takes place within the fluids
 650 through selective accumulation of drug and nanocarriers follows by the EPR effect [102] which is
 651 effectively confirmed by many research groups [103-105].

652 By the use of additional physical methods the EPR effect can be made more specific in its
 653 work process. For example, graphene or GO has high infra-red absorption capacity which allow
 654 photothermal effects for localized cell killing through hyperthermia, where the infrared light is
 655 applied only to the area being targeted [106,107].

656 Thus generalized heating through photothermal radiation also increase cell permeability
 657 and transfection efficiency of the graphene complexes in the area where the infrared light is applied

658 [108-110]. In the same way, prepared graphene-based magnetic nanoparticle composites helps
659 graphene particles to target specifically using generalized magnetic fields [111].

660 Feng *et al.* [112] used the pH difference in the tumormicroenvironment for modification in
661 their GBNs for efficient cellular uptake. The flakes were loaded with drug DOX and then it is
662 conjugated with PEG and a pH responsive polymer. When neutral or basic environments were
663 introduced the flakes become negatively charged and in an acidic environment their charge
664 becomes positive which creating interaction with the negative cell membrane and subsequent
665 endocytosis. The fluorescence imaging and flow cytometry is also used to increase in the cell death
666 followed by DOX-loading, results in significant improvement in cell uptake and drug delivery in
667 acidic conditions as compared to neutral conditions. Finally, photothermal heating was used to
668 further enhance cancer cell killing, which shows additional improvements on rates of cell death.

669

670 **4.2. Active Targeting**

671 It is noteworthy that the active targeting is essential for the delivery of drugs, genes and
672 theranostics to the location of interest avoiding the normal tissues and thereby enhances the
673 therapeutic efficiency and limits the side effects. Active targeting is able to significantly increase
674 the quantity of drug delivered to the target cell compared to free drug or passively targeted
675 nanosystems. After accumulation in the tumour region, the drug efficiency can be even increased
676 by the so-called active targeting. This is achieved through the decoration of the nanocarrier
677 surfaces with ligands binding to receptors overexpressed onto the malignant cells. This strategy
678 will improve the affinities of the nanocarriers for the surface of cancer cell and thus enhance the
679 drug penetration. In addition to the EPR effect, active targeting represents another strategy for
680 enhanced tumor uptake, which is generally achieved by conjugating or grafting a nanosystem with
681 affinity ligands to enable the specific recognition of tumor cells [113]. The active targeting directs
682 the nanoparticles towards the tumor sites through ligand-receptor interactions where antigens are
683 over expressed on the tumor surfaces, thus facilitating specific drug release inside the tumor. The
684 targeting ligands conjugated with graphene can be antibodies [114,115], peptides [116], aptamers
685 [117] or small molecules [118]. In a study Liu *et al.* took Transferrin (Tf) an iron-transporting
686 serum glycoprotein, as a ligand to develop Tf-conjugated PEGylated GO for loading and glioma
687 targeting delivery of anticancer drug DOX (Tf-PEG-GO-DOX). Tf-GO shows a high DOX loading
688 capacity. Tf-PEG-GO-DOX displayed greater intracellular delivery efficiency and stronger

689 cytotoxicity against C6 glioma cells as compared (PEG-GO-DOX) and free DOX. This
690 comparative experiment reveals that Tf was essential to glioma targeting *in vitro*. The HPLC assay
691 for DOX concentration in tumor tissue of the brain demonstrated that Tf-PEG-GO-DOX could
692 deliver more drug at tumor site *in vivo*. Hence Tf-PEG-GO-DOX exhibited significantly improved
693 therapeutic efficacy for glioma for both *in vitro* and *in vivo* [119]. Pursuing a similar study a double
694 targeted GO based delivery system has been formulated coupling both FA and Tf onto a Pluronic
695 F68 modified GO where DOX was loaded successfully (TGFP-DOX) and has been target
696 successfully against SMMC-7721 cancer cell line with improved therapeutic efficacy and lowered
697 toxicity [120]. In another study, hyaluronic acid, with a high affinity for CD44 (hyaluronan)
698 receptor, was conjugated onto GQDs for a targeted system using catechol as a linker. The *in vitro*
699 and *in vivo* results showed significantly enhanced uptake of the hyaluronic acid-conjugated GQD
700 system into cancer cells (A549) [121-124].

701 A vast number of receptors have been recognized as well as their antibodies were
702 successfully synthesized and investigated *in vitro* and *in vivo*. Inducing very strong ligand/receptor
703 binding, they can serve as potential models to promote active targeting technology. Among the
704 classical examples of ligands, we can cite the FA that specifically binds to the folate receptor as
705 well as present in TME. Folate itself has no toxicity and it is taken up via receptor endocytosis,
706 through different non-specific routes [125]. As a targeting ligand it provides a potential approach
707 to cell therapy, and also an approach for receptor-mediated targeting and intracellular drug-
708 targeting. Zhang *et al.* used graphene conjugated with carboxylated and sulfonated folate to target
709 the breast cancer cell line MCF-7 and deliver complex anti-cancer drug DOX and CPT via
710 graphene based nanocarrier [126]. Then the flakes were also conjugated with Rhodamine-B and
711 fluorescence microscopy images show that these flakes dispersed evenly in the cells with no
712 definite intracellular localisation. The result shows that folate-conjugated flakes significantly
713 induced greater toxicity than non-targeted flakes at similar level of cytotoxicity as free DOX.
714 These graphene based targeted drug delivery results have been confirmed by other groups with
715 different folate-receptor expressing cell lines such as HeLa and HepG2.

716

717 5. Drug Delivery Profiles and Systems

718 For a specific site-targeting approach, drug delivery profiles and systems must be précised
719 and well organized along with the potential effective technologies. Now a days, site-directed

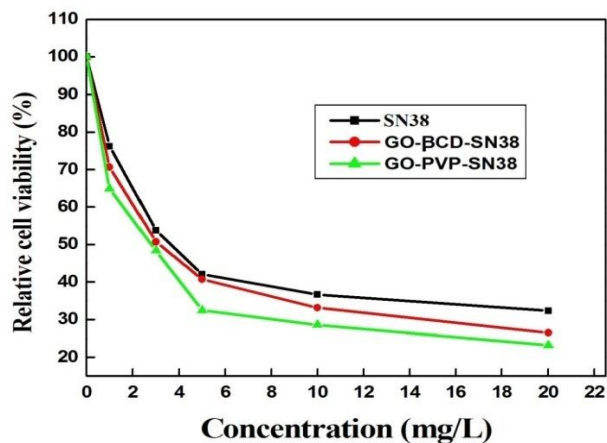
720 targeted drug delivery is a key research to improve the drug efficiency and decrease the side effects
721 of drugs. In this context, GO has emerged as a promising materials as it performs like drug delivery
722 vehicles due to its biodegradable, cost-effective easy to fabricate and nonimmunogenic
723 nature[127]. Also, GO and its derivatives are able to facilitate systemic pharmacokinetics which
724 are typically concerned with quantitative formulation of both carrier and load (any bioactive
725 compound) with controlled release at the specific site. With this specific characteristic of being a
726 carrier, GO based DDS can compete from the drawbacks of conventional administration of the
727 same drug by enhancing drug solubility, its prolonging duration, and retaining drug bioactivity
728 [128,129]. At the same time owing to the particular characteristic of crossing cell membranes and
729 potential delivery of bio-molecules like proteins, nucleic acids, and peptides into cells, GO
730 promotes the cellular uptake of micro molecules (e.g., anticancer, antibacterial, or antiviral agents)
731 and macromolecules [130]. This section is dedicated on and has illuminated the potential
732 applications of GO, especially the functionalized GO, as a nanocarrier in such DDSs.

733

734 **5.1. Delivery of single drug**

735 The presence of abundant functional groups on the surface and edges, allow GO to
736 conjugate with polymers and other biological moieties. Therefore, compared to GO, functionalized
737 GO has reactive groups which can provide the binding sites for some biological molecules such as
738 antibodies, enzymes, nucleic acids to form multifunctional materials, thus functionalized GO
739 provides a wide range of applications rather than pure GO [131]. Previously hydrophilic
740 biocompatible polymer PEG coated GO is the most common modification to improve the
741 biocompatibility as it can be functionalized on GO surface via both covalent and non covalent
742 approach [132]. Sun and co-workers [133, 134] have revealed PEGylated nano GO (PEG-NGO)
743 sheets that are soluble in buffers and biological media by covalently grafting PEG onto NGO for
744 the first time. Later on, the applications of PEG-NGO in drug delivery and cell imaging are studied
745 comprehensively. For the same, Wu *et al.* [135] reported that PEG-GO also has potential to be an
746 immune modulator for antigen-specific immune responses. They explained that the exposure to
747 PEG-GO significantly attenuated the serum level of ovalbumin specific immunoglobulin E. In
748 addition, PEG-GO augmented the metabolic activity of splenocytes restimulated with OVA but
749 not with the T-cell mitogen concanavalin A. Further Karki *et al.* [34] demonstrated the comparative
750 study of the drug SN-38 with two biocompatible polymer (β -CD) betacyclodextrin and PVP. Figure

751 3. clearly convinces the drug targeting with the modified GO as both polymers show enhanced
752 cytotoxicity against the MCF-7 cell.
753



755

756

757

758

759

760

761

762

763

764

765

766

767

768

769

770

771

772

773

774

775

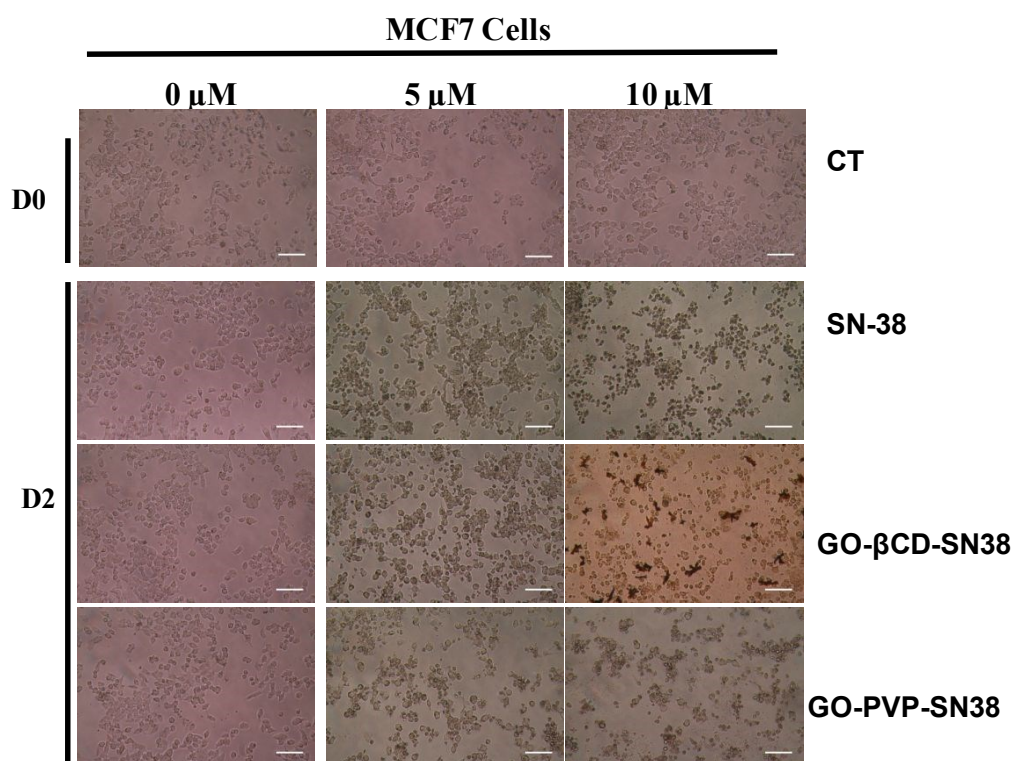
776

777

778

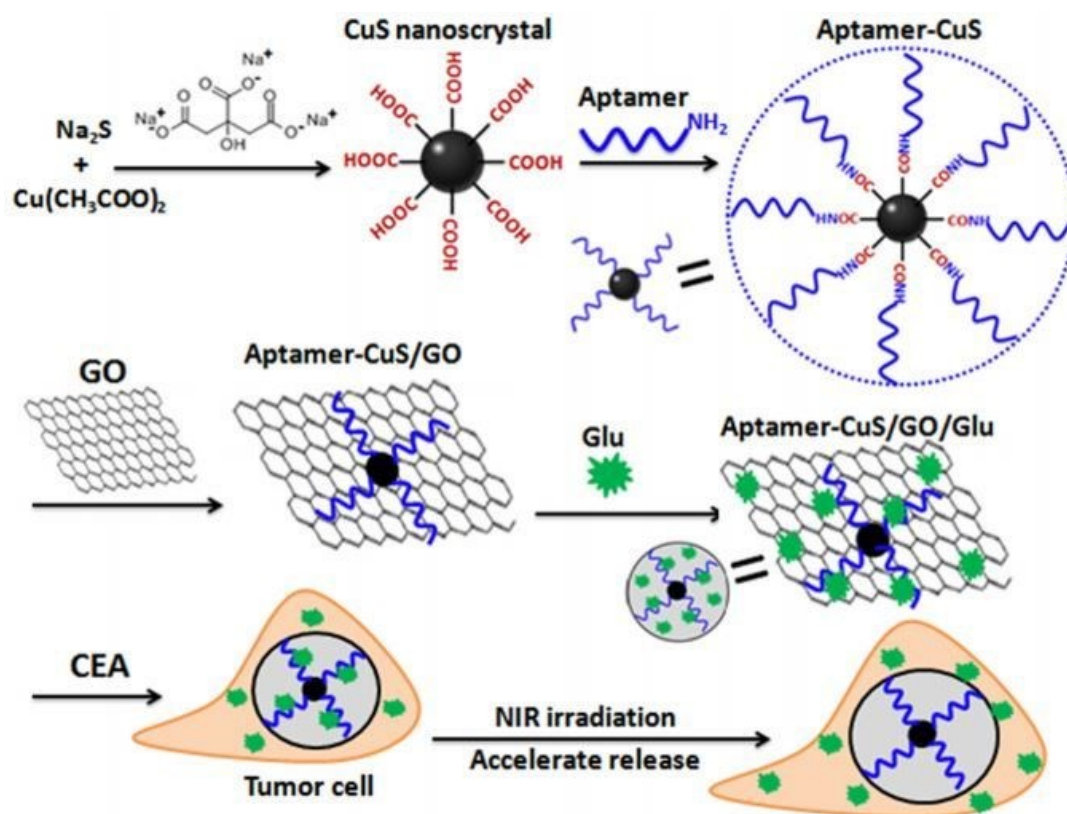
779

780



776 **Figure 3.** Morphological changes of MCF-7 cells after treatment with control, SN-38, GO-PVP-
777 SN-38 and GO-β-CD -SN-38 and cell viability of MCF-7 cells with different concentrations of SN-
778 38, GO-PVP-SN-38, and GO-β-CD-SN-38. Reprinted from [34], Copyright 2018, with permission
779 from Elsevier.

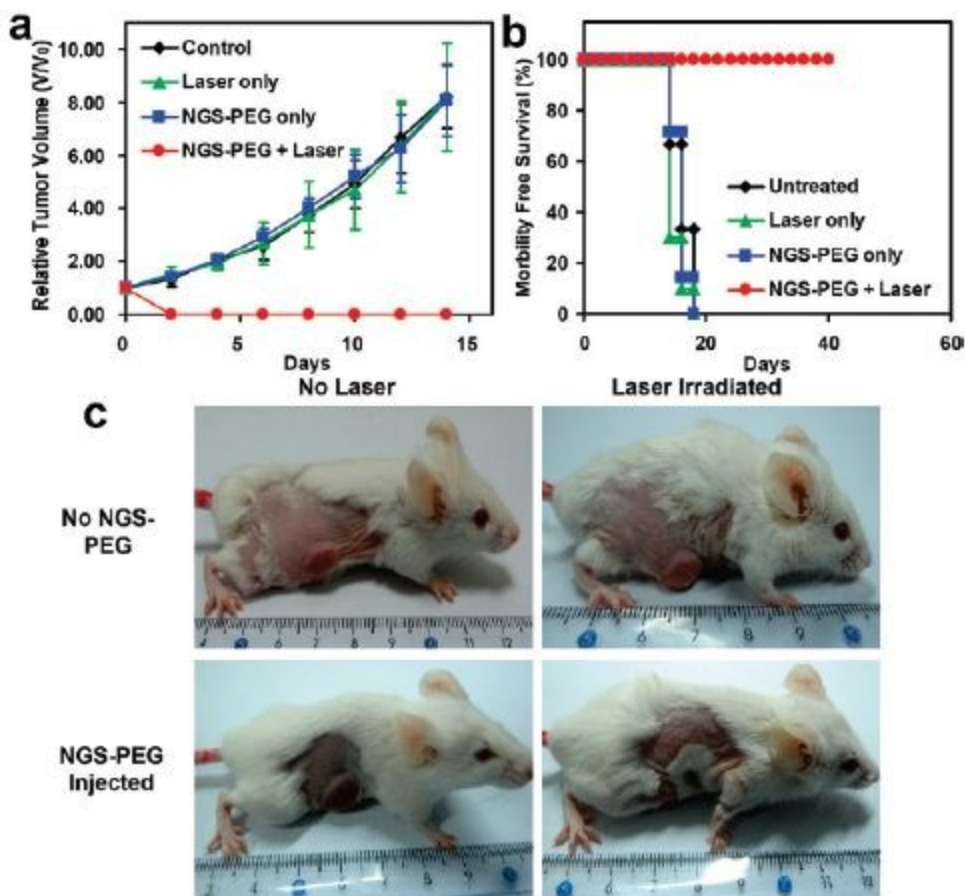
781 Xu and coworkers [136] discovered, a citrate-stabilized copper sulphide (CuS) nanocrystals
782 via NH_2 -terminated aptamer of carcinoembryonic (CEA) antigen to fabricate aptamer-CuS
783 complex *via* carbodiimide-activated coupling (Figure 4). Then, the complex was conjugated with
784 graphene oxide (GO) to form aptamer-CuS/GO conjugates *via* π - π stacking interactions. Finally,
785 glucosamine (Glu) was loaded into aptamer-CuS/GO conjugates to prepare aptamer-CuS/GO/Glu
786 composites. The composites enabled targeted and pH-sensitive Glu release against embryonic
787 carcinoma. They found that, under near-infrared light irradiation at 980nm, the composites have
788 photothermal-accelerated release of Glu and chemo-photothermal synergistic therapy *in vitro*. Due
789 to combined advantages from tumor biomarker-targeted, pH-sensitive, photothermal-accelerated
790 drug release, as well as chemo- photothermal therapy, the composites could be developed towards
791 multifunctional drug-delivery systems for highly efficient treatment against tumor cells. Thus
792 functionalization of GO nanosheets has created unexpected properties for advanced potential
793 applications.
794



795
796 **Figure 4.** Schematic representation of the systematic drug release of aptamer-CuS/GO/Glu composites.
797 Reprinted from [136], Copyright 2017, with permission from Elsevier.
798

799

800 Later on various metal and their respective oxide nanoparticles have also been proven as
801 promising materials for drug delivery with solitary or functionalized GO [137, 138]. Afzal *et*
802 *al.* worked on the zinc oxide nanoparticle (ZnO) doped GO nanosheets using a facile chemical
803 deposition method. The authors found significant increase in the absorption pattern of ZnO doped
804 GO in UV-Visible Absorption spectrum, which might have been due to the hydrogen bonding
805 between functional groups of GO and ZnO. Along with the high absorption spectra, GO doped ZnO
806 had higher drug loading efficiency of about 89% compared to pure ZnO (82%). These results
807 provided an efficient design of the drug delivery system for dissolution enhancement according to
808 the required drug release [139]. GO based nanometal composites have been emerged as a promising
809 material for anticancer therapeutics. Owing to their high drug loading capacity, photothermal and
810 synergizing effects, it is very important to exploit them for targeted chemo-thermal cancer
811 therapeutics. Chauhan *et al.* [140] explained the targeting behavior of gold nanoparticles (AuNPs)
812 with FA decorated GO. Here AuNPs composite-folate conjugated GO (FA-GO-AuNPs) nano-
813 platforms were synthesized and found to be NIR sensitive which results in intensified release of
814 anticancer drug DOX. Simultaneous delivery of DOX and AuNPs in the cellular vicinity was
815 further enhanced after localized NIR exposure which resulted in significantly improved cancer cell
816 toxicity. Also pharmacokinetics and organ distribution studies were carried out in healthy mice
817 tissues which further estimated the actual biological activity of these nanohybrids. *In vivo* studies
818 showed substantial tumor regression in solid tumor model in Balb/c mice and NIR exposure
819 induced photo-thermal effects further resulted in better tumor management. Yang *et al.*
820 explored nanographene sheets (NGS) with polyethylene glycol (PEG). PEG coated NGS show
821 several interesting *in vivo* behaviors including highly efficient tumor passive targeting and
822 relatively low retention in reticuloendothelial systems. Thus formulated system shows strong
823 optical absorbance of NGS in the NIR region for *in vivo* photothermal therapy,
824 achieving ultraefficient tumor ablation after intravenous administration of NGS [141]. Hence this
825 study simultaneously provided substantial evidences for both *in vitro* and *in vivo* level to support
826 the fact that this metal nanoparticle doped GO composite used as a tumor targeting tool.



827
 828 **Figure 5.** In vivo photothermal therapy study using intravenously injected NGS-PEG. (a) Tumor
 829 growth curves of different groups after treatment. (b) Survival curves of mice bearing 4T1 tumor
 830 after various treatments indicated. NGS-PEG injected mice after photothermaltherapy (c)
 831 Representative photos of tumors on mice after various treatments indicated. Thelaser irradiated
 832 tumor on NGS injected mouse was completely destroyed. Reprinted from [141], Copyright 2010,
 833 with permission from American Chemical Society.

834
 835
 836
 837 However, few studies have been carried out on the application of GO as a gene delivery
 838 system to treat various diseases caused by genetic disorders. In this regard, Dou and co-workers
 839 developed a new type graphene-based miRNA transfection system in which they functionalized
 840 graphene oxide with PEI. This complex was used to efficiently load miR-7b plasmid and deliver it
 841 into bone marrow macrophages. The entire system was targeted towards cell-cell fusion in bone
 842 marrow for inhibiting the formation of mature osteoclasts while preserving beneficial pre-
 843 osteoclasts [142]. Further, Huang *et al.* [143] reported PEI functionalized GO as the carrier of

844 siRNA against C-X-C chemokine receptor type 4 (CXCR4) which was a biomarker for cancer cell
845 metastasis to inhibit the cancer metastasis. Also we can conclude that the same DDSs can provide
846 multisensing approach as our prerequisite. Another approach with the same polymer was done by
847 Zhang *et al.* [144]. They demonstrate a new non-viral gene carrier bipolymer-functionalized
848 nanoscale GO (nGO-PEG-PEI) to increase the efficiency of plasmid DNA transfection in
849 *Drosophila* S2 cells. Small targeting biomolecules are usually minuscule and can be easily digested
850 in the body in a very short period. Therefore, it is critical to have carriers to convey these molecules
851 safely to the desired target site, and graphene and GO are recognized to be an excellent choice for
852 this particular issue. In this context several research groups reported that functionalized GO could
853 effectively deliver molecular beacons (MBs) and aptamers into cells for in situ specific detection
854 of biomolecules [145,146].

855 Recently antibacterial activity of GO has also received more attention in nanomedicine.
856 Nowadays, several research groups are extremely focused to formulate antimicrobial products with
857 GO. The synergistic effect of GO and silver (Ag) nanoparticle was examined by Ma *et al.* in order
858 to fabricate antimicrobial products. They explained the antibacterial activity of Ag-modified GO
859 materials through GO attachment onto *E. coli* cell surface that occurred *via* the formation of
860 hydrogen bonds between the lipopolysaccharides of the bacterial cell and the oxygen-containing
861 functional groups of GO [147]. They observed that GO decreased the intake of nutrition from the
862 surroundings while increasing the interaction between Ag and the bacteria. Ag is also reported to
863 disrupt the bacterial membrane, thereby inhibiting the respiration and replication of bacteria, which
864 eventually leads to cell death [148]. The Ag-modified GO exerts its antibacterial effect which
865 increases the deposition of bacteria as well as the contact between the cells and Ag-modified GO
866 nanoparticle. Thus Ag-GO is used as a novel antibacterial material, which exhibited a superior
867 antibacterial activity towards *Escherichia coli* (*E. coli*) due to the synergistic effect of graphene
868 oxide and silver nanoparticles [149].

869 The combination of carriers with specific ligands that can recognize corresponding
870 receptors on the cancer cell surface or respond to the specific stimulations in microenvironment,
871 has been widely used as an efficient approach to developing DDSs; this DDS strategy is called
872 internal-stimulation targeting DDS [150-154]. As the most commonly used magnetic stimuli
873 material for magnetic field-controlled drug-carrier systems, Fe_3O_4 is well known for its
874 supraparamagnetism, low toxicity, and favorable biocompatibility in physiological environments.

875 By applying Fe_3O_4 , Yang *et al.* [155] first prepared a supraparamagnetic GO- Fe_3O_4 hybrid through
876 chemical precipitation method. This nanohybrid had a high drug loading capacity, high dispersion,
877 and through the external magnetic field, it could move regularly to the action site. The
878 supraparamagnetic property allowed the nanocomposite to easily disperse in solution with
879 negligible magnetic interactions between each composite, avoid magnetic clustering, and deliver
880 drugs with high efficiency and accuracy with the assistance of an external magnetic field.

881 Turcheniuk in his work explained the role of GO in insulin delivery with the development
882 of insulin formulations that protected the native insulin from degradation under acidic pH in the
883 stomach. For the first time, they showed that a GO based matrix can ensure the stability of insulin
884 at low pH. GO doped with magnetic particle (MP) matrices loaded with insulin and the pH
885 triggered release of the insulin was examined. The loading of insulin on the GO nanomaterials
886 proved to be extremely high at $\text{pH} < 5.4$ with a loading capacity of $100 \pm 3\%$ on GO and $88 \pm 3\%$
887 on GO-MP doped. The insulin-containing GO matrices were stable at acidic pH, while insulin was
888 released when exposed to basic solutions ($\text{pH}=9.2$). These results suggest that GO based
889 nanomaterials are promising systems for the protection of insulin [156].

890 As an alternative way to battle against bacterial drug resistance, antibiotic-nanoparticle
891 combinations have been proposed by various research group [157-162]. However, studies on the
892 property of sustained release of drugs with such materials are limited. Developing antibiotic
893 graphene oxide nanocomposites to synergistically enhance the antibacterial activity and prolong
894 its activity is a novel approach to combat antibacterial resistance. Antibacterial activity based
895 nanocomposite for sustained release of Cephalexin (CEF) was explored by Katuwavila in his
896 recent work [163]. The enhancement of antibacterial activity of CEF, with GO in the
897 nanocomposite form, is observed. Encapsulation efficiency of 69% and a loading capacity of 19%
898 are obtained with the optimized formulation of GO-PEG-CEF. *In vitro* CEF release profiles
899 showed an initial burst release followed by a more sustained release over % days with cumulative
900 release of 80%. The half maximal inhibitory concentration (IC_{50}) values have both dose and time
901 dependent antibacterial activity for GO-PEG-CEF against both gram-positive and gram-negative
902 bacteria while pure CEF showed only dose dependent antibacterial activity. The minimum
903 inhibitory concentration values of GO-PEG-CEF have been 7.8 and 3.9 mg/mL against *S. aureus*
904 and *B. cereus*, respectively, while it was 10 mg/mL with pure CEF against both gram-positive
905 bacteria. This confirms the enhanced antibacterial activity of GO-PEG-CEF over pure CEF against

906 gram-positive bacteria. These findings therefore confront GO as nanoantibiotic system for
907 effective treatment against bacterial infections.

908 In a recent study, drug nanocarriers based on mesoporous silica-coated magnetic GO were
909 synthesized for anti-cancer drug delivery of DOX [164]. The addition of mesoporous silica
910 increases the surface area, thus drug loading efficiency, as well as the cellular uptake. Such carriers
911 were designed with a dendrimer-like structure based on supramolecular poly-
912 pseudorotaxane. They were commonly used in targeted drug delivery and acted as molecular gates
913 storing the drugs that can be opened by an external stimulus e.g. pH change. Thus the resulting
914 system, being pH-sensitive and positively charged, favored higher colloidal stability and improved
915 cellular uptake.

916 By means of significance of GO, there is great interest in functionalized GO as a
917 nanocarrier for both *in vitro* and *in vivo* drug delivery. Various works demonstrate the potential of
918 GO derivatives as exciting nanocarriers for the loading and delivery of biological agents.

919

920 **5.2. Delivery of binomial drugs**

921 Combined therapy with two or more drugs provides a promising strategy through co-
922 delivery of drugs within the same nanoparticle to increased synergistic effects of both the drugs.
923 [165]. It has been proved clinically that a variety of drug combinations can induce synergisms
924 among them and prevent from disease reappearance [166]. For achieving such therapeutic
925 selectivity for DDSs has been a major obstacle [167] as it requires precise target modulation, which
926 can be discontended by the compensatory mechanisms available to complex biological systems
927 [168]. To overcome this drawback high drug doses requires over and over again that results
928 unwanted side effects in other healthy and uninfected tissues [169,170].

929 Cytotoxicity can in principle be maximized if drugs with different activities can be
930 delivered simultaneously to the same cell. However, combination therapy with drugs having
931 distinct properties such as solubility generally requires use of multiple carriers or solvents, limiting
932 the likelihood of simultaneous delivery. Ahmed and his group briefly [171] described the *in*
933 *vivo* application of biodegradable polymersomes for systemic delivery of an anticancer cocktail.
934 These polymer-based shells exploit a thick hydrophobic membrane and an aqueous lumen to
935 efficiently carry both hydrophobic drug paclitaxel and hydrophilic drugs doxorubicin.
936 Polymersomes are long-circulating *in vivo* but also degrade and release their drugs on a time scale

937 of about 1 day, by which time the tumors treated here will otherwise have almost doubled in
938 volume. A single systemic injection of the dual drug combination shows a higher maximum
939 tolerated dose than the free drug cocktail and shrinks tumors more effectively and more sustainably
940 than free drug: 50% smaller tumors are seen at 5 days with polymersomes. The polymersomes
941 cause two-fold higher cell death in tumors than free drug and show quantitatively similar increases
942 in maximum tolerated dose and drug accumulation within the tumors.

943 However, one major challenge of combinatorial therapy is to unify the pharmacokinetics
944 and cellular uptake of various drug molecules, which will allow the precise control of the dosage
945 and scheduling of the multiple drugs, thereby maximizing the combinatorial effects. One of the
946 most popular approaches to overcoming this challenge is to load multiple types of therapeutic
947 agents onto a single drug-delivery vehicle and then concurrently deliver them to the sites of action
948 [170-174]. Several drug-delivery systems, such as polymeric nanoparticles and liposomes, have
949 shown the ability to co-deliver multiple drugs, but fine-controlling the comparative loading yield
950 and release kinetics of the multiple-drug payloads remains an unmet need.

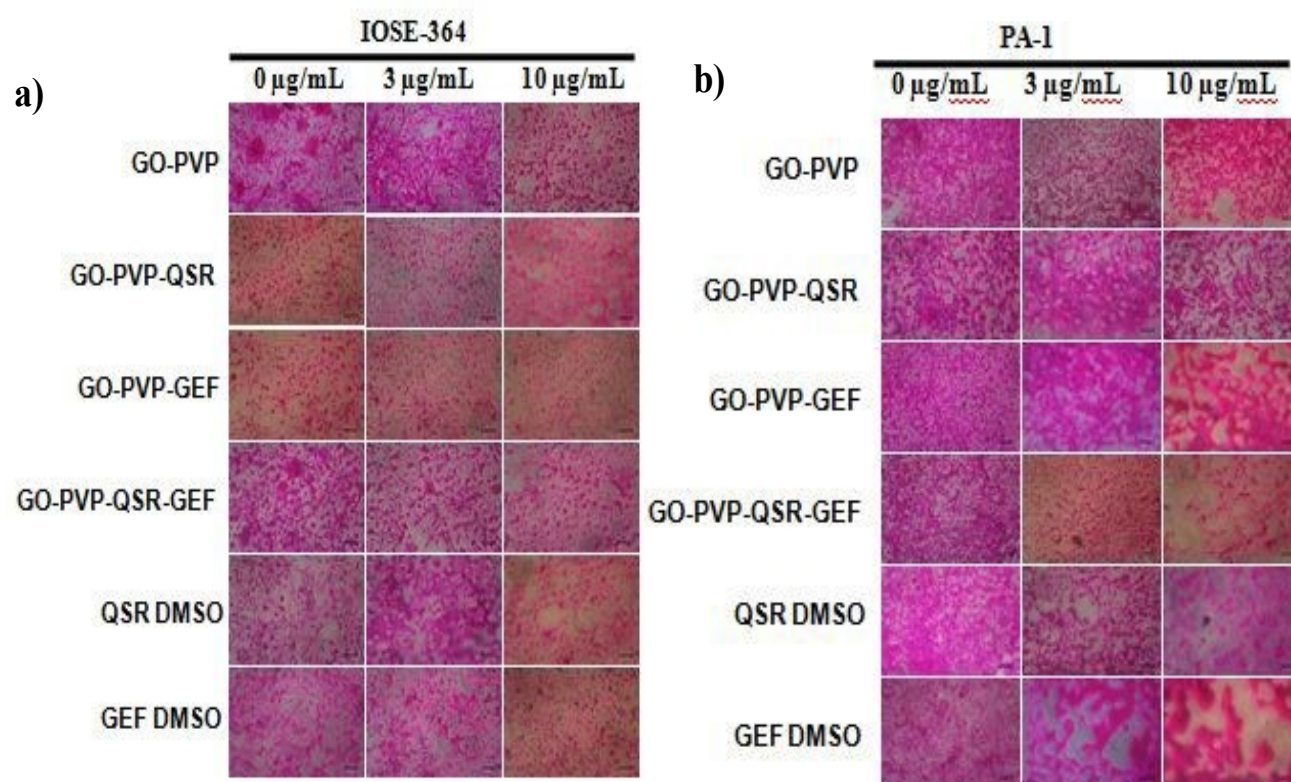
951 Herein, a combinatorial drug-conjugation strategy is to meet the aforementioned need by
952 covalently conjugating multiple therapeutic agents through hydrolysable linkers to form drug
953 conjugates prior to loading the drugs onto a delivery vehicle. In contrast to loading individual types
954 of drugs separately, this drug-conjugates approach enables multiple drugs to be loaded onto the
955 same drug carrier with a predefined stoichiometric ratio. The cleavable linkers allow the
956 therapeutic activity of the individual drugs to be resumed after the drug conjugates are delivered
957 into the target cells and unloaded from the delivery vehicles. In this regard Aryal and coworkers
958 [175] demonstrated the conjugation of PCT and gemcitabine hydrochloride (GEM) with a
959 stoichiometric ratio of 1:1 via a hydrolyzable ester linker, and have subsequently loaded the drug
960 conjugates into lipidcoated polymeric nanoparticles. The time-dependent kinetics of hydrolysis
961 and cytotoxic effect of the combinatorial drug conjugates against human pancreatic cancer cells
962 are studied. It is shown that the synthesized drug conjugates can be readily encapsulated into a
963 lipid-coated polymeric drug-delivery nanoparticle, which significantly improves the cytotoxicity
964 of the resulting combinatorial drug conjugates against human cancer cells which was comparable
965 to that of the corresponding free PCT and GEM mixtures after the conjugates were hydrolyzed. The
966 cytotoxicity of the drug conjugates was significantly improved after their encapsulation into drug-
967 delivery nanoparticles.

968 Herein Shen *et al.* presented [176] a novel method of synthesizing ultra-fine graphene
969 oxide (uGO) doped with (MNs composites is presented. This composite is fabricated by
970 combination of a simple and effective chemical deposition with further oxidation of iron ions on a
971 carboxylated uGO base, followed by coating oleic acid on MNs. Two anticancer drugs,
972 camptothecin (CPT) and methotrexate (MTX), are separately bound to uGO sheets and the
973 carboxyl terminals of uGO on the hybrid, forming a superparamagnetic & dual drug-loaded MTX-
974 uGO-COOH-MNs-OA-CPT nanocomposite. The size of the composite is approximately 80 nm
975 by DLS. The entrapment efficiencies of MNs, CPT, and MTX reach approximately 458 mg g⁻¹,
976 682 mg g⁻¹, and 896 mg g⁻¹, respectively. *In vitro* release and apoptotic assay results show that
977 the nanocomposite can cause the apoptosis and death of HepG2 cells by preferentially releasing
978 drugs to the tumor microenvironment. The tumor inhibitory rate of 73.9% in S-180 sarcoma-
979 bearing Balb/c mice suggests that the combination of nanocomposite-mediated dual drug synergic
980 chemotherapy with photothermal therapy has remarkable therapeutic potential against drug-
981 resistant tumors.

982 Moreover, FA-conjugated chitosan oligosaccharide (FA-CO) functionalized GO (GO-
983 FACO+) used for delivering DOX and siRNA was prepared for reversal of cancer drug resistance
984 [177]. GO-FACO+ could effectively load DOX and siRNA simultaneously through p-p stacking
985 and electrostatic interaction and specifically deliver to MCF-7 cells. siRNA could silence MDR
986 gene which induced the expression of P-glycoprotein (P-gp) to reduce the efflux of chemotherapy
987 drug DOX in MCF-7 cell. Therefore, this functionalized GO could be used as a novel drug carrier
988 to enhance the effect of chemotherapy.

989 Recently Tiwari *et al.* [178] reported an excellent carbonaceous nanocarrier modified with
990 polymer functionalities which was biodegradable and biocompatible, poly- vinylpyrrolidone
991 (PVP), to load dual drug combination gefitinib (GEF) as well as QSR and compared with it
992 individual drug therapy. The loading and cell cytotoxicity of both drug conjugated systems (i.e.
993 GO-PVP-GEF/GO-PVP-QSR and GO-PVP-GEF-QSR were investigated in PA-1 ovarian cancer
994 cells. They successfully showed that combined drug system loaded with modified nanocarrier,
995 GO-PVP, is significantly more toxic than individual drug therapy to the PA-1 ovarian cancer cells
996 compared to the toxicity toward IOSE-364 cells (Figure 6.). In another report of Yang and authors
997 [179], GO was functionalized by carboxymethyl chitosan. Afterwards, it was conjugated with
998 fluorescein isothiocyanate/ hyaluronic acid and subsequently anticancer drug doxorubicin was

999 loaded onto this conjugate. Similarly Jang and coauthors [180] have demonstrated that the
1000 combinatorial system of simvastatin and irinotecan was more effective than their separate systems.
1001 Their combination synergistically slowed down colon cancer cell proliferation in HT-29 cells
1002 with/without irinotecan resistance. They also showed the various fixed ratio combinations of
1003 irinotecan and simvastatin and revealed that 1 : 2 molar ratio shows good potential effect on HT-
1004 29 cells with or without irinotecan resistance and clearly suggested that simvastatin may be play
1005 advantageous role in the treatment of colon cancers and to triumph over irinotecan-resistance.



1006
1007
1008 **Figure 6.** Phase contrast microscopic images showing the morphological changes of (a) IOSE-
1009 364, and (b) PA-1 cells after treatment with indicated drug-loaded nanocarriers at 0, 1, 3, 5, and 10
1010 µg/ml concentrations. Reprinted from [178], Copyright 2019, with permission from Elsevier.

1011
1012
1013 Moreover, a multifunctional targeted delivery system based on GO that combined dual
1014 magnetic and molecular targeting was constructed by Song and co-workers [181]. In their study,
1015 lactoferrin (Lf) was used as a brain-targeted molecule to modify GO because its ability of crossing
1016 the blood brain barrier and combining Lf receptors (LfRs) overexpressed on the glioma cells.

1017 Fe₃O₄ nanoparticles with magnetic targeting ability can also improve target delivery efficiency of
1018 drugs under external guided magnetic field. Doxorubicin hydrochloride was loaded on the Lf-GO-
1019 Fe₃O₄ nanocomposites via π - π stacking, and the drug loading capacity achieved 0.8 mg/mg when
1020 the DOX concentration was 1 mg/mL and the drugs exhibited pH-dependent release. At pH 5.5,
1021 DOX can be rapidly released from GO-Fe₃O₄ and Lf-GO-Fe₃O₄ because of the protonation of
1022 DOX under acidic conditions, and the cumulative release rates were 20% and 26% in 72h,
1023 respectively. However, at pH 7.4, the cumulative release rate of DOX in both solutions was less
1024 than 10% in 72h. C6 glioma cells incubated with GO-Fe₃O₄ and Lf-GO-Fe₃O₄ without drug
1025 loading exhibited no appreciable toxicity even within the 250 μ g/mL concentration range for 72h,
1026 indicating that GO-Fe₃O₄ and Lf-GO-Fe₃O₄ can be a good carrier for drug delivery. Then C6
1027 glioma cells were cultivated with free DOX, GO-Fe₃O₄-DOX and Lf-GO-Fe₃O₄-DOX (the loading
1028 ratio of DOX was 1 mg/mg). The IC₅₀ of cells treated with GO-Fe₃O₄-DOX and Lf-GO-Fe₃O₄-
1029 DOX were found to be 31.30 μ g/mL and 23.95 μ g/mL, respectively.

1030 Wang *et al.* integrated chitosan onto rGO-SPIONs nanosheets to enhance their balance,
1031 solubility and biocompatibility for most cancers chemotherapy and gene remedy [182]. The
1032 resulting nanocarrier validated an efficient drug loading ability, pH dependent launch and precise
1033 cytotoxicity. DOX was then absorbed at the surface and the ensuing composite turned into
1034 encapsulated with a reporter DNA series and green fluorescent protein (GFP) *via* their interplay
1035 with the undoubtedly charged chitosan. The transport of each DOX and DNA was studied *in vitro*
1036 and in tumor bearing mice and observed through MRI, and the outcomes proven that the very last
1037 composite DOX-(chitosan magnetic-G)-GFP-DNA became fantastically dispensed alongside the
1038 tumor. Furthermore, toxicity research confirmed that there has been no frame weight loss of the
1039 treated mice. Following this pursuit, Zhang *et al.* 2010 [183] co-loaded DOX and CPT for efficient
1040 inhibition of cancer cell through topoisomerase intercalation only using nanomolar quantity of
1041 CPT. Furthermore, Owonubi 2015 reported that reduced GO (rGO)-acrylamide (AAm) pH
1042 responsive nanoconjugate when fabricated in wheat protein isolate based hydrogel, showed
1043 remarkable drug loading of drug duo Proguanil and Chloroquine. The entire system interestingly
1044 showed antidiabetic activity when targeted *In vivo* against relevant neoglucogenic receptors [184].
1045 Owonubi *et al* 2018 again reported that the same drug combination, when loaded simultaneously
1046 on functionalized rGO-whey protein based hydrogel, showed efficient activity as antimalarial with
1047 steady state release of both the drugs [185]. In 2019 Bullo *et al.* fabricated GO-PEG-FA (Folic

1048 acid) based target specific dual drug delivery system where protocatechuic acid and Chlorogenic
1049 acids were loaded and successfully delivered as antineoplastic combination [186]. As a beneficial
1050 cocktail Pei *et al.* 2017 reported that PEG functionalized GO when loaded with Cis-Pt and DOX,
1051 the therapeutic efficacy of the duo in cancer cell was higher than that of the individual candidate
1052 [187]. The authors also reported that the toxicity of the drug cocktail was also greatly reduced
1053 compared to the solitary ones. It has also been reported that GO or rGO can also be used to target
1054 other drug cocktails such as QSR-5 fluorouracil or epirubicin-temzolomide to target complex
1055 neoplasia such as paediatric brain tumours.

1056 However, the question lies that why dual drug loading onto GO/rGO or rGO-synthetic
1057 polymer conjugate improves stability or therapeutic efficiency? Computational studies revealed
1058 that much of the co-loading of drugs and synergistic release of the individual depends on drug-
1059 carrier or drug linker interaction. Alinejad *et al.* 2019 performed Density Functional Theory (DFT)
1060 and Molecular Dynamics (MD) simulation of DOX-CPT co-loaded system onto GO-FA hybrid
1061 and reported that the stability of this system has been a major contribution of drug-carrier
1062 interaction. They reported that DOX has reinforced stronger interaction with FA than CPT thus
1063 establishing the fact that FA has influenced DOX release kinetics in the medium more than CPT.
1064 Moreover, the major interaction between DOX/CPT-GO has been π - π stacking, while the
1065 interaction between DOX/CPT-FA has been hydrogen bonding (HB) due to heteroatom present
1066 onto the drugs and polar hydrogen present within the FA. Thus in this type of system, CPT
1067 adsorption is weaker facilitating faster release while DOX showed slower diffusion kinetics than
1068 CPT. FA improves both stability and therapeutic safety of the drug molecules [188]. Biomimetic
1069 peptides have emerged as a promising alternative tool of organic medicine which often binds with
1070 target cells due to high target specificity and produces potential therapeutic activity for their
1071 resemblance with actual protein or anti-protein in specific biochemical pathways. Exploiting this,
1072 a type of cell apoptosis peptide (KLAKLAK)₂(KLA) had been impregnated on GO matrix through
1073 a disulfide bond to achieve GO-SS-KLA. Then, anticancer drug doxorubicin (DOX) was charged
1074 on the engineered GO through π - π conjugation and hydrogen bonding. Finally, bovine serum
1075 albumin (BSA) was used stabilize DOX-GO-SS-KLA/BSA. The authors reported that KLA and
1076 DOX were released based on the reductive and pH stimulation inside the cells, respectively, and
1077 reaped a synergetic remedy for most cancers [189]. A summary of delivery systems has been
1078 summarized in Table 2.

1079

1080 **6. Dual Drug Delivery Systems over Single Drug Delivery Systems**

1081 Synergistic combinations of two or more agents can overcome toxicity and other side
1082 effects associated with high doses of single drugs by countering biological compensation, allowing
1083 reduced dosage of each compound or accessing context-specific multitarget mechanisms [190-
1084 192]. Thus combination of multiple drug components may offer a rational molecular basis in novel
1085 chemotherapeutic strategies. In current era, numbers of combinational therapies are in tradition in
1086 which the radiotherapy, immunotherapy with chemotherapy, hormone therapy and combination of
1087 multiple chemotherapeutic agents, are most common strategies for revolutionizing treatment of
1088 many diseases.

1089

1090 **Limitations of single drug delivery system towards cancer therapy**

1091 Single chemotherapeutic system is limited to act on cancer survival pathways with little
1092 response rate and relapse of tumor for which when system treated on the cancer patients, it were
1093 found to fail in clinical setting [193]. The most important limiting factors are significant toxicity,
1094 multi-drug resistance (MDR) and uninvited side effects with single chemotherapeutic systems
1095 when treated in cancer patients. These factors are major aims of significant drug delivery systems.
1096 In individual drug delivery system with or without carrier or pro-moiety no synergistic effects are
1097 available which enhance targeting, therapeutic activity and helps to reduce side effects.

1098

- 1098 • Low drug loading
- 1099 • Not proper release
- 1100 • *In vivo* variability in single unit drug delivery system.
- 1101 • Immediate withdrawal of drug is not possible.
- 1102 • Drug dose manipulation in case of child and elder patients is not possible

1103

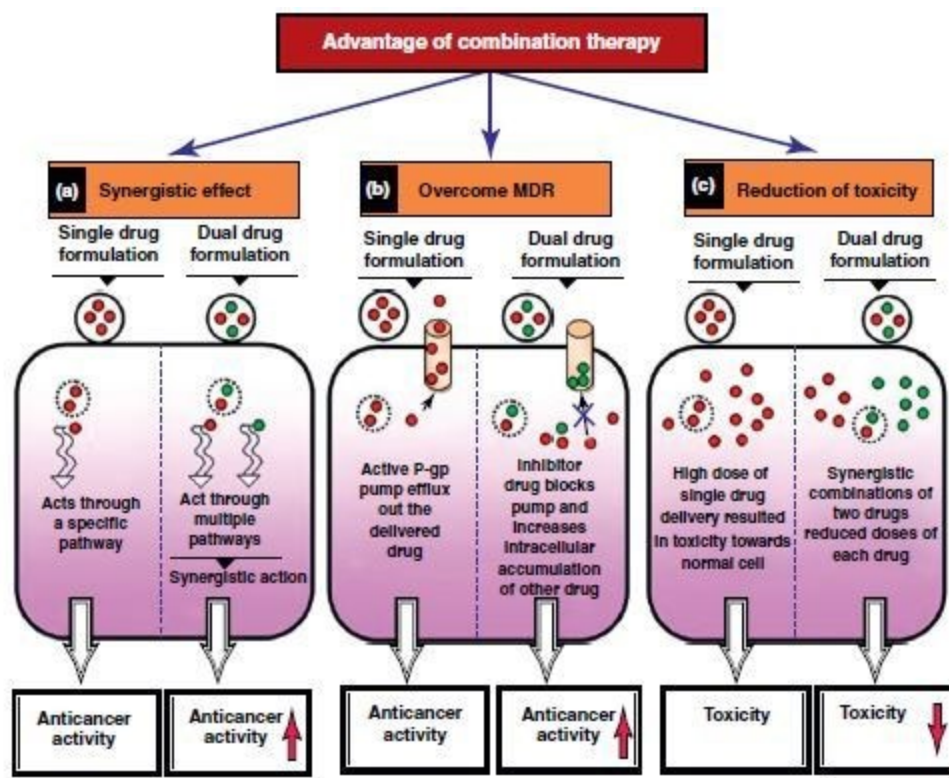
1104 **Advantages of combinational strategies towards cancer therapy**

1105

1106 Unlike individual drug therapy, combination or co-drug therapy not only can alter different
1107 signaling pathways but also triumph over toxicity or reduces individual drug-related toxicity and
1108 resulting in improved therapeutic effects. Moreover this combination strategy can act as a
1109 conqueror to the mechanisms of drug resistance associated with cancer treatment. Multiple drug

1110 effect/combination index (CI) isobologram analysis can be effective in calculating which drug
1111 combination is best therapeutic combination with maximum antitumor efficacy and also an
1112 efficient tool to demonstrate that therapeutics are performing synergistically [194]. Figure
1113 7 shows the various advantages of combination drug delivery for cancer therapy. In recent years,
1114 the use of combination therapy has been well conventional to the different cancer treatment and
1115 its advantages in cancer therapy are pointed below.

- 1116 • The overall therapeutic advantage of the drugs in co-drug system is found to be superior
1117 to the sum of the effects of individual drugs [195].
- 1118 • Synergistic modulation can offer the opportunity to alter the doses of the parent
1119 therapeutic in order to improve efficiencies and reduce drug toxicities [196].
- 1120 • Enhanced stability due to synergistic effect of partner drug without impairing its
1121 properties.
- 1122 • Major and considerable advantage is to maximize release performance [197-198].
- 1123 • Modulation of odour: for example, parent drug with a strong unsympathetic odour can be
1124 reduced by attaching a co-drug that increase BP (boiling point) so as to interpret it less
1125 volatile, thus reducing or removing odour [196].
- 1126 • Modulation of taste: groups like carboxylic acid groups which bestow the sensation of
1127 bitterness can be reduced or modulated [196].
- 1128 • Anchoring GO with drug along with anticancer peptide can improve the viability, target
1129 specificity and synergism of the therapeutic cocktail; in addition can reduce the toxicity
1130 of the dosage regimen.



1131

1132 **Figure 7.** Schematic representation depicting various advantages shown by combination drug
 1133 delivery for cancer therapy. Reprinted from [194], Copyright 2012, with permission from Elsevier.

1134

1135 7. Role of GO in Bioimaging

1136

1137 To improve the survival rate of patients suffering from cancer, early diagnosis is crucial.
 1138 For different kinds of cancer imaging techniques, the development of contrast agents and imaging
 1139 probes is essential. Bioimaging has a crucial role in both research and clinical practice. Owing to
 1140 their unique physical/ chemical properties, extensive research has been devoted to carbon
 1141 nanostructure (CNT, graphene, fullerene, and nanodiamond) based platforms for cancer imaging.
 1142 The surfaces of these carbon nanostructures can be engineered via functionalization to manipulate
 1143 their physicochemical/biological characteristics [199]. Many reports also explained that
 1144 functionalized GO nanocomposites were utilized as a contrast agent in various biological imaging
 1145 such as fluorescence imaging, photoacoustic imaging and magnetic resonance imaging (MRI)
 1146 [104, 200]. It has been observed that most commonly used imaging agents are unable to cross the
 1147 cell membrane. On the other hand, carbon-based nanostructures (e.g. CNTs) can be helpful to
 1148 deliver such contrast agents intracellularly for cell tracking with high selectivity, and great
 potential [201].

1149 7.1. Optical Imaging

1150 Optical imaging is a passive technique, having superior advantages over other imaging
1151 techniques with comparatively low-cost, high multiplexing capability, relatively high sensitivity
1152 and real time imaging [202]. This technique provides the detailed images of microorganism's tissues
1153 and cells with the help of visible light and photons. Despite of these advantages, optical imaging is
1154 highly affected by the poor tissue penetration due to tissue autofluorescence and light adsorption
1155 by macromolecules such as heme groups, proteins etc. To overcome these problems nowadays,
1156 particularly, NIR wavelength is suitable when it was applied in organisms, because tissues are
1157 transparent to light at such a wavelength [203].

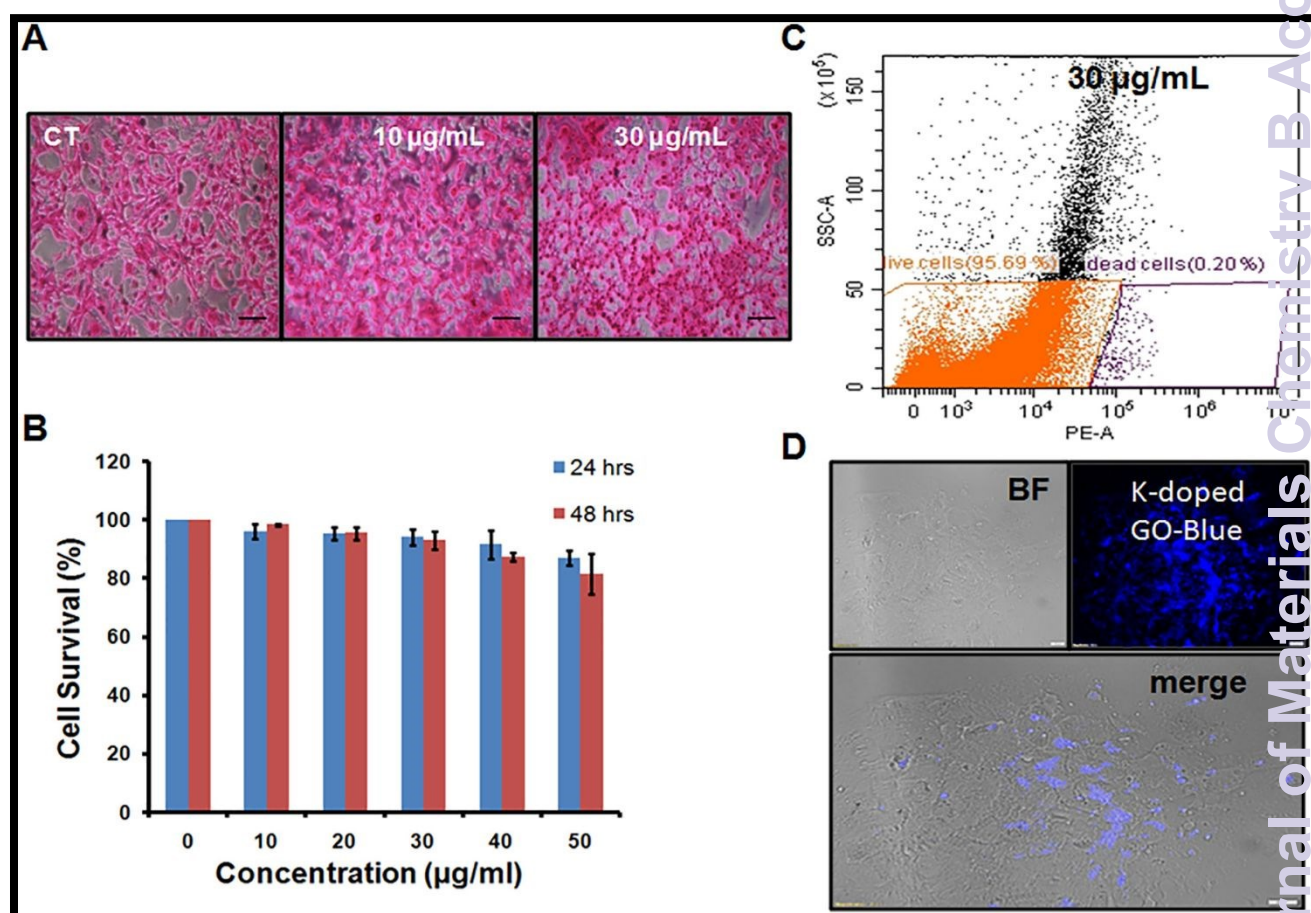
1158 GO acquires strong photoluminescence characteristic in NIR region due to the presence of
1159 surface and edge defects, suitable band gaps and exceptional photostability [204]. Along with the
1160 above GBNs have interesting chemical, mechanical, and optical properties which makes them
1161 excellent imaging probes in biomedical field [133,140,205].

1162 Optical imaging is studied through fluorescence imaging [FI], two-photon FL imaging
1163 [TPFI], and Raman imaging [RI] in which GBNs are functionalized with various molecular dyes,
1164 quantum dots, upconversion nanoparticles etc.

1165 7.1.1. Fluorescence Imaging

1166 Fluorescence is a phenomenon in which fluorescent probes absorb the quanta of a
1167 significant energy, then stimulated from ground state to allowed excited state, where the excited
1168 electron stays for a short period of ($\sim 10^{-9}$ s) and then come back to its ground state by simultaneously
1169 emitting the stored energy in form of photon which results in emission of light. Owing to this emitted
1170 light FI enables the extensive range of interaction between the molecules in tissues and cells to
1171 observe the location and dynamics of gene, protein expression etc [206, 207]. Chauhan *et al.*,
1172 reported binding and recognizing of Raji B cells through PEGylated nano GO (NGO) in which
1173 NGO has been covalently conjugated by antibody Rituxan (anti-CD20) for selective *in vitro* killing
1174 of cancer cells. The photoluminescent property of NGO used in field of bioimaging application as
1175 it is NIR active and its π - π stacked structure further provides efficient loading of aromatic
1176 anticancer drug DOX [140]. Based upon these specific properties of GBNs many researchers
1177 explore GBNs in bioimaging field. Recently, Chetna *et al.* in 2019 reported a greener and cost
1178 effective route for synthesis of potassium-doped GO using agricultural waste i.e. *Quercus ilex*.
1179 This nanomaterial shows low toxicity, good biocompatibility and strong PL properties and

1180 reflected as an excellent probe for bioimaging. To determine the cytotoxic effect of K-doped GO,
 1181 they performed Sulphorhodamine B colorimetric assay using tumorigenic ovarian epithelial IOSE-
 1182 364 cells (Fig. 8.) and the result showed greater than 90% cell viability at a concentration of 30
 1183 $\mu\text{g/mL}$, whereas inhibitory concentration (IC) value was greater than 50 $\mu\text{g/mL}$. Further, they
 1184 confirmed its biocompatibility by using IOSE-364 cells, executed *invitro* MTT assay at 24 and 48
 1185 h and results indicated around 80% cell viabilities after treatment with K-doped GO for 48 h at
 1186 highest concentration of 50 $\mu\text{g/mL}$, indicates its non-toxic nature for this cells. This material shows
 1187 bright blue fluorescence when incubated with IOSE-364 cells for 4h, followed by washing the
 1188 images was taken using fluorescence microscope, indicates material is excellent bioimaging probe
 1189 for detection of IOSE-364 cells [208].
 1190



1191
 1192
 1193 **Fig. 8.** Biocompatibility and bio-imaging studies of K-doped GO in non-tumorigenic ovarian
 1194 epithelial IOSE-364 cells, (A) Representative light microscopic images of cells stained with

1195 Sulphorhodamine B after treatment with different concentrations of K-doped GO for 24 h. (B) Cell
1196 viability MTT assay of K-doped GO at different indicated concentrations using IOSE-364 cells at
1197 24 and 48 h. (C) Flow cytometry data showing the live and dead cells populations after PI staining
1198 (D) Confocal microscopic images of cells using K-doped GO as fluorescent probe. Reprinted from
1199 [208], Copyright 2019, with permission from Elsevier.

1200
1201

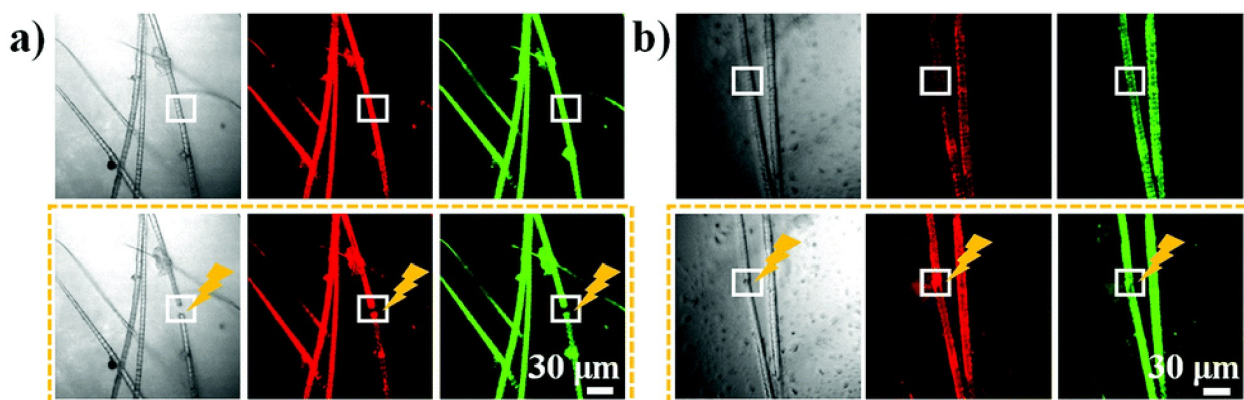
1202 In addition to FI, QDs with quantum captivity and edge effects have possessed optical
1203 properties, hence used for bioimaging applications. QDs have a wide optical absorption, from
1204 UV to NIR region, with the strongest peak located in the UV region. The size of the QDs is the
1205 key factor responsible for the fluorescence color e.g. Panet *al.* found QDs with blue
1206 fluorescence [209] while Zhu *et al.* explained green colored QDs in their experiment [210]. Dong *et al.*
1207 functionalized QDs with dual biocompatible polymers i.e. poly (L-lactide) (PLL) and PEG
1208 for intracellular imaging of miRNA along with gene transport to provide improved therapeutic
1209 efficacy [211]. The PLL-PEG-decorated-QDs showed excellent physiological stability
1210 with steady photoluminescence. PLL-PEG-decorated-QDs were conjugated to agents targeting
1211 miRNA-21 and survive in as a gene vector into HeLa cells; and as a result green fluorescence
1212 appeared inside the cells when observed under a confocal microscope. This allowed improved
1213 observation of regulation in gene delivery through QDs. Fascinated with the properties of
1214 QDs further, Wen *et al.* applied the fluorescent property of organosilane and fabricated them
1215 with QDs (producing Si-QDs) that were further encapsulated into mesoporous hollow silica
1216 nano-spheres [212]. The Si-QDs hybrid nanospheres displayed blue and green colors in the
1217 visible range at cellular uptake in HePG2 cells. The results again demonstrate QDs as promising
1218 candidates.

1219 In addition to FI, in 2015 Liet *al.* reported a novel label-free highly sensitive transient
1220 imaging technique for the fast imaging and computable layer study of graphene and GO, along
1221 with the on time imaging of GO *in vitro* with cells and *ex vivo* in circulating blood, based on the
1222 transient absorption process [213]. They used modulation range of MHz that effectually dodged the
1223 low-frequency laser noise. With this imaging modality, they were able to attain high-speed as well
1224 as real time imaging of GO with quantitative analysis of the intracellular concentration of well-
1225 dispersed PEG-GO. This eventually opened up new windows for GO to emerge as a bioimaging
1226 marker grounded on the transient absorption imaging process.

1227 7.1. 2. Two-Photon Fluorescence Imaging (TPFI)

1228 FI imaging has poor tissue penetration which somewhere limits its application in field of
 1229 bioimaging. To overcome these complications, TPF1 is used in field of medical diagnostics
 1230 [214]. TPF1 is capable to get the more detailed information regarding the activities of deep located
 1231 tumor targets. It generates high level of special resolution than FI by using its nonlinear excitation
 1232 mode and results in photobleaching reduction. Now a days, GBNs are on high demand in TPF1
 1233 based techniques. Li *et al.* demonstrated, GO as an excellent optical imaging probe due to their
 1234 strong two-photon luminescence. They labelled the target cells with GO, which resulted in
 1235 extremely confined and low energy therapy. Thus highly efficient GO, after combining with an
 1236 ultrafast pulsed laser, proved to be promising material for 3D TPF1 [215]. In recent years,
 1237 fluorescence resonance energy transfer (FRET) has been evolving as a fascinating tool to strategize
 1238 novel two photon PDT (TP-PDT) bioimaging systems. In this perspective, Sun and his group [216]
 1239 synthesized a system, in which nitrogen doped GQD was coupled with a photosensitive drug Rose
 1240 Bengal (RB) and applied it for TP-PDT based FRET (Figure 9). They found that the system N-
 1241 GQD-RB possessed high photostability as well as biocompatibility. The N-GQD helped to excite
 1242 the photosensitive drug RB with one or two photon laser. Further TP-PDT was also examined *via*
 1243 blocking the targeted blood vessels with high precision utilizing small amount of RB and low dose
 1244 of two photon irradiations.

1245



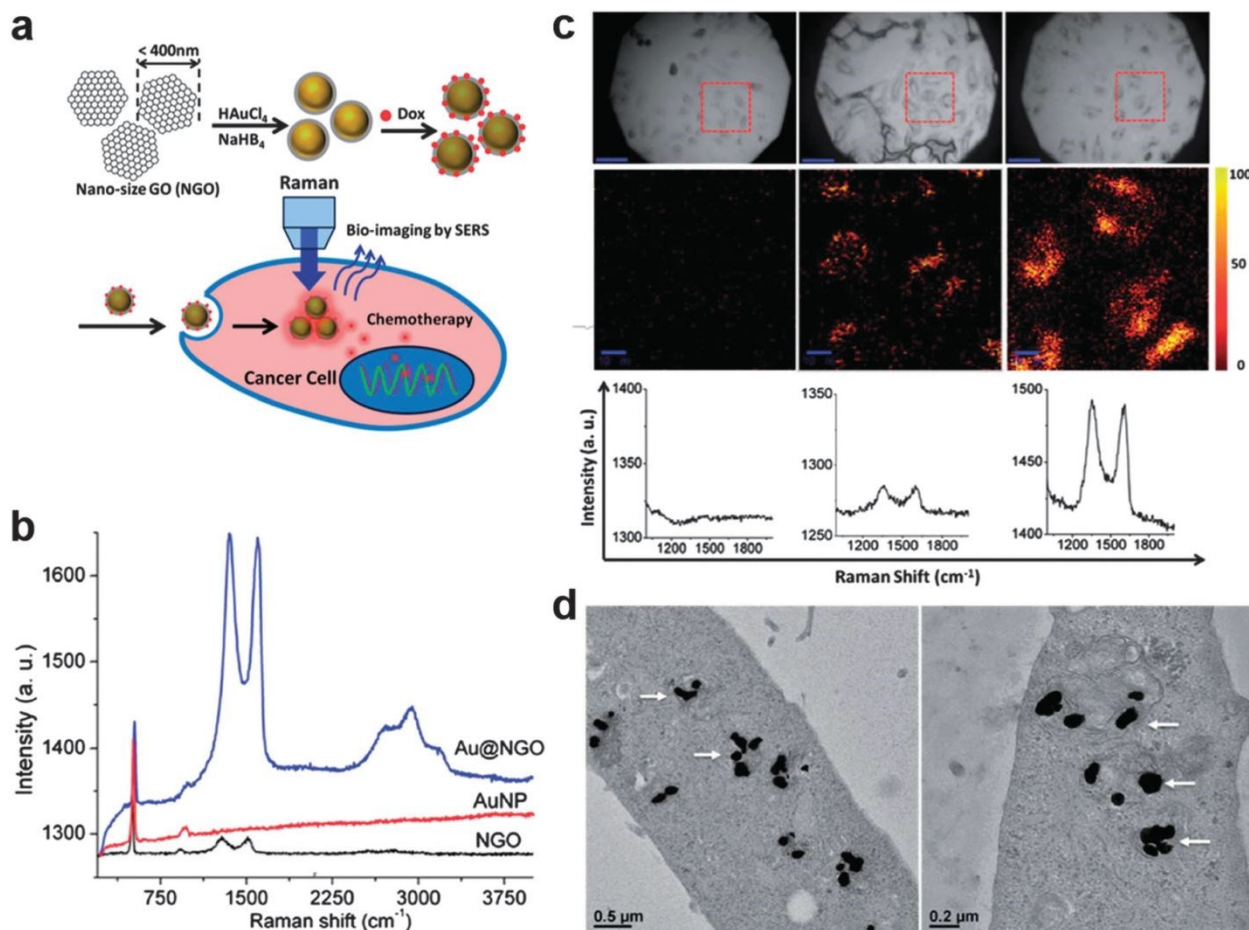
1246

1247 **Fig. 9.** Pre-irradiation and post-irradiation images of the ear blood vessels of mouse treated with a)
 1248 N-GQD-RB or b) FITC-dextran and two-photon excitation. Reprinted from [216], Copyright 2018,
 1249 with permission from John Wiley and Sons.

1250

1251 7.1.3. Raman Imaging

1252 This is a quantitative and qualitative technique to investigate the inelastic scattering of phonons
1253 originated from molecular vibration excitation mode of various molecules and biological samples
1254 [214]. It works in a nonperturbing and nondestructive manner with high signal to noise ratio and
1255 negligible photobleaching. Both graphene and GO exhibit unique intrinsic Raman signals that can
1256 be further enhanced by integrating GBNs metal NPs [217]. Wang *et al.*, reported direct reduction
1257 of silver (Ag^+) on GO to form Ag-GO hybrids which exhibited an outstanding surface-enhanced
1258 Raman spectroscopy (SERS) effect [218] and further found it helpful for effective SERS imaging
1259 of cancer cells. Hence Raman spectra of GBNs have also been applied for bioimaging. In addition
1260 to this, Song *et al.* described the dual metal doped graphene (GP) NPs by developing multi layers of
1261 graphene onto the surface of silver (Ag) and copper (Cu) alloy NPs [219]. The Ag-Cu-GP have
1262 been employed to develop characteristic Raman signals from the graphitic shell, making Ag-Cu-
1263 GP an ideal candidate for cell labeling, rapid RI and SERS detection. Further in this series Ma and
1264 co-workers reported gold nanoparticle (Au NPs) doped GO as an active imaging probe, (Figure 10)
1265 [220]. These GO-Au nanocomposites could be utilized for both intracellular bioimaging markers
1266 and DDSs.



1267

1268 Figure 10. In vitro Raman imaging using the SERS effect. (a) Schematic diagram of Au
 1269 nanoparticle–GO (Au@NGO) synthesis. (b) Raman spectra of Au@NGO and both bare materials
 1270 (AuNP and NGO). (c) In vitro Raman imaging of HeLa cells. (d) TEM images of HeLa cells
 1271 incubated with Au@NGO. Reproduced from ref. [220], with permission from The Royal Society
 1272 of Chemistry.

1273

1274

1275 7.2. Radionuclide Imaging

1276

1277 Optical imaging generally affected by auto fluorescence of tissues and cannot provide
 1278 quantitative results, while the excellent properties such as negligible penetration and high
 1279 sensitivity ($\sim 10^{-11}$ – 10^{-12} mol/L) of Radionuclide Imaging (RAI) were extensively applied for
 1280 labeling the substance *in vivo* and also for the quantitative analysis [221]. Radio labeling method
 1281 mainly contains positron emission tomography (PET) and single-photon emission computed
 1282 tomography (SPECT). The main difference between these two imaging methods is based on the

1283 characteristic of radiotracers used. In PET scans positrons produced by a specific dye containing
1284 radioactive tracers while SPECT scans is based on gamma rays scanning [222]. Hong *et al.* reported
1285 GO-PEG labeled with radioactive ^{125}I on the edges of GO. The radio labeling of nGO-PEG
1286 with ^{64}Cu was explored for active tumor targeting and imaging [223].

1287 Cao *et al.* [224] proposed an ultra-small NGO-PEG (usNGO-PEG) and NGO-PEG, then ^{125}I -
1288 radiolabeling was labeled on them for comparative retention of different sizes of NGO in the tumor
1289 via single SPECT imaging. After that six-arm branched PEG was modified to both system to
1290 compare their biocompatibility. According to longitudinal visualization of non-invasive SPECT
1291 imaging, us NGO-PEG showed longer and higher tumor accumulation than NGO-PEG, which was
1292 attributed to EPR effect and good passive targeting.

1293

1294 7.3. Magnetic Resonance Imaging (MRI)

1295 Due to the high spatial resolution and non-invasive feature, magnetic resonance imaging (MRI)
1296 has been widely applied in bioimaging field [221]. Owing to the nonselective coordination with
1297 biomolecules, paramagnetic metals ions i.e. manganese (Mn) and gadolinium (Gd) show high
1298 toxicity [225]. GO with various oxygen containing functional groups can be easily chelated with
1299 these toxic ions by clutching the ions between graphene layers, which moderate the toxic effect of
1300 these ions [214]. Gizzatov *et al.* 2014 chelated Gd^{3+} ions with carboxyphenylated graphene
1301 nanoribbons (GNRs) for enhanced MRI relaxivity [226]. Gd^{3+} ions and GNRs displayed better
1302 MRI contrast images in both longitudinal and transverse environment.

1303 Ma and Yan *et al.* developed a model for specific gene-targeting and chemotherapeutic drugs
1304 by combining of dendrimer and gadolinium-functionalized NGO (Gd-NGO) [227]. Gd-NGO can
1305 be controlled by MRI to locate the tumor area and justify quantitatively the concentration of
1306 therapeutics within the tumor. Nanosized ferrites spinel possessed supermagnetic properties and
1307 emerged as a promising contrasting agent for MRI. But due to small size, they show physiological
1308 instability. To overcome this problem, the spinels required support of dispersible agents as per
1309 authors' conclusion. Recently Alazmi *et al.* used GO as a precursor to make composites of cobalt
1310 ferrite (CoFe_2O_4) which affected greatly the average size, dispersion and magnetic behaviour of the
1311 grafted spinels nanoparticles. Results showed that GO, as a precursor, effectively enhanced the
1312 proton relaxation rate by two folds in the proposed system [228]. In addition, the aggregation of
1313 Fe_3O_4 NPs often leads to precipitation, causing shortening of circulation time in blood.

1314 Hence Fe_3O_4 NPs coated ligands have been doped with GO to make it supermagnetic hybrid
1315 conjugate (GO/IONP), which are extensively used to shorten the relaxation time of protons. For
1316 example, Chena *et al.* [200] developed a GO based system for contrasting agent by forming the
1317 aggregates of aminodextran-capped Fe_3O_4 NPs that can grip onto GO sheets to form clusters,
1318 allowing enhanced contrast for enhanced MRI compared to the isolated Fe_3O_4 NPs.

1319 **7.4. Photoacoustic Imaging**

1320 For diagnostic imaging, Photoacoustic Imaging (PAI) has generally employed due to its
1321 specific features of depth imaging and spatial resolution [229]. In PAI, the non ionizing laser pulses
1322 of lower energy are applied which causes low energy wave to penetrate deeper into the tissues and
1323 provide effective imaging.

1324 As a new diagnostic imaging modality, PAI typically requires the contrast agents (CAs) to
1325 further improve their imaging performance. Nanoprobes with strong NIR absorbances are generally
1326 regarded as the desirable CAs for this particular imaging [230].

1327 Based on the excellent NIR-absorbance performance, Patel *et al.* (2013) synthesized
1328 microwave-enabled low-oxygen graphene (ME-LOGr) which could be easily dispersed in water
1329 and used to generate PA signals with the help of NIR excitation [231]. Further, Wang and group
1330 prepared Indocyanine green (ICG) dye enhanced GO nanohybrid (ICG-GO). They found ICG-GO
1331 exhibited relatively high absorbance in the NIR region and displayed outstanding photothermal
1332 properties under NIR irradiation. After complexing the system with folic acid, *in vitro* experiments
1333 revealed that the complex could be used for targeted photothermal cancer cell destruction and for
1334 PAI demonstration [232] where this complex was used as a CA.

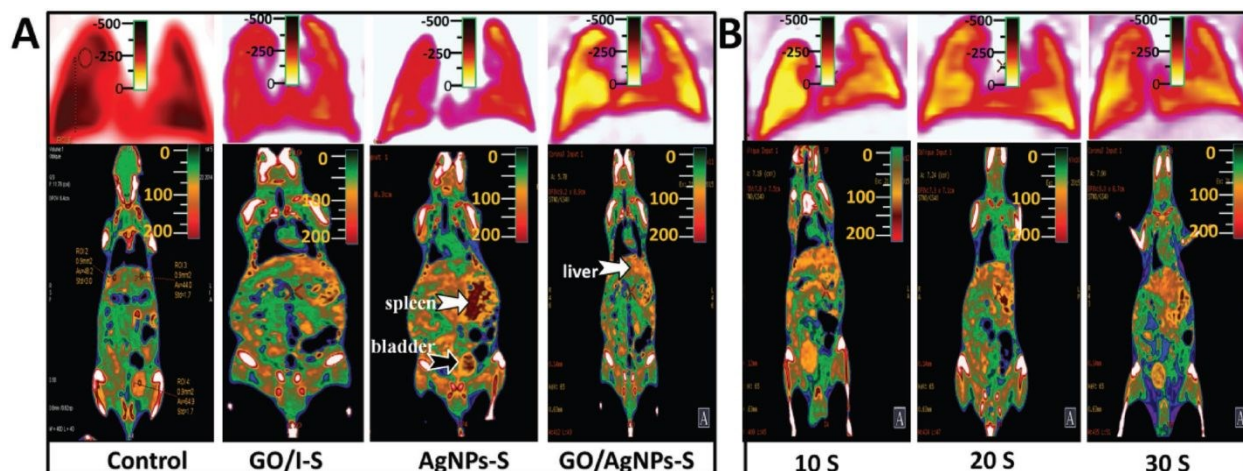
1335 Among GBNs, especially rGO and GO have cosmic application in field of medical science.
1336 Lalwani *et al.*, in 2013 reported a comparative study in context of PA effect between oxidized
1337 singlewalled GNRs (O-SWGNRs) and oxidized multiwalled GNRs (O-MW-GNRs). They found
1338 5-10 times intense signal for PAI and concluded O-GONRs as promising CAs for PAI [233].

1339

1340 **7.5. Computed Tomography**

1341 Computed Tomography (CT) is a painless imaging technique through which detailed
1342 images of the inner organs are analysed by means of X-rays. In CT the anatomic details of inner
1343 parts are subjected under X-rays which provide the detailed images of the objects. With the help
1344 of CAs such as GBNs, the diagnosis of renal dysfunction is proposed by Li *et al.* (Figure 11). They

1345 developed the GO/AgNPs composite, by deposition of AgNPs on the surface of GO, and
 1346 simultaneously injected with simvastatin to eliminate *in vivo* toxicity. They found GO/AgNPs at
 1347 even very lower dose (≈ 0.5 mg per kg bw) could enhance the imaging of CT into the liver, lung,
 1348 and kidney of mice for a long time period of approximately 1 day. Hence the modified GO has
 1349 arisen as an imaging agent, for highly sensitive CT [234].



1350
 1351
 1352 **Figure 11.**(A) CT imaging of Control, GO/I-S, AgNPs-S, and GO/AgNPs-S in mice *in vivo* after
 1353 coinjection with simvastatin for 20 min. Doses of GO/I, AgNPs, and GO/AgNPs are 5 mg per kg
 1354 bw, simvastatin dose is 20 mg per kg bw. (B) Effect of simvastatin dose on CT imaging of
 1355 GO/AgNPs, 10 S is 10 mg per bw, 20 S is 20 mg per bw, 30 S is 30 mg per bw, white bone tissue
 1356 is not included in color bar (1000 HU). Reprinted from [234], Copyright 2017, with permission
 1357 from John Wiley and Sons.

1358
 1359 Recently many literatures are published regarding the applications of GBNs sponges
 1360 (GBNSs) in biomedical field including antimicrobial activity, bioimaging etc. The applicability
 1361 and scope of their advantages depends on the post synthesis step in which the metals nanoparticles
 1362 are introduced in the carbon matrix. Smith *et al.*, reported GBCS based CT after the uptake of
 1363 silver and iron nanoparticles which provide information of nanoparticles deposition on the internal
 1364 and external structure of 3D GBNSs[235].

1365 7.6. Multimodal Imaging

1366 Each imaging modality has some specific characteristics and drawbacks which somehow limits
 1367 their application in bioimaging field. For overcome this issue and gathering the information
 1368 provided by advantages of individual imaging modality, the idea of integration of several imaging
 1369 modalities comes in the form of multimodal imaging (MI) [236]. MI provides signals *via* multiple

1370 imaging techniques simultaneously and gather all required information from various imaging
1371 modalities by eliminating the drawbacks generated due to the particular imaging technique [222].

1372 Recently, GBNs are used as building blocks for multimodal imaging due to its multifunctional
1373 chemistry and large surface area. Bai *et al.*, group designed a multi modal imaging probe based on
1374 iron oxide nano particle (IONP) doped rGO with PEG for FL, PAI, and MRI [157]. In 2014, Rong
1375 *et al.* reported the GO-PEG loaded with photosensitizer 2-(1-hexyloxyethyl)-2-devinyl
1376 pyropheophorbide- α for PDT of tumors [237]. They found GO-PEG-HPPH complex allows
1377 dual-modality FL and PET imaging.

1378 In addition to that, Zhang and group developed a system with BaGdF₅ NPs directly grown on
1379 the surface of GO nanosheets in the presence of PEG. The comparative study between Iohexol
1380 (contrast agent) and GO/BaGdF₅/PEG sheets reveals that GO/BaGdF₅/PEG shows low
1381 cytotoxicity, positive magnetic resonance (MR) contrast effect and better X-ray attenuation
1382 property than Iohexol, which enables effective dual-modality MR and X-ray CT imaging [238].

1383

1384 **8. Challenges and Outlooks**

1385

1386 **8.1. Prevention of drug from biological degradation**

1387 The drugs stability in GO is a big bottleneck in GO based drug delivery *in vivo*. The loading
1388 mechanics of drugs in GO nanosheets largely influences the drugs stability and its release which,
1389 in turn, depends on the molecular chemistry as well as their inter-matrix interactions. In pursuit,
1390 McCallion *et al.* 2016 acknowledged that various drugs can undergo binding with GO nanosheet
1391 by multivariate bonding interactions. For example, SN38 binds with GO with π - π interaction while
1392 DOX binds with GO largely due to its hydrogen bonding with GO based hydroxyl and carbonyl
1393 groups. Thus pH based stimuli govern the release of DOX under specific microenvironment which
1394 does not hold true for SN38 [239]. Furthermore, gene targeting has become an efficient tool for
1395 drug delivery which involves combining antisense oligonucleotides with drug co-loads. The
1396 stability of gene-drug combination has also scaled a different height exploiting GO based
1397 interaction cum protection. Lu *et al.* 2010 acknowledged that gene wrapped in GO matrix, either
1398 cross linked with molecular beakon or such kind of adaptors, remain stable *in vivo* and deliver
1399 payload on specific tissue targets. Linkers such as polyethylene amine (PEI) or polyamidoamine
1400 (PAMAM) may serve excellently to acquiesce such kind of gene-GO loading. The authors also
1401 discussed that the genes become resistant to the DNase attack upon such kind of loading [240]. In

1402 addition, we have mentioned that computational studies have already discovered loading
1403 mechanism to improve stability of the drugs. For example, Molecular dynamics simulation on
1404 DOX loaded GO showed that functionalizing GO with polymer like PEG improves drug's stability
1405 in matrix [241]. Furthermore, stable loading of hydrophobic drug on GO may be achieved using
1406 supramolecular GO nanosheets where secondary carrier like beta cyclodextrin may be nested with
1407 the former. This augments drug stability due to its interactions with both GO and cyclodextrin.
1408 Thus for improving drug stability inside GO matrix, we may suggest the following key scores:

- 1409 1) Choice of suitable polymer for functionalizing GO depending upon the drug molecule or
1410 combination.
- 1411 2) Choice of Janus structure discussed earlier, if required, for concomitant loading of hydrophilic
1412 and hydrophobic drugs
- 1413 3) Choice of linkers such as PEI or PAMAM for improving stability of loaded gene on GO matrix.
- 1414 4). Consideration of secondary carrier such as cyclodextrin nested in GO for improving stability
1415 and release of drugs.

1416 **8.2. Effective targeting**

1417 In last a few years, a lot of engineering approaches have been reported to formulate target
1418 specific drug delivery system, still the complexity of target tissue, disease specific gene or protein
1419 expression, system metabolomics, microenvironment of the target cell have been laying spectrum
1420 of challenges in designing target specific drug delivery. One of the potential outlooks of these
1421 challenges is to endow the delivery system with cDNA or siRNA whose shorter version has been
1422 the application of aptamers. Now, the stability of cDNA or siRNA inside body is another challenge
1423 to the scientists, so a balance between between target specificity and chemical modification of the
1424 cDNA or siRNA is required in the outlook to solve this challenge. RGD or other peptidomimetics
1425 based targeting has also been another alternative to this approach where surface of the GO is
1426 manipulated with such peptides to lead the delivery to the target. Cellular uptake and cleavage by
1427 proteolytic enzymes in blood or other body fluids are major challenges of using peptides in drug
1428 delivery system. Furthermore, using folic acid (FA) or other epitopes have evolved as potential
1429 outlooks herein, challenges have still remained to perturb myriads of complex cases *in vivo* through
1430 target specific drug delivery which is also true for our GO based system. For example, as per our
1431 previous discussion, Hyaluronic acid (HA) solitarily can be coated over GO nanodevice to target
1432 this towards cancerous cells. To add to this, HA conjugated with RGD peptide (Arg-Gly-Asp)

1433 could be effectively used to target DOX loaded GO towards cancer endosomes [242]. Thus
1434 effective targeting of GO based drug delivery has been being studied through various avenues and
1435 reasonable success of these routes has promised solution of off-target accosting of such devices in
1436 physiological system.

1437

1438 **8.3. Cost effectiveness**

1439 Cost effectiveness is always a challenge for engineered or smart drug delivery system
1440 (DDS) over the decades. The use of natural, synthetic or co-polymers; use of primary nanocarriers,
1441 operational or manufacturing cost have been some of the primary cost influencing factors which
1442 are unique for the process and product. Choice of drug depends on the target disease whereas
1443 distribution, marketing and such others are inevitable constant parameters which levy a fixed
1444 percentage of cost into the final product pricing. Thus, the first stated factors usually help to tune
1445 the cost of an engineered DDS. For fabrication of a nanodevice, the choice of nanomaterial and its
1446 procurement cost is a prime important factor. In this context, GBNs or GO has already been
1447 acknowledged by various authors as cheaper raw materials compared to other nano fabricating
1448 materials [35]. Recently Pandey *et al* 2019 has devised a new technology to synthesize graphene
1449 nanosheets from waste plastic in bulk scale which has showed a new way to produce graphene in
1450 considerably lower cost compared to other technologies [243]. The authors calculated the cost of
1451 produced graphene with all expense parameters and compared with that of commercially available
1452 graphene sheets in the market. While 1 gram of commercially available graphene costs around 100
1453 USD-200 USD, the cost of 1 gram of graphene obtained from waste plastic recycling has projected
1454 around 1 USD [244]. The technology transfer is under process, and once finalized, may
1455 revolutionalize the graphene based industries round the globe by bringing down the production
1456 cost of raw graphene significantly.

1457

1458 **9. Conclusion and future prospective**

1459 Hence from the entire review, it can be concluded that graphene oxide either its own or in
1460 reduced form can be an excellent carrier for fabricating various biomedical devices. Although GO
1461 due to its high carbonaceous structure, has significant toxicity *in vivo*, the toxicity is often
1462 minimized by covalently crosslinking it with biocompatible cosolvents such as PEG, PVA or
1463 PVP). The GO-PEG or GO-PVA/PVP system could be efficiently utilized as functionalized

1464 nanocarrier for further biomedical applications. Graphene oxide can be efficiently designed with
1465 various polymer and co-polymers (such as PAm, PNIPAAm, PMA) to deliver single drugs where
1466 depending on polymers surface chemistry, its π -electron cloud, ring opening reaction, electron
1467 donating or accepting capacity, various drugs of differential polarity can be loaded onto GO-
1468 polymer conjugate. While delivered *in vitro* or *in vivo*, the drug-carrier shows excellent stability,
1469 steady drug release and improved biocompatibility. This type of single drug delivery has been
1470 widely used in cancer therapy on trial basis, where the actual formulation of GO based anticancer
1471 therapy is yet to come. In addition, when used for administering combination drugs such as DOX-
1472 CPT, DOX-5FU, Epirubicin-Temozolomide, QSR-GEF, the synergistic action of the component
1473 drugs have been revealed. Although this type of dual drug loading is challenging and requires lots
1474 of surface engineering of GO-Polymer conjugate, the final dual drug-GO sandwich is one
1475 promising potential for tackling critical diseases since synergistic action of drugs herein improves
1476 therapeutic potential of them in many folds. To further engineer its release pattern, cell
1477 permeability and stability, various engineered GO micro devices such as GO nanosheets (GON),
1478 GO SPION nanosheets, GQDs, ZnO doped GO, GO-hyaluronic acid combination with peptide
1479 modification have been fabricated. Janus structured nano device based on GO and especially
1480 surface engineered GO (such as using SI-RAFT technology) have been blessings to potentiate
1481 combination drug loading of various polarity or to improve its biocompatibility. Stimuli responsive
1482 GO based drug delivery has been another promising toolkit of modern days biomedical sciences.
1483 Since GO or rGO can be surface engineered with temperature, pH or photosensitive polymers or
1484 dyes; subsequent thermoresponsive, pH responsive or photosensitive (leading to PDT) GO or rGO
1485 nanoboats have been fabricated which have shown promising drug release under special
1486 microenvironment inside body with controlled irradiation with laser or NIR in cases. The surface
1487 of GO can be further wrapped with various cell recognition genes or peptides which can redirect
1488 the GO-drug micromotor towards desired site, attach onto this and subsequently infiltrate within
1489 the cell or endosome. This finally leads to reduced toxicity and improved output of the candidate
1490 drug under the specific disease condition. Using the electrical property of graphene, its high
1491 conductivity and high energy electron emission, GQDs have been positively used in MRI imaging
1492 or photon based imaging. Using its ability to couple with other nanoparticles such as Ag or Fe₃O₄
1493 nanoparticle, which leads to formation of supramagnetic nanohybrid, has facilitated MRI imaging
1494 in biomedical sciences. The GO has been further coupled with radioisotopes, fluorescent dyes to

1495 devise radionucleotide based or fluorescent based imaging. Recently FRET based imaging devices
1496 on GO have also been brought into limelight which has opened the gateway of finely tuned
1497 bioimaging operations under highly sensitive microenvironment inside body.

1498 Graphene oxide has a huge potential in futuristic applications of biomedical field. The first
1499 application we can suggest is its antibacterial and antiviral potential. Due to its unique polygonal
1500 structure of catenated carbon atoms, GO possess the ability to damage cell membrane of microbes.
1501 Plus, Graphene oxide produces cluster of free radicals which may damage the microbial cell
1502 membrane as well as other organelles [245,246]. This encompasses huge potential in devising non-
1503 antibiotic antimicrobial that may help in combating antibiotic resistance all over the globe.

1504 Another future application of GBNs is heat-therapy which achieved by raising the surface
1505 temperature upon photon irradiation through tactful modification of the same. For example, Jiang
1506 *et al* 2019 reported that bacterial cellulosed entrapped graphene oxide can be used as antibacterial
1507 candidate, which upon reduction with chemical treatment forms nanocomposite of reduced
1508 graphene oxide (rGO) in cellulosic membrane. This nanocomposite upon irradiation with normal
1509 light undergoes thermal activation sensed by its temperature elevation. In Jiang's work this
1510 technology has been used to fabricate biomembrane which killed microbe and deterred biofouling
1511 [247]. We propose that this technology can be implemented *in vivo* to treat resistant microbe or
1512 acrid tumours (malignant or benign) which are otherwise hard to treat by simple chemical or
1513 peptide based therapies. In addition Chen *et al* 2019 showed that, the surface -COOH groups, if
1514 functionalized with sulfhydryl (-SH) groups of L-cysteine, becomes photothermally active. The
1515 authors reported that when challenged against microbes, this nanodevice efficiently invaded the
1516 microbial cells by first tearing their cell membranes with its knife edged polycarbonaceous surface,
1517 later subjected then to photothermal ablation [248]. This therapeutic supremacy may be utilized
1518 against various kinds of tedious infections such as pneumonia, gonorrhea, tuberculosis, blood
1519 poisoning and food borne diseases as suggested by the authors.

1520 Next futuristic application of Graphene based polymer is application of the same in stimuli
1521 responsive form thus making it more target specific as well more potent in executing therapeutic
1522 payloads. As discussed earlier, pH responsive and temperature sensitive GBN has been
1523 successfully designed with selective polymer coupling and allowing their ring opening mechanism
1524 under the particular stimuli. Even electroresponsive graphene based nanomaterial has been
1525 undertaken as a drug carrier where pulsatile release of drugs under various voltages have shown

1526 great promise [249]. Furthermore, tagging the GBNs with photosensitizing electrophores such as
1527 Ce6 or other porphyrin derivatives, PDT has been evolved. We suggest that this kind of therapy in
1528 future may be used to treat various form of malignant tumours or microbial endosome *in vivo*
1529 which in otherwise, be extremely difficult to treat. In this era of Covid-19 pandemic, where
1530 mutated microbe is endowed with indomitable penetration power in respiratory organs, this kind
1531 of therapy may be an alternative to virostatic or virocidal agents in respective organs.

1532 Surface engineered Graphene oxide with oligonucleotides can also be used as successful
1533 candidate to design target specific therapy in future. As described earlier, aptamer functionalized
1534 Graphene oxide was successfully used to deliver drug molecules in target specific fashion. The
1535 abundant –COOH groups on GO help in aptamer conjugation through cross linking of its –
1536 NH₂ groups with former's carboxyl terminal. We also propose that this target specific therapy can
1537 be effectively utilized to deliver any kind drug molecules to desired targets.

1538 Another promising application of using GBNs in biomedical field lies in strategic and smart drug
1539 loading within its matrices. For example, GO so far has been used mostly to incorporate
1540 hydrophobic drug such as DOX in solitary fashion. However, one of the most interesting and
1541 potential approach of loading combination drugs is application of Janus based nanostructure over
1542 GBNs which has already been discussed in this review. Since two drug molecules often have
1543 differential polarity, simultaneous loading of both the drugs on symmetrically functionalized
1544 GBNs have often faced with adverse interactions. This kind of orthodox loading has led to either
1545 poor loading of drugs or sub-optimum release of drug particles in the solution. However, in Janus
1546 structure GBNs where two surfaces of GO matrix have been functionalized with two differently
1547 polar polymers, loading of hydrophilic-hydrophobic drug combination has reached new efficiency
1548 with potential release kinetics as described earlier. The application of Janus based GBNs in drug
1549 delivery has started in recent past and holds great promise in vast pool of biomedical sciences in
1550 future.

1551 Apart from Janus nanostructure, how could the drug loading and release be improved in future
1552 GBNs applications? In this pursuit, Molecular dynamics (MD) simulation has been a popular
1553 approach to delineate drug-polymer dynamics and thus design the future drug-nano conjugate for
1554 improved stability and bioavailability. In a few MD simulation studies related to GO and its cross
1555 linking polymer and drugs like DOX has revealed that functionalization GO with PEG has a great
1556 impact on stability and release of DOX from the polymer matrix [241]. In other MD simulation

1557 studies, it has also been revealed that the diameter of the guest molecules together with dimension
1558 of GO nanosheets greatly influences binding energy, molecular cross-walking of the candidates,
1559 diffusion and release of them in liquid mediums. Not only that but also it is the molecular structure
1560 and chemistry of the candidates which determine their best loading mode on GO through either
1561 single or double surfaces of it [250]. Although it has been explored only on a few molecules and
1562 functional polymer such as PEG, there is a huge scope to explore such kind of molecular dynamics
1563 between other kinds of drug molecules and various functional polymers such as PVA, PVP, PAm.
1564 NIPAAm, DDMAT. This would help to design properly functionalized GBNs, choosing right drug
1565 molecules, resulting in better loading of drugs with improved release kinetics both *in vitro* and *in*
1566 *vivo*.

1567 The next futuristic application of GBN is to build supramolecular GO using nested GO structure
1568 using cross linking with inclusion complexes with cyclodextrins (CD). Since cyclodextrins have
1569 excellent capacity to accommodate hydrophobic molecules in its inner core using hydrogen
1570 bonding with its multiple functional –OH groups, tethering GO with such channel lattice or
1571 clathrates may revolutionize drug delivery in future application. Since β -CD and Hydroxypropyl
1572 propyl beta cyclodextrin (HP- β -CD) have improved aqueous solubilities, drug release from both
1573 these matrices are steady and efficient in biological fluids. Exploiting this property, poor drug
1574 release from functionalized GO which is largely hydrophobic and hold the drug with π - π
1575 interactions, could be solved. The supramolecular β -CD-GO nanocage would have the
1576 amalgamated potential of efficient targeting the drug within the cell, trigger its stimuli responsive
1577 performance and release the molecule efficiently at the end. One of such attempt has already been
1578 discussed by Cruz and Coworker at 2019.

1579 Genetherapy has been a promising target now a days where genes are delivered within the
1580 recipient cell either to correct a malfunctioning gene or to make the gene act as a therapeutic
1581 candidate within the cell. Exploiting this, attempts have been made to co-administer gene and drug
1582 together in order to potentiate each other's action. As discussed earlier in our review, siRNA or
1583 plasmid DNA protected gene therapy *via* GO based carrier can efficiently deliver the genes to the
1584 target cell. It has been acknowledged that suitable grafting of GO by PEI or polyamidoamine
1585 (PAMAM) together with GO-PEG or GO-chitosan can successfully deliver gene towards target
1586 cell. We are hopeful that this gene delivery can be very beneficial in future to boost administration
1587 of gene-drug cocktail to various diseases such as cancer, AIDS, different viral infections, various

1588 gene associated disorders such as Glucose-6-phosphate deficiency, haemolytic anemia,
1589 autoimmune disorders, Huntington's disease and many others.

1590 Due to its unique chemistry and energy potential GO or its derivative can effectively cross blood
1591 brain barrier. As reported in our earlier discussion, using this potential epirubicin and temzolomide
1592 combination has been effectively targeted to treat paediatric brain tumour. Thus, there is a great
1593 future potential of treating various brain related disorders using functionalized GO encapsulating
1594 drug-drug or drug gene combination.

1595 Although acknowledged in review, graphene oxide has been mainly studied so far against cancer
1596 and tumours in medical science field, Owonubi *et al* in 2015 and 2018 studied the effect of GO
1597 with binomial drug cocktail against other diseases such as diabetes and malaria. Following this,
1598 Ge *et al* 2019 reported that bionomially coated GO, one surface with docetaxel and other surface
1599 with anticoagulant heparin, was successfully used in Cardiovascular stent which showed no
1600 noticeable aggregation or thrombosis when implanted inside zebrafish body [251]. In addition,
1601 various scientists are trying to envisage the pulmonary application of GO by studying its toxicity
1602 and biotransformation within alveolar fluids, subsequently the effect of biotransformation on the
1603 drug delivery pattern of GO [252]. Another interesting observation has been revealed by Afzali
1604 and coworkers that GO could increase the number of Kupffer cells in liver when tested in mouse
1605 embryo [253]. Thus it is very encouraging to observe GO applications being studied in other
1606 biomedical fields apart from cancer with a strategic effort to down-regulate its toxicity. These
1607 efforts can be further channelized in future to utilize GO against various other diseases such as
1608 atherosclerosis, liver disfunction, cardiovascular diseases, coronary thrombosis, bone
1609 regeneration, osteoporosis, Type I and II diabetes mellitus and many others.

1610 In bioimaging field, plethora of improved technology have been being tried with GO and as in
1611 the review, all of them have been reported to provide image of target organ or organelles
1612 successfully. Radionucleotide based imaging, photoacoustic imaging, two photon based imaging,
1613 fluorescence based imaging, MRI, CT to FRET based imaging all have provided scientists wider
1614 windows to capture snapshots of various organs or cell stages at different diseased conditions. We
1615 hope that exploiting various unique properties of GO as discussed above, the imaging science can
1616 galore to a different benchmark with holograms of captivating various life patterns with or without
1617 abnormalities. This would aid scientists propose various dogmas, technicalities and solutions of
1618 biological sciences which world has not witnessed so far.

1619 Overall, we would like to be optimistic in utilizing GO and its multifaceted grafted systems for
1620 multimodal applications in biomedical field which has yet to be explored in coming eras. As a part
1621 of that, in this review we have tried to revisit some recent advancements of it involving polynomial
1622 drug delivery from single GO based switches, its current status and mechanisms, advancements in
1623 grafting technology to manufacture such smart switches and various alleys of bioimaging sciences
1624 that has progressed to ultrasensitivity in capturing different microcosms of life. We have also
1625 discussed the unfathomable opportunities to explore GO based nanodevices in biomedical
1626 applications which may scale a different height in drug delivery or bioimaging science. We hope,
1627 our small attempt of this review would help scientists to plan, dive and progress in this ocean in
1628 future days.

1629

1630 **Acknowledgements**

1631 The author(s) are greatly thankful for the financial assistance from the National Mission of
1632 Himalayan Studies (NMHS), Kosi Kataramal, Almora, India.

1633

1634

1635

1636

1637

1638 **10. References**

- 1639 1. S. Virani, J. A. Colacino, J. H. Kim and L. S. Rozek, *ILAR J.*, 2012, **53**, 359–369.
- 1640 2. A. Lage and T. Crombet, *Int. J. Environ. Res. Public Health*, 2011, **8**, 683–697.
- 1641 3. S. Goel, C. G. England, F. Chen and W. Cai, *Adv. Drug Delivery Rev.* 2017, **113**, 157-176.
- 1642 4. H. Kim, K. Chung, S. Lee, D. H. Kim and H. Lee, *Wiley Interdiscip. Rev.: Nanomed.*
1643 *Nanobiotechnol.* 2016, **8**, 23–45.
- 1644 5. O. L. Gobbo, K. Sjaastad, M. W. Radomski, Y. Volkov and A. P. Mello, *Theranostics*,
1645 2015, **5**, 1249–1263.
- 1646 6. G. D. Crozals, R. Bonnet, C. Farre and C. Chaix, *Nano Today*, 2016, **11**, 435-463.
- 1647 7. A.K. Geim, K.S. Novoselov, *Nat. Mater.*, 2007, **6**, 183-191.
- 1648 8. W.S. Hummers, R.E. Offeman, *J. Am. Chem. Soc* 1958, **80**, 1339.

- 1649 9. X. Sun, Z. Liu, K. Welsher, J. Robinson, A. Goodwin, S. Zaric, H.J. Dai, *Nano Res.*, 2008,
1650 1, 203-212.
- 1651 10. Z. Liu, J. Robinson, X. Sun, and H. Dai, *J. Am. Chem. Soc.*, 2008, **130**, 10876-10877.
- 1652 11. G. Modugno, C. M. Moyon, M. Prato and A. Bianco, *Br. J. Pharmacol.*, 2015, **172**, 975–
1653 991.
- 1654 12. X. Zhu, Y. Liu, P. Li, Z. Nie and J. Li, *Anst.*, 2016,**141**, 4541-455.
- 1655 13. N. Karki, H. Tiwari, M. Pal, A. Chaurasia, R. Bal, P. Joshi and N. G. Sahoo, *Colloids and*
1656 *Surfaces B: Biointerfaces*, 2018, **169**,265–272.
- 1657 14. N. G. Sahoo, Y. Pan, L. Li and C. B. He, *Nanomedicine*, 2013, **8**, 639-653.
- 1658 15. A. Nandi, C. Ghosh, A. Bajpaib and S. Basu, *J. Mater. Chem. B*, 2019,**7**, 4191.
- 1659 16. C. Nie, L. Ma, S. Li, X. Fan, Y. Yang, C. Cheng, W. Zhao and C. Zhao, *Nano Today*,
1660 2019, 26, 57-97.
- 1661 17. X. Fan, F. Yang, C. Nie, Y. Yang, H. Ji, C. He, C. Cheng and C. Zhao, *ACS Applied*
1662 *Materials & Interfaces*, 2018, 10, 296-307.
- 1663 18. C. Argyo, V. Weiss, C. Bräuchle and T. Bein, *Chem. Mater.* 2013, **26**, 430–434.
- 1664 19. F. Li, H. Pei, L. Wang, J. Lu, J. Gao, B. Jiang, X. Zhao and C. Fan, *Adv. Fun. Mater.* 2013,
1665 **23**, 4140-4148.
- 1666 20. C. Cheng, S. Li, A. Thomas, N. A. Kotov and R. Haag, *Chem. Rev.*, 2017, **117**, 1826–1914.
- 1667 21. T. Kuila, S. Bose, A. K. Mishra, P. Khanra, N. H. Kim and J. H. Lee, *Prog. Mater. Sci.*,
1668 2012, **57**, 1061–1105.
- 1669 22. A. Battigelli, C. M. Moyon and A. Bianco, *J. Mater. Chem. B*, 2014, **2**, 6144-6156.
- 1670 23. J. G. Yu, F. P. Jiao, X. Q. Chen, X. Y. Jiang, Z. G. Peng, D. M. Zeng and D. S. Huang, *J.*
1671 *Cancer Res. Ther.* 2012, **8**, 348–354.
- 1672 24. H. Sadegh and R. Shahryari-ghoshekandi, *Nanomed. J.* 2015, **2**, 231–248.
- 1673 25. Z. M. Markovic, L. M. Harhaji-Trajkovic, B. M. Todorovic-Markovic, D. P. Kepic K. M.
1674 Arsikin, S. P. Javanovic, A. C. Pantovic, M. D. Dramicanin and V. S. Trajkovic,
1675 *Biomaterials*, 2010, **32**, 1121–1129.
- 1676 26. A. K. Geim, K. S. Novoselov, *Nat. Mater.* 2007, **6**, 183-191.
- 1677 27. E. Widenkvist, *Fabrication and functionalization of graphene and other carbon*
1678 *nanomaterials in solution*, 2010, *Acta Universitatis Upsaliensis*, Uppsala.

- 1679 28. T. L. Moore, R. Podilakrishna, A. Rao and F. Alexis, *Part. Part. Syst. Charact.* 2014, **31**,
1680 886–894.
- 1681 29. X. Pei, Z. Zhu, Z. Gan, J. Chen, X. Zhang, X. Cheng, Q. Wan and J. Wang, *Sci. Rep.* 2020,
1682 **10**, 1-15.
- 1683 30. K. Butte, M. Momin, S. Kurhade and S. Kar, *Int. J. Pharm. Chem. Biol. Sci.*, 2013, **3**, 680–
1684 681.
- 1685 31. Z. Liu, W. B. Cai, L. He, N. Nakayama, K. Chen, X. Sun, X. Chen and H. Dai, *Nat.*
1686 *Nanotech.* 2007, **2**, 47–52.
- 1687 32. X. Zhang, Y. Feng, S. Tang and W. Feng, *Carbon*, 2010, **48**, 211–216.
- 1688 33. N. V. Medhekar, A. Ramasubramaniam, R. S. Ruoff and, V. B. Shenoy, *ACS Nano*, 2010,
1689 **4**, 2300-2306.
- 1690 34. M. Hu and B. Mi. *J. Membrane Sci.* 2014, **469**, 80-87.
- 1691 35. C. Lin, Y. T. Liu, and X. M. Xie, *Aust. J. Chem.* 2014, **67**, 121-126.
- 1692 36. P. Song, Z. Xu, Y. Wu, Q. Cheng, Q. Guo and H. Wang, *Carbon*, 2017, **111**, 807-812.
- 1693 37. J. Liu, W. Yang, L. Tao, D. Li, C. Boyer and T. P. Davis. *J. Polym. Sci.* 2010, **48**, 425-
1694 433.
- 1695 38. M. Zhi, W. Huang, Q. Shi, and K. Ran, *J. Mater. Sci. Mater. Electron.* 2016, **27**, 7361–
1696 7368.
- 1697 39. H. Hu, J. Yu, Y. Li, J. Zhao and H. Dong, *J. Biomed. Mater. Res. A*, 2012, **100**, 141-148.
- 1698 40. D. Depan, J. Shah and R.D.K. Misra, *Mater. Sci. Eng. C*, 2011, **31**, 1305-1312.
- 1699 41. L. Yan, Y. N. Chang, L.N. Zhao, Z. J. Gu, X. X. Liu, G. Tian, L. J. Zhou, W. L. Ren,
1700 S. Jin, W.Y. Yin, H. Chang, G. Xing, X. Gao and Y. Zhao, *Carbon*, 2013, **57**, 120-129.
- 1701 42. L. Zhang, J. Xia, Q. Zhao, L. Liu and Z. Zhang, *small*, 2010, **6**, 537-544.
- 1702 43. X. Yang, Y. Wang, X. Huang, Y. Ma, Y. Huang, R. Yang, H. Duan and Y. Chen, *J. Mater.*
1703 *Chem.* 2011, **21**, 3448-3454.
- 1704 44. H. Mok, J. W. Park and T. G. Park, *Bioconjug. Chem.*, 2008, **19**, 797–801.
- 1705 45. Y. Lei, G. Zhang and H. Li, *Mater. Sci. Eng.*, 2017, **274**, 012115.
- 1706 46. H. Kim, D. Lee, J. Kim, T. I. Kim and W. J. Kim, *ACS Nano* 2013, **7**, 6735–6746.
- 1707 47. J. Q. Chen, H. Y. Liu, C. B. Zhao, G. Q. Qin, G. N. Xi, T. Li, X. P. Wang and T. S. Chen,
1708 *Biomaterials*, 2014, **35**, 4986–4995.

- 1709 48. L. Yan, C. L. Z. Ya-Nan, G. Zhanjun, L. Xiaoxiao, T. Gan, Z. Liangjun.
1710 Carbon, 2013, **57**, 120-129.
- 1711 49. S. Guo, Y. Nishina, A. Bianco and C. Ménard-Moyon, *Angew. Chem.* 2020, **59**, 1542-
1712 1547.
- 1713 50. B. P. Jiang, B. Zhou, Z. Lin, H. Liang and X. C. Shen, *Chem. Eur. J.* 2019, **25**, 3993-4004.
- 1714 51. N. Cheeveewattanagul, E. Morales-Narváez, A.R. H. A. Hassan, J. F. Bergua, W.
1715 Surareungchai, M. Somasundrum and A. Merkoçi, *Adv. Funct. Mater.* 2017, **27**, 1702741-
1716 1702748.
- 1717 52. J. A. Burger and T. J. Kipps, *Blood*, 2006, **107**, 1761–1767.
- 1718 53. C. J. Shih, S. Lin, R. Sharma, M. S. Strano and D. Blankschtein. *Langmuir*, 2012, **28**, 235–
1719 241
- 1720 54. U. Ahn, H. Gaiji, T. Kim, M. Abderrabba, H. W. Lee and B. S. Kim, *J. Membr. Sci.* 2019,
1721 **585**, 191-198.
- 1722 55. X. Yang, X. Zhang, Z. Liu, Y. Ma, Y. Huang and Y. Chen, *J. Phys. Chem. C*, 2008, **112**,
1723 17554–17558.
- 1724 56. J. Bytesnikova, L. Richtera, K. Smerkova and V. Adam, *Environ. Sci. Poll. Res.* 2019,
1725 **26**, 20148–20163.
- 1726 57. S. Stankovich, D. A. Dikin, R. D. Piner, K. A. Kohlhaas, A. Kleinhammes, Y. Jia, Y. Wu,
1727 S. T. Nguyen and R. S. Ruoff, *Carbon*, 2007, **45**, 1558–1565.
- 1728 58. X. Li, G. Zhang, Y.; X. Bai, X. Sun, X. Wang, E. Wang and H. Dai, *J. Nat. Nanotechnol.*
1729 2008, **3**, 538–542.
- 1730 59. C.J Shih, S. Lin, R. Sharma, M. S. Strano, and D. Blankschtein, *Langmuir*, 2012, **28**, 235–
1731 241.
- 1732 60. F. Kim, L. J. Cote and J. K. Huang, *Adv. Mater.* 2010, **22**, 1954–1958.
- 1733 61. J. Kim, L. J. Cote, F. Kim, W. Yuan, K. R. Shull and J. X. Huang, *J. Am. Chem. Soc.* 2010,
1734 **132**, 8180–8186.
- 1735 62. H. Bai, C. Li, X. Wang and G. Shi, *Chem. Commun.* 2010, **46**, 2376–2378.
- 1736 63. X. Yang, X. Zhang, Z. Liu, Y. Ma, Y. Huang and Y. Chen, *J. Phys. Chem. C*, 2008, **112**,
1737 17554–17558.
- 1738 64. J. T. Chen, Y. J. Fu, Q. F. An, S. C. Lo, S. H. Huang, W. S. Hung, C. C. Hu, K. R. Lee,
1739 and J. Y. Lai, *Nanoscale*, 2005, **5**, 9081–9088.

- 1740 65. A. Pourjavadi, M. Kohestanian and M. Yaghoubi, *New J. Chem.* 2019, **43**, 18647-18656.
- 1741 66. J. C. Sung, B. L. Pulliam and D. A. Edward, *Trends Biotechnol.* 2007, **25**, 563-570.
- 1742 67. G. R. Bardajee and Z. Hooshyar, *J. Polym. Res.* 2017, **24**, 1-8.
- 1743 68. Y. Lei, G. Zhang and H. Li, *IOP Conf. Series: Mater. Sci. Eng.* 2017, **274**, 012115.
- 1744 69. H. Wang, D. Sun, N. Zhao, X. Yang, Y. Shi, J. Li, Z. Su and G. Wei, *J. Mater. Chem. B*,
- 1745 2014, **2**, 1362.
- 1746 70. L. Yang, Y.T. Tseng and G. Suo, *ACS Appl Mater Inter.* 2015, **7**, 5097-5106.
- 1747 71. L. Yan and L. Qiu, *Nanomedicine*, 2015, **10**, 361-373.
- 1748 72. A. Sahu, W. I. Choi, J. H. Lee and G. Tae, *Biomaterials*, 2013, **34**, 6239-6248.
- 1749 73. P. Kalluru, R. Vankayala, C. S. Chiang and K. C. Hwang, *Biomaterials*, 2016, **95**, 1-10.
- 1750 74. P. Agostinis, K. Berg, K. A. Cengel, T. H. Foster, A. W. Girotti, S. O. Gollnick, S. M.
- 1751 Hahn, M. R. Hamblin, A. Juzeniene, D. Kessel, M. Korbelik, J. Moan, P. Mroz, D. Nowis,
- 1752 J. Piette, B. C. Wilson and J. Golab, *CA Cancer J Clin.* 2011, **61**, 250-281.
- 1753 75. Y. Cho, H. Kim and Y. Choi, *Chem Commun (Camb)*. 2013, **49**, 1202-1204.
- 1754 76. T. F. Cabada, C. S. L. de Pablo and A. M. Serrano, *Int. J. Nanomed.* 2012, **7**, 1511-1523.
- 1755 77. M. Vila, M.C. Matesanz and G. Gonçalves, *Nanotechnol.* 2014, **25**, 035101.
- 1756 78. L. Ma, M. Zhou, C. He, S. Li, X. Fan, C. Nie, H. Luo, L. Qiu and C. Cheng, *Green Chem.*
- 1757 2019, **21**, 4887-4918.
- 1758 79. P. Dua, J. Yanb, S. Longa, H. Xiongb, N. Wena, S. Caib, Y. Wanga, D. Pengc, Z. Liub and
- 1759 Y. Liua, *J. Mater. Chem. B*, 2020, **8**, 4046-4055.
- 1760 80. Y. Li, H. Dong, Y. Li and D. Shi, *Int. J. Nanomedicine*, 2015, **10**, 2451.
- 1761 81. Y. Ding, L. Zhou and X. Chen, *Int. J. Pharmaceut.* 2016, **498**, 335-346.
- 1762 82. Y. Cho and Y. Choi, *Chem Commun.* 2012, **48**, 9912-9914.
- 1763 83. S. Khoei and M. R. Karimi, *Polymer*, 2018, **142**, 80-98.
- 1764 84. X.M. Li, L. Zhou, Y. Wei, A.M. El-Toni, F. Zhang and D.Y. Zhao, *J. Am. Chem. Soc.*
- 1765 2014, **136**, 15086-15092.
- 1766 85. X. Zhao and P. Liu, *RSC Adv.* 2014, **4**, 24232-24239.
- 1767 86. J. Wang, C. Liu, Y. Shuai, X. Cui and L. Nie, *Colloids Surf. B*, 2014, **113**, 223-229.
- 1768 87. D. Li, M. B. Muller, S. Gilje, R. B. Kaner and G. G. Wallace, *Nat. Nanotechnol.* 2008, **3**,
- 1769 101-105.

- 1770 88. I. Chowdhury, M. C. Duch, N. D. Mansukhani, M. C. Hersam and D. Bouchard, Environ,
1771 Sci. Technol. 2013, **47**, 6288–6296.
- 1772 89. M. M. Gudarzi, Langmuir, 2016, **32**, 5058-5068.
- 1773 90. S. Stankovich, R. D. Piner, X. Chen, N. Wu, S. T. Nguyen and R. S. Ruoff, J. Mater. Chem.
1774 2005, **16**, 155-158.
- 1775 91. M. Wang, Y. Niu, J. Zhou, H. Wen, Z. Zhang, D. Luo, D. Gao, J. Yang, D. Liang and Y.
1776 Li, Nanoscience, 2016, **8**, 14587-14592.
- 1777 92. Z.S. Singh, Nanotechnol. Sci. Appl. 2016, **9**, 15–28.
- 1778 93. E. L. Chng and M. Pumera, Chem-Eur J. 2013, **19**, 8227-8235.
- 1779 94. Y. Li, L. Feng and X. Shi, Small, 2014, **10**, 1544-1554.
- 1780 95. S. F. Kiew, L. V. Kiew, H. B. Lee, T. Imae and L.Y. Chung, J. Control. Release. 2016,
1781 **226**, 217-228.
- 1782 96. C. Cheng, S. Nie, S. Li, H. Peng, H. Yang, L. Ma, S. Sun and C. Zhao, J. Mater. Chem. B,
1783 2013, **1**, 265-275.
- 1784 97. X. Guo and N. Mei, J. Food Drug Anal. 2014, **22**, 105-115.
- 1785 98. N. A. Elyamany, F. F. Mohamed and T. A. Salaheldin, Exp. Toxicol. Pathol. 2017, **6**, 383-
1786 392.
- 1787 99. N. Chatterjee, J. S. Yang and K. Park K, Environ. Health-Glob. Toxic. 2015, **30**, 2015007.
- 1788 100. Y. Zhang, T. R. Nayak, H. Hong and W. Cai, Nanoscale. 2012, **4**, 3833-3842.
- 1789 101. X. Zhi, H. Fang, C. Bao, G. Shen, J. Zhang, K. Wang, S. Gao, T. Wan and D. Cui,
1790 Biomaterials, 2013, **34**, 5254-5261.
- 1791 102. T.L. Moore, R. Podilakrishna, A. Rao and F. Alexis, Part. Part. Syst. Charact., 2014,
1792 **31**, 886–894.
- 1793 103. C. S. Lee, H. Kim, J. Yu, S. H. Yu, S. Ban, S. Oh, D. Jeong, J. Im, M. J. Baek and
1794 T. H. Kim, Eur. J. Med. Chem., 2017, **142**, 416–423.
- 1795 104. K. Yang, L. Hu, X. Ma, S. Ye, L. Cheng, X. Shi, C. Li, Y. Li and Z. Liu, Adv. Mater.,
1796 2012, **24**, 1868–1872.
- 1797 105. X. X. Ma, H. Q. Tao, K. Yang, L. Z. Feng, L. Cheng and X. Z. Shi, Nano Res.,
1798 2012, **5**, 199–212.
- 1799 106. W. Zhang, Z. Guo, D. Huang, Z. Liu, X. Guo and H. Zhong, Biomaterials, 2011,
1800 **32**, 8555–8561.

- 1801 107. W. Miao, G. Shim, G. Kim, S. Lee, H.-J. Lee, Y.B. Kim, Y. Byun and Y. K. Oh, J.
1802 Control. Release, 2015, **211**, 28–36.
- 1803 108. P. Huang, C. Xu, J. Lin, C. Wang, X. Wang, C. Zhang, X. Zhou, S, Guo and D.
1804 Cui, 2011, **1**, 240–250.
- 1805 109. L. Feng, X. Yang, X. Shi, X. Tan, R. Peng, J. Wang and Z. Liu, Small, 2013, **9**,
1806 1989–1997.
- 1807 110. Y. Zhou, Y. Wang, X. Zhang, J. Peng, H. Li and Z. Li, J. Nanosci. Nanotechnol,
1808 2015, **15**, 2009–2014.
- 1809 111. L. Yao, T Lei and S. W. A. Bligh, Mat. Sci. Eng. C-Mater., 2016, **59**, 652-660.
- 1810 112. L. Z. Feng, K.Y. Li, X.Z. Shi, M. Gao, J. Liu, and Z. Liu, Adv. Healthcare Mater.,
1811 2014, **3**, 1261–1271.
- 1812 113. J. H. Park, S. Lee, J. H. Kim, K. Park, K. Kim, and I. C. Kwon, Prog. Polym. Sci.,
1813 2008, **33**, 113-137.
- 1814 114. H. Hong, Y. Zhang, J. W. Engle, T. R. Nayak, C. P. Theuer, R. J. Nickles, T. E.
1815 Barnhart, and W. Cai, Biomaterials, 2012, **33**, 4147-4156.
- 1816 115. L. Fiandra, S. Mazzucchelli, C. De Palma, M. Colombo, R. Allevi, S. Sommaruga,
1817 E. Clementi, M. Bellini, D. Prospero, and F. Corsi, ACS Nano, 2013, **7**, 6092-6102.
- 1818 116. S. Jager, A. Jahnke, S. Adebar, F. N. Vogtle, E. Delima-Hahn, D. Pfeifer, T. Berg,
1819 M. Lubbert, and M. Trepel, 2008, **31**, 100.
- 1820 117. O. C. Farokhzad, J. Cheng, B. Tepiy, A. Khademhosseini, S. Jon, E. Levy-
1821 Nissenbaum, and R. Langer, EJC Suppl., 2005, **3**, 229-230.
- 1822 118. X. F. Cao, F. L. Feng, Y. S. Wang, X. Y. Yang, H. Q. Duan, and Y. S. Chen, J.
1823 Nanopart. Res., 2013, **15**, 1965.
- 1824 119. G. Liu, H. Shen, J. Mao, L. Zhang, Z. Jiang, T. Sun, Q. Lan, and Z. Zhang, ACS
1825 Appl. Mater. Inter., 2013, **5**, 6909-6914.
- 1826 120. T. Lu, Z. Nong, L. Wei, M. Wei, G. Li, N. Wu, C. Liu, B. Tang, Q. Qin, X. Li and
1827 F. Meng, J. Biomater. App., 2020, 1-13.
- 1828 121. N. Abdullah Al, J.-E. Lee, I. In, H. Lee, K. D. Lee, J. H. Jeong, and S. Y. Park,
1829 Mol. Pharm., 2013, **10**, 3736-3744.
- 1830 122. C. Zhan, B. Li, L. Hu, X. Wei, L. Feng, W. Fu and W. Lu, 2011, **50**, 5482–5485.

- 1831 123. C. Zhan, X. Wei, J. Qian, L. Feng, J. Zhu and W. Lu, *J. control release*, 2012, **160**,
1832 630-636.
- 1833 124. C. Zhan, Z. Yan, C. Xei and W. Lu, *Mol. Pharm.*, 2010, **7**, 1940–1947.
- 1834 125. S. Sabharanjak and S. Mayor, *Adv. Drug Deliv. Rev.*, 2004, **56**, 1099–1109.
- 1835 126. L. Zhang, J. Xia, Q. Zhao, L. Liu and Z. Zhang, *Small*, 2010, **6**, 537–544.
- 1836 127. G. Poste and R. Kirsh, 1983, **1**, 869–878.
- 1837 128. H. Mok, J. W. Park and T. G. Park, *Bioconjug. Chem.*, 2008, **19**, 797–801.
- 1838 129. C. He, S. W. Kim and D. S. Lee, 2008, **127**, 189–207.
- 1839 130. X. Zhang, J. Yin, C. Peng, W. Hu, Z. Zhu, W. Li, C. Fan and Q. Huang, 2011, **49**,
1840 986-995.
- 1841 131. K. Yang, L. Feng, X. Shi and Z. Liu, *Chem. Soc. Rev.*, 2013, **42**, 530-547.
- 1842 132. L. Du, S. Wu, Y. Li, X. Zhao, X. Zu and Y. Wang, *Bio-Med. Mater. Eng.*, 2014,
1843 **24**, 2135-2141.
- 1844 133. Z. Liu, J. Robinson, X. Sun, and H. Dai, *J. Am. Chem. Soc.*, 2008, **130**, 10876-
1845 10877.
- 1846 134. X. Sun, Z. Liu, K. Welsher, J. T. Robinson, A. Goodwin, S. Zaric, and H. Dai,
1847 *Nano. Res.*, 2008, **1**, 203-212.
- 1848 135. H. Y. Wu, K. J. Lin, P. Y. Wang, C. W. Lin, H. W. Yang, C. C. M. Ma, Y. J. Lu and
1849 T. R. Jan, *Int. J Nanomed.*, 2014, **9**, 4257- 4266.
- 1850 136. Z. Xu, S. Wu, G. Huang, H. Ding, R. Gui and B. Zhu, *Mater. Lett.*, 2017, **195**, 131-
1851 135.
- 1852 137. K. R. Javed, M. Ahmad, S. Ali, M. Z. Butt, M. Nafees, A. R. Butt, M. Nadeem and
1853 A. Shahid, *Medicine*, 2015, **94**, 1–6.
- 1854 138. M. Naz, N. Nasiri, M. Ikram, M. Nafees, M. Z. Qureshi, S. Ali and A. Tricoli, *Appl.*
1855 *Nanosci.*, 2017, **7**, 793–802.
- 1856 139. H. Afzal, M. Ikram, S. Ali, A. Shahzadi, M. Aqeel, A. Haider, M. Imran, S. Ali,
1857 *Mater. Res. Express*, 2020, **7**, 015405.
- 1858 140. G. Chauhan, V. Chopra, A. Tyagi, G. Rath, R. K. Sharma and A. K. Goyal, *Eur. J.*
1859 *Pharm. Sci.*, 2017, **96**, 351-361.
- 1860 141. K. Yang, S. Zhang, G. Zhang, X. Sun, S.-T. Lee and Z. Liu, *Nano Lett.*, 2010, **10**,
1861 3318–3323.

- 1862 142. C. Dou, N. Ding, F. Luo, T. Hou, Z. Cao, Y. Bai, C. Liu, J. Xu and S. Dong, *Adv.*
1863 *Sci.*, 2018, **5**.
- 1864 143. Y. P. Huang, C. M. Hung, Y. C. Hsu, C. Y. Zhong, W. R. Wang, C. C. Chang and
1865 M. J. Lee, *Nanoscale Res. Lett.*, 2016, **11**, 247.
- 1866 144. J. Zhang, L. Feng, X. Tan, X. Shi, L. Xu, Z. Liu and R. Peng, *Part. Part. Syst. Char.*,
1867 2013, **30**, 794-803.
- 1868 145. Y. Wang, Z. Li, J. Wang, J. Li and Y. Lin, *Trends Biotechnol.*, 2011, **29**, 205–212.
- 1869 146. Y. Wang, Z. Li, D. Hu, C. T. Lin, J. Li and Y. Lin, *J. Am. Chem. Soc.*, 2010, **132**,
1870 9274–9276.
- 1871 147. J. Ma, J. Zhang, Z. Xiong, Y. Yong and X.S. Zhao, *J. Mater. Chem.*, 2011, **21**,
1872 3350-3352.
- 1873 148. S.W. Chook, C.H. Chia, S. Zakaria, M.K. Ayob, K.L. Chee, N.M. Huang, H.M.
1874 Neoh, H.N. Lim, R. Jamal and R.M.F.R.A. Rahman, *Nanoscale Res. Lett.*, 2012, **7**, 1-7.
- 1875 149. W. P. Xu, L. C. Zhang, J. P. Li, Y. Lu, H. H. Li, Y. N. Ma, W. D. Wang and S. H.
1876 Yu, *J. Mater. Chem.*, 2011, **21**, 4593-4597.
- 1877 150. Z. Wang, D. Wu, J. Zou, Q. Zhou, W. Liu, W. Zhang, G. Zhou, X. Wang, G. Pei,
1878 Y. Cao and Z. Y. Zhang, *J. Mater. Chem. B*, 2017, **5**, 62-73.
- 1879 151. Z. Li, B. H. Tan, T. Lin and C. He, *Prog. Polym. Sci.*, 2016, **62**, 22-72.
- 1880 152. A. A. Karim, Q. Dou, Z. Li and X. J. Loh, *an Asian journal*, 2016, **11**, 1300-1321.
- 1881 153. X. Fan, Z. Li and X. J. Loh, *Polym. Chem.*, 2016, **7**, 5898-5919.
- 1882 154. X. Fan, J. Y. Chung, Y. X. Lim, Z. Li and X. J. Loh, *ACS Appl. Mater. Interfaces*,
1883 2016, **8**, 33351-33370.
- 1884 155. X. Yang, X. Zhang, Y. Ma, Y. Huang, Y. Wang and Y. Chen, *J. Mater. chem.*, 2009, **19**,
1885 2710-2714.
- 1886 156. K. Turcheniuk, M. Khanal, A. Motorina, P. SubRamanian, A. Barras, V.
1887 Zaitsev, V. Kuncser, A. Leca, A. Martoriati, K. Cailliau, J. F. Bodart, R.
1888 Boukherrouband S. Szunerits, *RSC Adv.*, 2014, **4**, 865-875.
- 1889 157. R. G. Bai, K. Muthoosamy, F. N. Shipton, A. Pandikumar, P. Rameshkumar, N. M.
1890 Huang and S. Manickam, *RSC Adv.*, 2016, **6**, 36576-36587.
- 1891 158. O. Akhavan and E. Ghaderi, *ACS Nano.*, 2010, **4**, 5731-5736.
- 1892 159. O. Akhavan and E. Ghaderi, *J. Phys. Chem.*, 2009, **113**, 20214-20220.

- 1893 160. J. Li, G. Wang, H. Zhu, M. Zhang, X. Zheng, Z. Di, X. Liu and X. Wang, *Sci. Rep.*,
1894 2014, **4**, 1-8.
- 1895 161. O. Akhavan, E. Ghaderi and A. Akhavan, *Biomaterials*, 2012, **33**, 8017-8025.
- 1896 162. A. M. Allahverdiyev, K. V. Kon, E. S. Abamor, M. Bagirova and M. Rafailovich,
1897 *Expert Rev. Anti Infect. Ther.*, 2011, **9**, 1035-1052.
- 1898 163. N. P. Katuwavila, Y. Amarasekar, V. Jayaweera, C. Rajapaksha, C. Gunasekara,
1899 I. C. Perera, G. A. J. Amaratunga, and L. Weerasinghe, *J. Pharma. Sci.*, 2020, **109**, 1130-
1900 1135.
- 1901 164. A. Pourjavadi, Z. Tehrani and A. Shakerpoor, *Supramol.Chem.*, 2016, **28**, 624-633.
- 1902 165. F. Calabro, V. Lorusso, G. Rosati, L. Manzione, L. Frassinetti, T. Sava, E. D. Di
1903 Paula, S. Alonso and C. N. Sternberg, *Cancer*, 2009, **115**, 2652– 2659.
- 1904 166. H. M. McDaid and P. G. Johnston, *Clin. Cancer Res.*, 1999, **5**, 215–220.
- 1905 167. A. L. Hopkins, *Nat. Chem. Biol.*, 2008, **4**, 682–690.
- 1906 168. H. Kitano, *Nat. Rev. Drug Discov.*, 2007, **6**, 202–210.
- 1907 169. W. Kassouf, C. PDinney, G. Brown, D. J. McConkey, A. J. Diehl, M. Bar-Eli and
1908 L. Adam, *Cancer Res.*, 2005, **65**, 10524–10535.
- 1909 170. I. G. Zarraga and E. R. Schwarz, *J. Am. Coll. Cardiol.*, 2007, **49**, 1–14.
- 1910 171. F. Ahmed, R. I. Pakunlu, A. Brannan, F. Bates, T. Minko and D. E. Discher, *J.*
1911 *Control Release*, 2016, **116**, 150–158.
- 1912 172. S. Sengupta, D. Eavarone, I. Capila, G. Zhao, N. Watson, T. Kiziltepe and R.
1913 Sasisekharan, *Nature*, 2005, **436**, 568–572.
- 1914 173. Y. Wang, S. Gao, W. H. Ye, H. S. Yoon and Y. Y. Yang, *Nat. Mater.* 2006, **5**, 791–
1915 796.
- 1916 174. L. Zhang, A. F. Radovic-Moreno, F. Alexis, F. X. Gu, P. A. Basto, V. Bagalkot, S.
1917 Jon, R. S. Langer and O. C. Farokhzad, *Chem. Med. Chem.*, 2007, **2**, 1268–1271.
- 1918 175. S. Aryal, C. J. Hu, and L. Zhang, *Combinatorial Drug Conjugation Enables*
1919 *Nanoparticle Dual-Drug Delivery*, *small*, 2010, **6**, 1442–1448.
- 1920 176. J. M. Shen, F. Y Gao, L. P. Guan, W. Su, Y. J. Yang, Q. R. Li, and Z. C. Jin, *Rsc.*
1921 *Advances*, 2014, **4**, 18473-18484.
- 1922 177. X. Cao, F. Feng, Y. Wang, X. Yang, H. Duan and Y. Chen, *J. Nanopart Res.*, 2013,
1923 **15**, 965.

- 1924 178. H. Tiwari, N. Karki, M. Pal, S. Basak, R.K. Verma, R. Bal, N. D. Kandpal, G. Bisht
1925 and N. G. Sahoo, *Colloids Surf. B*, 2019, **178**, 452–459.
- 1926 179. H. Yang, D.H. Bremner, L. Tao, H. Li, J. Hu and L. Zhu, *Carbohydr. Polym.*, 2016,
1927 **135**, 72–78.
- 1928 180. H. J. Jang, E. M. Hong, J. Jang, J. E. Choi, S. W. Park, H. W. Byun, D. H. Koh, M.
1929 H. Choi, S. H. Kae, and J. Lee, *Research and Practice*, 2016, 1-9.
- 1930 181. M. M. Song, H. L. Xu, J. X. Liang, H.H Xiang, R. Liu and Y. X. Shen, *Mat. Sci.*
1931 *Eng. C-Mater.*, 2017, **77**, 904-911.
- 1932 182. C. Wang, S. Ravi, U. Garapati, M. Das, M. Howell, J. Mallela, S. Alwarappan, S.
1933 S. Mohapatra and S. Mohapatra, *J. Mater. Chem. B*, 2013, **1**, 4396-4405.
- 1934 183. L. Zhang, J. Xia, Q. Zhao, L. Liu and Z. Zhang, *Small*, 2010, **6**, 537–544.
- 1935 184. B. A. Aderibigbe, S. J. Owonubi, J. Jayaramudu, E. R. Sadiku and S. S. Ray,
1936 *Colloids and Poly. Sci.*, 2015, **2**, 409-420.
- 1937 185. S. J. Owonubi, B. A. Aderibigbe, E. Mukwevho, E. R. Sadiku and S. S. Ray,
1938 *International J. of Indus. Chem.*, 2018, **9**, 39-52.
- 1939 186. S. Bullo, K. Buskaran and R. Baby, *Pharm. Res.*, 2019, **36**, 91.
- 1940 187. X. Pei, Z. Zhu, Z. Gan, J. Chen, X. Zhang, X. Cheng, Q. Wan and J. Wang, *Sci.*
1941 *Rep.*, 2020, **10**, 2717.
- 1942 188. A. Alinejad, H. Raissi and H. Hashemzadeh, *J. Bio. Struc. and Dynamic.*, 2019, 1-
1943 9.
- 1944 189. J. Zhang, L. Chen, B. Shen, L. Chen, J. Mo and J. Feng, *Langmuir*, 2019, **35**, 6120-
1945 6128.
- 1946 190. J. R Sharom., D. S. Bellows and M. Tyers, *Curr. Opin. Chem. Biol.*, 2004, **8**, 81–
1947 90.
- 1948 191. W. G. Jr. Kaelin, *Nat. Rev. Cancer*, 2005, **5**, 689–698.
- 1949 192. C. T. Keith, A. A. Borisy, and B. R. Stockwell, *Nat. Rev. Drug Discov.*, 2005, **4**,
1950 71–78.
- 1951 193. A. Persidis, *Nat. Biotechnol.*, 1999, **17**, 94–95.
- 1952 194. T. C. Chou, *Cancer Res.*, 2010, **70**, 440–446.
- 1953 195. P. Parhi, C. Mohanty and S. K. Sahoo, *Drug Discov. Today*, 2012, **17**, 1044-1052.

- 1954 196. W.M. Lau¹, A.W. White¹, S.J. Gallagher, M. Donaldson, G. McNaughton and C.M.
1955 Heard, *Curr. Pharm. Des.*, 2008, **14**, 794-802.
- 1956 197. Ali Pourjavadi, S. Asgari, S. H. Hosseini, and M. Akhlaghi, *Langmuir*, 2018, **34**,
1957 15304-15318.
- 1958 198. R. K. Thapa, Y. Choi, J. H. Jeong, Y. S. Youn, H. G. Choi, C. S. Yon and J. O.
1959 Kim, *Pharm. Res.*, 2016, **33**, 2815–2827.
- 1960 199. B. Haley and E. Frenkel, *Urol. Oncol.*, 2008, **26**, 57–64.
- 1961 200. D. Chena, C. A. Dougherty, K. Zhu and H. Hong, *J. Control Release*, 2015, **210**,
1962 230–245.
- 1963 201. W. Chen, P. Yi, Y. Zhang, L. Zhang, Z. Dang and Z. Zhang, *ACS Appl. Mater.*
1964 *Inter.*, 2011, **3**, 4085-4091.
- 1965 202. M. H. Rivera, N. G. Zaibaq and L. J. Wilson, *Biomaterials*, 2016, **101**, 229–240.
- 1966 203. C. Wang, J. Li, C. Amatore, Y. Chen, H. Jiang and X. M. Wang, *Angew. Chem. Int.*
1967 *Ed. Engl.*, 2011, **50**, 11644–11648.
- 1968 204. M. Nurunnabi, Z. Khatun and G. R. Reeck, *ACS Appl. Mater. Inter.*, 2014, **6**,
1969 12413-12421.
- 1970 205. J. L. Li, B. Tang and B. Yuan, *Biomaterials*, 2013, **34**, 9519-9534.
- 1971 206. Z. Liu, S. Tabakman, K. Welsher, H. Dai, *Nano Res.*, 2009, **2**, 85–120.
- 1972 207. S. N. Baker and G. A. Baker, *Angew. Chem. Int. Ed.*, 2010, **49**, 6726–6744.
- 1973 208. C. Tewari, G. Tatrari, M. Karakoti, S. Pandey, M. Pal, S. Rana, B. SanthiBhushan,
1974 A. B. Melkani, A. Srivastava, and N. G. Sahoo, *Mater. Sci. Eng. C*, 2019, **104**, 109970.
- 1975 209. D. Pan, J. Zhang, Z. Li and M. Wu, *Adv. Mater.*, 2010, **22**, 734–738.
- 1976 210. S. Zhu, J. Zhang, C. Qiao, S. Tang, Y. Li, W. Yuan, B. Li, L. Tian, F. Liu, R. Hu,
1977 H. Gao, H. Wei, H. Zhang, H. Sun and B. Yang, *Chem. Commun.*, 2011, **47**, 6858–6860.
- 1978 211. H. Dong, W. Dai, H. Ju, H. Lu, S. Wang, L. Xu, S. F. Zhou, Y. Zhang and X. Zhang,
1979 *ACS Appl. Mater Interfaces*, 2015, **7**, 11015–11023.
- 1980 212. T. Wen, B. Yang, Y. Guo, J. Sun, C. Zhao, S. Zhang, M. Zhang and Y. Wang, *Phys.*
1981 *Chem. Chem. Phys.*, 2014, **16**, 23188–23195.
- 1982 213. J. Li, W. Zhang, T. F. Chung, M. N. Slipchenko, Y.P. Chen, J. X. Cheng, and C.
1983 Yang, *Sci. Rep.*, 2015, **5**, 12394.
- 1984 214. J. M. Yoo, J. H. Kang, and B. H. Hong, *Chem. Soc. Rev.*, 2015, **44**, 4835–4852.

- 1985 215. J. L. Li, H. C. Bao, X. L. Hou, L. Sun, X. G. Wang, M. Gu, *Angew. Chem. Int.*
1986 *Ed.*, 2012, **51**, 1830–1834.
- 1987 216. J. Sun, Q. Xin, Y. Yang, H. Shah, H. Cao, Y. Qi, J. R. Gong and J. Li, *Chem*
1988 *comm.*, 2018, **54**, 715–718.
- 1989 217. Z. Liu, Z. Guo, H. Zhong, X. Qin, M. Wan and B. Yang, *Phys. Chem. Chem. Phys.*,
1990 **15**, 2961–2966.
- 1991 218. X. Wang, P. Huang, L. Feng, M. He, S. Guo, G. Shen and D. Cui, *RSC Adv.*, 2012,
1992 **2**, 3816–3822.
- 1993 219. Z. L. Song, Z. Chen, X. Bian, L.Y. Zhou, D. Ding, H. Liang, Y. X. Zou, S. S. Wang,
1994 L. Chen, C. Yang and X. B. Zhang, *J. Am. Chem. Soc.*, 2014, **136**, 13558–13561.
- 1995 220. X. Ma, Q. Qu, Y. Zhao, Z. Luo, Y. Zhao, K. W. Ng and Y. Zhao, *J. Mater. Chem.*
1996 *B*, 2013, **1**, 6495–6500.
- 1997 221. S. M. Janib, A. S. Moses, J. A. MacKay, *Adv. Drug Deliv. Rev.*, 2010, **62**, 1052–
1998 1063.
- 1999 222. K. Park, S. Lee, E. Kang, K. Kim, K. Choi, I. C. Kwon, *Adv. Funct. Mater.*, 2009,
2000 **19**, 1553–1566.
- 2001 223. H. Hong, K. Yang, Y. Zhang, J. W. Engle, L. Feng, Y. Yang, T. R. Nayak, S. Goel,
2002 J. Bean, C. P. Theuer, T. E. Barnhart, Z. Liu and W. Cai, *ACS Nano*, 2012, **6**, 2361–2370.
- 2003 224. T. Cao, P. You, X. Zhou, J. Luo, X. Xu, Z. Zhou, S. Yang Y. Zhang, H. Yang and
2004 M. Wang, *J Mater Chem B.*, 2016, **4**, 6446–6453.
- 2005 225. P. Caravan, J. J. Ellison, T. J. McMurry and R. B. Lauffer, *Chem. Rev.*, 1999, **99**,
2006 2293–2352.
- 2007 226. A. Gizzatov, V. Keshishian, A. Guven, A. M. Dimiev, F. Qu, R. Muthupillai, P.
2008 Decuzzi, R. G. Bryant, J. M. Tour and L. J. Wilson, *Nanoscale*, 2014, **6**, 3059–3063.
- 2009 227. H. W. Yang, C. Y. Huang, C. W. Lin, H. L. Liu, C. W. Huang, S. S. Liao, P.Y.
2010 Chen, Y. J. Lu, K. C. Wei, and C. C. Ma, *Biomaterials*, 2014, **35**, 6534–6542.
- 2011 228. A. Alazmi, V. Singaravelu, N. M. Batra, J. Smajic, M. Alyami, N. M. Khashab,
2012 and P. M. Costa, *RSC advances*, 2019, **9**, 6299–6309.
- 2013 229. L. H. V. Wang and S. Hu, *Science*, 2012, **335**, 1458–1462.
- 2014 230. L. Cheng, J. Liu, X. Gu, H. Gong, X. Shi, T. Liu, C. Wang, X. Wang, G. Liu, H.
2015 Xing, W. Bu, B. Sun and Z. Liu, *Adv. Mater.*, 2014, **26**, 1886–1893.

- 2016 231. M. A. Patel, H. Yang, P. L. Chiu, D. D. Mastrogiovanni, C. R. Flach, K. Savaram,
2017 L. Gomez, A. Hemnarine, R. Mendelsohn, E. Garfunkel, H. Jiang, and H. He, *ACS Nano*,
2018 2013, **7**, 8147–8157.
- 2019 232. Y. W. Wang, Y. Y. Fu, Q. Peng, S. S. Guo, G. Liu, J. Li, H. H. Yang and G. N.
2020 Chen, *J. Mater. Chem. B* 1, 2013, **1**, 5762–5767.
- 2021 233. G. Lalwani, X. Cai, L. Nie, L. V. Wang, and B. SithaRaman, 2013, **1**, 62–67.
- 2022 234. Z. Li, L. Tian, J. Liu, W. Qi, Q. Wu, H. Wang, M.C. Ali, W. Wu and H. Qiu, *Adv.*
2023 *Healthc. Mater.*, 2017, **6**, 1700413.
- 2024 235. C. T. Smith, C. A. Mills, S. Pani, R. Rhodes, J. J. Bailey, S. J. Cooper, T. S. Pathan,
2025 V. Stolojan, D. J. Brett, P. R. Shearing, and S.R.P.Silva, *Nanoscale*, 2019, **11**, 14734-
2026 14741.
- 2027 236. D. E. Lee H. Koo, I. C. Sun J. H. Ryu, K. Kim and I. C. Kwon, *Chem. Soc. Rev.*,
2028 2012, **7**, 2656-2672.
- 2029 237. P. Rong, K. Yang, A. Srivastan, D. O. Kiesewetter, X. Yue, F. Wang, L. Nie, A.
2030 Bhirde, Z. Wang, Z. Liu, G. Niu, W. Wang and X. Chen, 2014, **4**, 229–239.
- 2031 238. H. Zhang, H. Wu, J. Wang, Y. Yang, D. Wu, Y. Zhang, Y. Zhang, Z. Zhou, S.
2032 Yang, *Biomaterials*, 2015, **42**, 66–77.
- 2033 239. C. McCallion, J. Burthem, K. Rees-Unwin, A. Golovanov and A. Pluen, 2016, **104**,
2034 235–250.
- 2035 240. C. H. Lu, C. L. Zhu, J. Li, J. J. Liu, X. Chen and H. H. Yang, *Chem. Commun*,
2036 2010, **46**, 3116–3118.
- 2037 241. M. Mahdavi, A. Fattahi, E. Tajkhorshid, and S. Nouranian, *ACS Applied Bio.*
2038 *Materials*, 2020, **3**, 1354-1363.
- 2039 242. Y. Guo, H. Xu , Y. Li , F. Wu , Y. Li , Y. Bao , X. Yan , Z. Huang and P. Xu, *J*
2040 *Biomater. Appl.*, 2017, **32**, 54-65.
- 2041 243. S. Pandey, M. Karakoti, S. Dhali, N. Karki, B. SanthiBhushan, C. Tewari, S. Rana,
2042 A. Srivastava, A. B. Melkani and N. G. Sahoo, *Waste Management*, 2019, **88**, 48–55.
- 2043 244. N. G. Sahoo, Sandeep, M. Karakoti and V.D. Punetha, "A process of Manufacturing
2044 Graphene", Application No. 201611016081.
- 2045 245. T. Pullingam, K. L. Thong, J. N. Appaturi, N. I. Nordin, I. J. Dinshaw, C. W. Lai
2046 and B. F. Leo, *Eur. J. Pharm. Sci.*, 2020, **142**, 105087.

- 2047 246. M. Y. Xia, Y. Xie, C. H. Yu, G. Y. Chen, Y. H. Li, T. Zhang and Q. Peng, *J. Control*
2048 *Release*, 2019, **10**, 16-31.
- 2049 247. Q. Jiang, D. Ghim, S. Cao, S. Tadepalli, K. K. Liu, H. Kwon, J. Luan, Y. Min, Y.
2050 S. Jun, and S. Singamaneni, *Environ. Sci. Technol.*, 2019, **53**, 412-421.
- 2051 248. X. Chen, X. Dai, Y Yu, X. Wei, X Zhang and C. Li, *New j. of Chem.*, 2019, **43**,
2052 917-925.
- 2053 249. D. Aycan and N. Alemdar, 2018, Berlin, Germany.
- 2054 250. X. Wang, Y. Liu, J. Xu, S. Li, F. Zhang, Q. Ye, X. Zhai and X. Zhao, *J. Nanomater.*,
2055 2015, 1-14.
- 2056 251. S. Ge, Y. Xi, R. Du, Y. Ren, Z. Xu, Y. Tan, Y. Wang, T. Yin and G. Wang,
2057 *Regenerative Biomaterials*, 2019, 299–309.
- 2058 252. Y. Liu, Y. Qi, C. Yin, S. Wang, S. Zhang, A. Xu, W. Chen and Sijin L,
2059 *Nanotheranostics*, 2018, **2**, 222-232.
- 2060 253. M. Afzali, K. Parivar, N. H. Roodbari and A. Badiei, *Special Issue of Curr World*
2061 *Environ*, 2015, 10.

2062 **Table 1. Summary of advantages and disadvantages of GO**

2063

Advantages	Disadvantages
<p>Pi- Conjugated Structure:</p> <ul style="list-style-type: none"> ➤ GO and its derivatives provide the high π electrons density on their basal plane which favor the addition of different therapeutics in their surface [1-4]. 	<p>Hydrophobic Nature:</p> <ul style="list-style-type: none"> ➤ Primitive graphene is hydrophobic in nature. ➤ Surfactants or stabilizing agents are required for making stable suspension or preventing from agglomeration in water or biological fluids [13].
<p>Polar basal plane:</p> <ul style="list-style-type: none"> ➤ GO makes stable suspension in water due to the presence of polar basal plane and negative charge (carboxylate group) on edge site [9-12]. ➤ GO acts as an amphiphilic molecule and can be used as surfactant to stabilize hydrophobic species in water [13]. 	<p>Aggregation in Biological Media:</p> <ul style="list-style-type: none"> ➤ GO has poor colloidal stability in buffered saline and cell cultured medium. ➤ GO exfoliates and shows stable dispersions in polar organic solvents [67]. ➤ Functionalization can be utilized to improve the stability of these species [68].
<p>Optical Properties:</p> <ul style="list-style-type: none"> ➤ GO has excellent optical properties. ➤ Single layer of GO transmits 97.7% of incident light. Their high light transmittance and charge 	<p>Toxicity:</p> <ul style="list-style-type: none"> ➤ GO produces singlet oxygen species which destroy or affect the function of normal tissues [52].

<p>mobility tendency and photoluminescence property make graphene a valuable material for MRI [26-28].</p> <ul style="list-style-type: none"> ➤ GO has ability to manage separation or recombination of surface electrons can be fully utilized in the development of Bio- imaging applications [29-30]. 	<ul style="list-style-type: none"> ➤ High zeta potential of GO damages cells. On the other hand if electronic charge is too high then toxicity is not affects strongly [53]. ➤ <i>In vivo</i> and <i>in vitro</i> experiments have shown that GO displayed observable dose-dependent toxicity [78].
<p>Interaction with DNA:</p> <ul style="list-style-type: none"> ➤ GO and functionalized GO have affinity to interact with DNA or RNA, which make these species as an attractive candidate for DNA or RNA sensing and delivery carrier [34-36]. ➤ GO preferentially adsorbs ssDNA over to double strand (ds) DNA and protects them it from nuclease enzyme [37]. 	

2064

2065

2066

2067 **Table 2. Summary of therapeutic applications of GO.**

2068

Functionalized Graphene Oxide (FGO)	Therapeutic Agents (TA)	Interaction between FGO and TA	Highlights of the study	Stimuli	Ref.
GO-β-CD and GO-PVP	SN-38	Noncovalent	Functionalized GO with both polymers show enhanced cytotoxicity against the MCF-7 cell.	pH	[13]
GO-CuS	CEA and Glu	Noncovalent	GO-CuS-CEA-Glu shows photothermal accelerated release of Glu and <i>in vitro</i> chemo-photothermal synergistic therapy.	NIR, PTT, pH	[91]
GO-ZnO	DOX	Noncovalent	GO=ZnO shows higher drug loading efficiency(89%) compared to pure ZnO (82%) and provides enhanced	pH	[94]

			dissolution according to the drug release.		
GO-FA-AuNPs	DOX	Covalent and Noncovalent	Substantial <i>in vivo</i> tumor regression in solid tumor model in Balb/c mice	NIR-PTT	[95]
GO-PEI	mi-RNA	Covalent	Efficient loading of miR-7b plasmid and delivers it into bone marrow macrophages for inhibiting the formation of mature osteoclasts while preserving beneficial pre-osteoclasts.	NIR	[97]
nGO-PEG-PEI	Plasmid DNA	Noncovalent	Efficiency of plasmid DNA transfection in <i>Drosophila</i> S2 cells increased	pH	[99]
GO-AgNPs	<i>E. coli</i>	Noncovalent	Antibacterial activity of GO-AgNPs on <i>E. coli</i> surface decreases the intake of nutrition from the surroundings while increases the interaction between Ag and the bacteria.	pH	[102]
GO-Fe ₃ O ₄	DOX	Noncovalent	GO-Fe ₃ O ₄ shows a high drug loading capacity, high dispersion through the external magnetic field.	External Magnetic Field	[110]
GO-FeNPs	Insulin	Noncovalent	GO-FeNPs-Insulin is stable at acidic pH, and released when exposed to basic solutions.	pH	[111]
GO-PEG	CEF	Covalent	GO-PEG-CEF shows both dose and time dependent antibacterial activity against both gram-positive and gram-negative bacteria while pure CEF shows only dose dependent antibacterial activity	pH	[118]
GO-Fe ₃ O ₄ -mSiO ₂	DOX	Noncovalent	The addition of mSiO ₂ on GO-Fe ₃ O ₄ increases the surface area, thus drug	pH	[119]

			loading efficiency, as well as the cellular uptake.		
GO-Fe ₃ O ₄	CPT and MTX	Noncovalent	<i>In vitro</i> shows that the nanocomposite can cause the apoptosis and death of HepG2 cells by preferentially releasing drugs to the tumor microenvironment	NIR-PTT	[131]
GO-FA-CS	DOX and siRNA		GO-FA-CS could effectively load DOX and siRNA simultaneously through p-p stacking and electrostatic interaction and specifically delivers to MCF-7 cells.	pH	[132]
GO- PVP	GEF and QSR	Noncovalent	The loading and cell cytotoxicity of GO-PVP-GEF, GO-PVP-QSR and GO-PVP-GEF-QSR in PA-1 ovarian cancer cells are significantly more cytotoxic than individual drug therapy to the PA-1 ovarian cancer cells compared to the toxicity toward IOSE-364 cells.	pH	[133]
rGO-AAm	PRG and CHL	Noncovalent	The rGO-AAm-PRG-CHL system interestingly shows antidiabetic activity when targeted <i>In vivo</i> against relevant neoglucogenic receptors	pH	[139]
GO-PEG	Cis-Pt and DOX	Noncovalent	GO-PEG-Cis-Pt-DOX shows more tumor cell growth inhibition than pure drug alone.	pH	[142]
GO-FA	CPT and DOX	Noncovalent	DOX has reinforced stronger interaction with FA than CPT thus establishing the fact that FA has influenced DOX release kinetics in the medium more than CPT.	pH	[143]

2070

Published on 18 August 2020. Downloaded on 8/21/2020 5:19:18 AM.

Journal of Materials Chemistry B Accepted Manuscript

Table of Content

Functionalized Graphene Oxide as a Vehicle for Targeted Drug Delivery and Bioimaging Applications

Neha Karki, Himani Tiwari, Chetna Tewari, Anita Rana, Neema Pandey, Souvik Basak, Nanda Gopal Sahoo*

